PTM 2025
ABSTRACTS

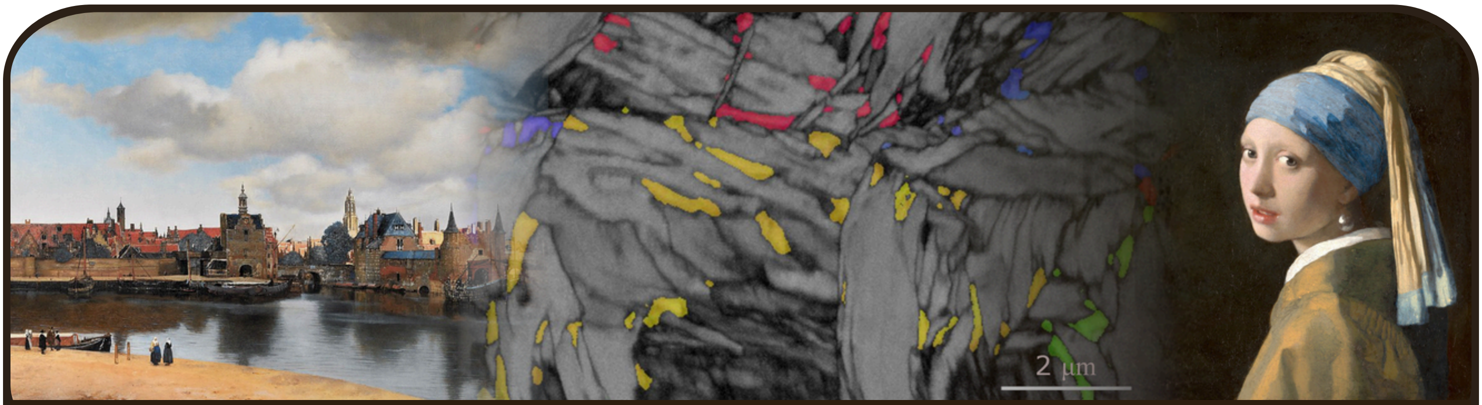

View at Delft [Vermeer, 1660] Q&P microstructure [Santofimia, 2011] Girl with a Pearl Earring [Vermeer, 1665]

The 9th International Conference on Solid-Solid Phase Transformations in Inorganic Materials

7 - 11 July 2025 | Delft, The Netherlands

Welcome to PTM2025

Scientific conferences represent knowledge sharing and mutual understanding. In the turbulent world we are living in, these unfortunately appear to be rare attributes. Still, we wish that this conference not only serves to its core values, but will also be an event of tolerance and dialogue. With this wish, we are excited to present the scientific programme of the 9th International Conference on Solid-Solid Phase Transformations in Inorganic Materials, PTM 2025, which will be held from 7 to 11 July 2025 at the Aula of Delft University of Technology, Delft, the Netherlands. The programme includes 42 sessions, six keynote lectures, the Hillert-Cahn lecture, the Aaronson Award ceremony and a poster session. There are over 200 registered delegates.

The conference aims at exchanging high-level fundamental knowledge on phase transformations in inorganic materials, i.e. the microscopic processes by which the microstructure can be tailored and thus by which the properties and performance of the material can be optimised. Although many types of materials have been used for centuries, the in-depth knowledge on these microstructural processes is still far from complete and still strongly developing, for instance through experimental observations at ever smaller length and time scales. Such observations and physics-based model development are mutually stimulating and lead to the design of new materials with enhanced performance. Fundamental science as developed and disseminated by the PTM conferences forms the basis for the materials transition towards sustainable production and circularity.

We hope that you will be inspired by the conference, catching up with old colleagues and making new contacts. There will be excursions to the Mauritshuis museum in The Hague with seventeenth-century paintings of Vermeer, the Dutch windmills in Kinderdijk and the war monument Oranjehotel in Scheveningen on Wednesday 9 July in the afternoon. The conference dinner will be held at the beach of Scheveningen on Thursday 10 July.

We are grateful for the sponsorship that we received from Groeien met Groen Staal, ThermoCalc, CAMECA, Access/Micress, Tata Steel, and Journal of alloys and compounds of Elsevier. We are grateful for the support of the department of Materials Science and Engineering of TU Delft and our fellow members of the PTM 2025 Scientific Committee: Annika Borgenstam (KTH Royal Institute of Technology), Leo Kestens (Ghent University), Joakim Odqvist (KTH Royal Institute of Technology), Jilt Sietsma (Delft University of Technology).

We look forward to meeting you in Delft,

Erik Offerman and Maria Santofimia, Conference Chairs

Monday, July 7

Plenary 1. Solid-state phase transformations during metal additive manufacturing: A case study on laser powder bed fusion of tool steels. Caballero[1], Santana[1], El hamouchia[1], Eres-Castellano[2], Rementeria[3], Królicka[4], Poplawsky[5], Capdevila[1].

[1] CENIM-CSIC, Madrid, Spain.

[2] Los Alamos National Lab, Los Alamos, United States.

[3] ArcelorMittal Global R&D, SLab—Steel Labs, Aviles, Spain.

[4] Wroclaw University of Science and Technology, Wroclaw, Poland.

[5] Oak Ridge National Laboratory, Oak Ridge, United States.

Laser powder bed fusion (LPBF) is thought to be the additive manufacturing (AM) technology best suited for producing complex functional parts that can be scaled up to an industrial level for metallic components. The microstructure produced by traditional processing differs from that of grade steels used in AM. Understanding phase-transformation in additively made tool steels during the LPBF process and subsequent post-heat treatments is the goal of this investigation. Phase formation in the solid state and during solidification are investigated. During AM processes, the impact of cooling rates, thermal gradients, and thermal cycling is considered. Particular focus is paid to demonstrating the potential effects of the solute distribution during solidification on the phase transitions.

M1a.1-4: Ferrite formation in steels (I).

Invited. **Combinatorial experiments for fast mapping of the austenite-to-ferrite transformation kinetics.** Hugo Landeghem1 Imed-Eddine Benrabah[2], Amani Ksibi[1], Vuk Manojlovic[1,3], Benoit Denand[2], Guillaume Geandier[2], Veijo Honkimaki[3], Alexis Deschamps[1].

[1]SIMaP, Grenoble, France.

[2]Institut Jean Lamour, Nancy, France.

[3]ESRF, Grenoble, France.

The transformation of austenite into ferrite is a ubiquitous transformation in steel processing. It is of particular importance in the case of advanced high strength steel (AHSS) grades such as dual phase and transformation induced plasticity grades where precise control of the ferrite fraction is required in order to achieve the desired mechanical properties. The multi-component character of those grades complicates the modeling of the transformation kinetics due to the interactions of substitutional alloying elements with the transformation interface leading to solute drag. One of the main obstacles to the integration of solute drag in ferrite growth models is the need for a thermodynamic description of the interface. Given the spatial extent of the interface and the temperature at which the interface exists, direct measurements required for this description are impractical and it is usually determined by inverse method instead. The present work aims at providing a method to gather kinetic records of the transformation across the composition space in order to make this determination faster and more reliable. This method relies on the combined use of compositionally graded samples and time- and space-resolved in situ synchrotron X-ray diffraction experiments. The quasi-continuous mapping of the composition space it produces helps in determining not only the interaction of elements with the interface but also the interaction between those elements at the interface. These interactions were found to closely match the corresponding ones in austenite for the investigated elements.

Ferrite and austenite transformations in Fe-N based alloys. Tadashi Furuhara , Mitsutaka Sato, Goro Miyamoto.

Tohoku University, Sendai, Japan.

Microstructures formed during ferrite transformation and austenite reversion were analyzed in Fe-0.3mass%N based alloys prepared by gaseous nitriding. By isothermal holding in the ferrite+austenite two-phase region after austenitization, two ferrite morphologies, allotriomorphic and Widmanstatten, are formed at austenite matrix grain boundary. At 500°C, on the other hand, nitride-free bainitic ferrite was formed at the beginning, and later changed to bainite accompanied with γ' precipitation. In reverse transformation by intercritical annealing of initial nitrogen martensite, two morphologies of acicular and globular austenite are formed. These phase transformation behaviors are similar to those of carbon-containing steels. Non-equilibrium partitioning of nitrogen and third alloying elements are recognized in both forward and reverse transformations. In the presentation, various factors causing energy dissipation in ferrite/austenite boundary migration will be discussed in comparison to carbon-containing steels.

Unravelling the kinetics of austenite to acicular ferrite transformation in a low alloy steel during continuous cooling using a physical-based model. Antoine Kieffer[1,2], Flore Villaret[1], Frédéric Delabrouille[1], Xavier Boulnat[2], Michel Perez[2], Alexandre Brosse[3], Corentin Chavignon[4].

[1]EDF - R&D, Moret sur Loing, France.

[2]INSA Lyon, MateIS UMR5510 Villeurbanne, France.

[3]Framatome, Lyon, France.

[4]Framatome Centre Technique, Saint-Marcel, France.

Acicular ferrite is historically a microstructure that was most commonly found in welded joints. However, with the development of additive manufacturing techniques using welding processes, this microstructure has regained interest among the steel community. In this work, the authors aim at modeling the formation kinetics of acicular ferrite in a low-alloy steel. This using a physical based nucleation and growth mid-field model under continuous cooling. Nucleation sites for the microstructure, that are the finely dispersed inclusions, have been characterized using SEM for the volume fraction and TEM-EDX for the chemical composition. Results of these characterizations have helped in predicting the number of potent nucleation sites using both the chemical composition of the manufactured parts and the processing parameters. Austenite decomposition kinetics will be investigated using dilatometry analysis. Firstly Fe-C-X ternary alloys with X being either Mn, Ni or Mo will be studied in order to isolate the effect of each major alloying element on the decomposition kinetics and parameterize the physical based model. Secondly, industrial alloys will be investigated using dilatometry in order to tailor the nucleation fitting parameter. This step will also help evaluating if the size and morphology of acicular ferrite is well predicted. At last, thermal cycles representative of a manufacturing cycle will be applied on said industrial alloys to evaluate the soundness of the model.

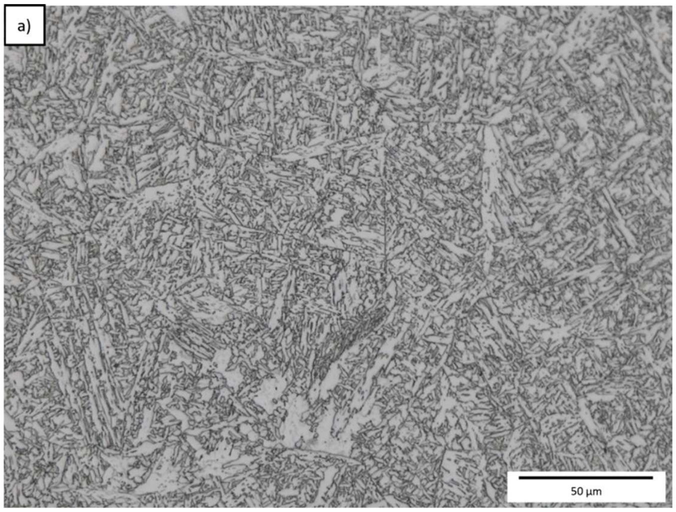

Acicular ferrite resulting of a 10°C/s continuous cooling observed using a light optical microscope after a 5%Nital etching.

The effects of material heterogeneities on diffusional ferrite formation. Martin Strangwood.

University of Warwick, Coventry, United Kingdom.

Increased use of thermo-mechanical processing to generate wider property mix ranges with leaner steel grades means that improved microstructural development models are required. Many models currently do not consider fully the effects of material heterogeneities on microstructural development, e.g. using average / mode prior austenite grain size (PAGS) and bulk composition. The significance of features such as residual segregation on ferrite nucleation and growth needs to be determined so that whether, where and how to incorporate these features into models can be assessed. High speed dilatometry has been carried out for low carbon steel weldments (containing de-oxidation products) and a series of low carbon steels (including those matching the weldmetal composition) in the hot-rolled (containing residual segregation) and homogenised conditions for a single starting PAGS distribution. Nucleation effects have been studied through the generation of continuous cooling transformation (CCT) curves and indicate strong effects of non-metallic inclusions and segregation on the start temperature for formation of allotriomorphic (and idiomorphic) ferrite. Isothermal time-temperature-transformation (TTT) curves have been generated in the two phase (alpha + gamma) field to follow the effects of heterogeneities on the diffusional growth behaviour of ferrite. The effects shown by the results of these studies will be discussed in terms of modifications necessary to microstructural models.

M1b.1-4: Ti alloys (I).

Invited. **Exploring the strength-ductility space of alpha-beta Ti alloys through a quenching and partitioning approach.** Stéphane Godet[1], Harena Rakotozafy[1], Loïc Malet[1], Odeline Dumas[1], Frédéric Prima[2].

[1]Université Libre de Bruxelles, Brussels, Belgium.

[2]ChimieParisTech, Paris, France.

The microstructure-mechanical property relationships of α+α’ dual phase microstructures are studied in different a-b Ti alloys. The study first focuses on Ti-6Al-4V. Various annealing temperatures in the α+β field are analyzed and the decomposition of the metastable martensite phase is also investigated. Low annealing temperatures lead to large work-hardening that is attributed to the occurrence of the concurrent deformation of a composite structure where the martensite is the softer phase and the occurrence of Reorientation Induced Plasticity in the martensite (RIP effect). This is studied by Electron Backscatted Diffraction (EBSD) and in-situ tensile testing combined with Digital Image Correlation (DIC). High annealing temperatures lead to a large decrease in work hardening due to the disappearance of RIP and of the mechanical contrast between α and α’. Further annealing of the α+α’ microstructures goes along with the disappearance of RIP associated with the decomposition of the metastable martensite. The decomposition mechanism is shown to be a reversion phenomenon with the β phase precipitating within the martensite and at interfaces while retrieving its high temperature orientation. The precipitation of the β phase is shown to largely increase the strain to fracture of the samples annealed at high temperatures. The precipitates act as reinforcement of the larger laths that form within the large β grains associated with the high annealing temperatures. The dual-phase microstructure is finally extended to various α+β alloys and several design rules to optimize the work-hardening by Reorientation Induced Plasticity are proposed and experimentally validated.

Effect of electric current on phase diagram of pure titanium. Heung Nam Han[1], Howook Choi[1], Siwhan Lee[1], Yijae Kim[1], Wan Chuck Woo[2], Sung-Tae Hong[3], In-Ho Jung[1].

[1]Seoul National University Seoul, South Korea.

[2]Korea Atomic Energy Research Institute, Daejeon, South Korea.

[3]University of Ulsan, Ulsan, South Korea.

It is generally known that thermodynamic stability of material is primarily dictated by temperature, pressure, and chemical composition. Gibbs free energy, which is influenced by atomic interactions in materials, is critical in determining the spontaneity of phase transition, serving as a tool to predict material phase stability. In this study, we attempt to examine whether applying an electric current to a material can change the free energy, which ultimately affects the phase stability of the material. First, we analyzed the difference in α/β phase transition temperature of pure titanium under the current-applied condition and the heat treatment condition reflecting the temperature increase due to former Joule heating. For the pure titanium samples with various initial microstructures, the phase transformation temperatures were measured using in-situ neutron and ex-situ X-ray diffraction. Subsequently, the athermal effect of electric current could be quantified as a form of additional Gibbs free energy, resulting in a pseudo phase diagram plotted with the microstructure of titanium and the applying electric current as state variables. This finding provides the evidence that the athermal effect of electric current originates from the change of free energy due to the charge imbalance near defects.

Contribution of the ω/β interfaces to the electrical resistivity of a Ti-15Mo β-metastable titanium alloy. Benoît Denand[1], Yann Le Bouar[2], Vladimir Esin[1], Benoît Appolaire[1].

[1]Université de Lorraine - CNRS / Institut Jean Lamour, Nancy, France.

[2]CNRS - Onera / Laboratoire d'Étude des Microstructures, Châtillon, France.

Electrical resistivity can be very effective in monitoring phase transformations and determining their kinetics. It is a particularly valuable technique when dilatometry is not sufficiently sensitive, such as in Ti alloys where the transformations do not involve significant volume changes. In general, the assumption of a simple mixing law between the resistivities of the coexisting phases gives good estimates of the phase fractions compared to in situ high energy X-ray diffraction (HEXRD). However, when the isothermal precipitation of the ω phase in a β-metastable Ti-15Mo alloy is monitored quantitatively, such a law fails to describe the evolution of the electrical resistivity. The present work shows that in such a case the interfaces should be taken into account for a reliable description of the transformation kinetics. In order to obtain accurate data on ω formation in Ti-15Mo, HEXRD experiments were first carried out at 300, 350 and 400 °C, followed by microstructural characterisation by TEM. Two stages were observed: growth and coarsening. Secondly, using the phase fractions as well as the mean precipitate size from the experimental study, a quantitative model is proposed to predict the evolution of the electrical resistivity during the different stages of ω precipitation. The model relies on the intrinsic ω and β resistivities and the ω/β interface resistivity as input parameters. A good agreement between the measured and calculated resistivities is obtained. This work thus demonstrates that the contribution of interfaces must be taken into account when applying electrical resistivimetry to the evolution of nanometric precipitates.

Non-conserved migration mode of semicoherent interfaces during precipitate growth. Jin-Yu Zhang[1, 2], Frédéric Mompiou[3], Shigenobu Ogata[1], Wen-Zheng Zhang[2].

[1]Osaka University, Osaka, Japan.

[2]Tsinghua University, Beijing, China.

[3]Université de Toulouse, Toulouse, France.

The property enhancement of many structural materials relies on the precise control of precipitate attributes - size, morphology, and distribution - achieved through various mechanical and heat treatments. Despite extensive research, many aspects of precipitate growth, which involves the migration of a two-phase interface, remain unclear. We study this process using atomistic simulations in diffusive time scale (such as phase field crystal and diffusive molecular dynamics) and theoretical analyses in a FCC/BCC and HCP/BCC system, in which interfaces are anisotropic and semicoherent. We unveil the intricate interplay between nucleation and motion of interfacial defects, together with fine details about the development of a characteristic lath morphology. Based on the O-lattice theory, we offer a novel explanation for the positioning of interfacial dislocation networks during migration. Our findings underscore the pivotal role of non-conservative dislocation motion in the nucleation and migration of growth ledges - a critical factor for the evolution of the precipitate morphology, which classical molecular dynamics simulations cannot model. The results are consistent with the observed crystallography of γ precipitates in duplex stainless steels and β precipitates in titanium alloys, where nano-sized growth ledges on facets are characterized by our in-situ TEM study. This comprehensive analysis of precipitate growth contributes to the quantitative description of interface migration in terms of dislocations and growth ledges, offering valuable insights towards understanding morphological evolution during phase transformations.

M1c.1-4: Additive manufacturing (I).

Invited. **3D-Printed heterostructured copper-iron composite manufactured by direct energy deposition.** Jairo Alberto Muñoz Bolaños[1], José María Cabrera Marrero[1], Pere Barriobero Vila[1], Rayan Nemmour [2].

[1]Polytechnic University of Catalunya, Barcelona, Spain.

[2]Université de Lorraine, Lorraine, France.

Through millions of years of evolution, natural materials have inspired the creation of functional metallic materials. This research seeks to delve into the development of advanced metallic materials with superior mechanical properties using bio-inspired designs aided by additive manufacturing processes. In this investigation, we produced a metallic composite that mimics the structure of the abalone shell combining layers of a Cu-Zr-Cr alloy with an austenitic stainless steel. It was found that the interfaces between soft and hard regions in the heterostructured metallic material exhibited an extra strengthening mechanism that needs to be optimized in order to solve the reported conflict between strength and ductility in metallic materials. Hence, this investigation delves into the study and comprehension of the mechanical performance and hardening mechanisms of a heterostructured metallic composite made of copper and stainless steel designed by additive manufacturing. Advanced characterization and manufacturing techniques such as electro-backscattering diffraction and direct energy deposition were used to reach this goal.

Robust design of additive manufacturable Ni superalloys. Hao Yu[1], Wei Xu[1], Sybrand Van der Zwaag[2].

[1]Northeastern University, Shenyang, China

[2]Delft University of Technology, Delft, Netherlands.

To achieve an effective design of additively manufacturable Ni superalloys with decent service performance, a hybrid computational design model has been developed, where the strategy to tailor local elemental segregations was integrated within a scheme of minimizing the cracking susceptibility. More specifically, the phase boundary of primary NbC / γ matrix was introduced into the design routine to tune the spatial distribution of critical solutes at an atomic scale, thereby inhibiting the formation of borides and segregation-induced cracking. Based on the output of the design, new grades of Ni superalloy have been developed with excellent additive manufacturability, as confirmed by the robustness of printing parameters in fabricating low-defect-density samples. The capability of the phase boundaries to evenly distribute boron atoms was validated experimentally, and the cracking induced by uncontrolled boron segregation at grain boundaries was effectively prevented. The newly designed alloys showed good tensile properties and decent oxidation resistance at different service temperatures, which are comparable to those of conventionally produced superalloys. The finding that phase boundaries can be employed to prevent undesirable clustering of boron atoms can be extended to manipulate the distributions of other critical elements, which provides a new path for designing novel Ni superalloys with balanced printability and mechanical properties.

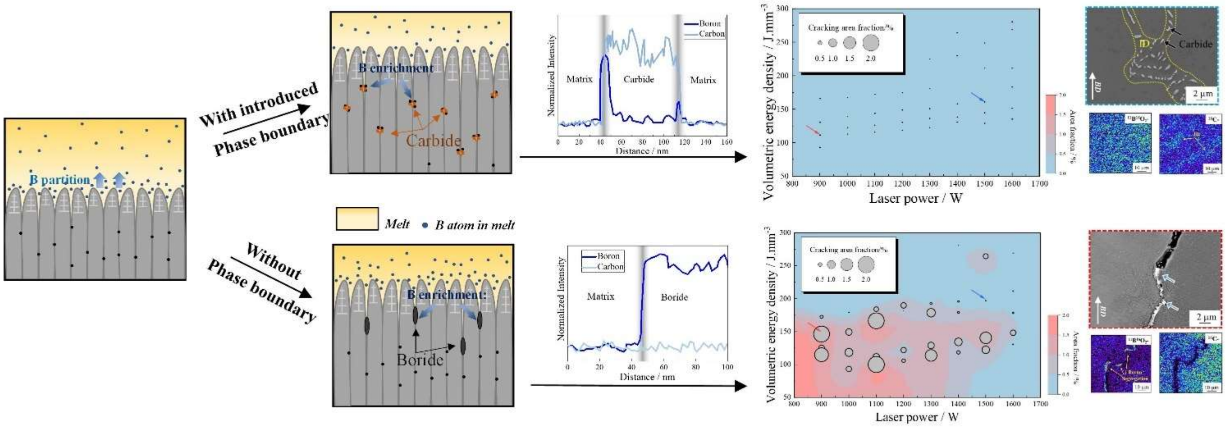

In-situ lamination during 3D printing of high silicon steel. Soran Birosca, Babak Haghighat.

University of Portsmouth, Portsmouth, United Kingdom.

Theorists, experimentalists, and industrialists have all acknowledged that further improvements of electrical steel (ES) magnetic properties with the current chemical composition and manufacturing routes is extremely challenging. However, to enable the prevailing vehicle and aircraft electrifications revolution, further developments in materials and electrical machine design are required. Today, additive manufacturing (AM) unlocks opportunities for novel machine designs and production of higher Si steels than previously available via standard manufacturing routes. However, challenges around their inferior magnetic properties remain to be overcome. Here, the in-situ lamination during 3D printing of 6.5%Si steel is demonstrated. The in-situ steel lamination via “Coating and Fusion” was conducted through a combination of powder coating and printing strategies that enabled a production of a near net shape laminated high Si steel. The Ar atomised 6.5 wt% Si steel powder was coated with Fe-(Mn,Zn) ferrite by sol-gel auto-combustion method and with SiO_2 by sol-gel method for comparison purposes. Various Ferrite/ES and SiO_2/ES ratios were explored to determine the desired coating thickness. The coated powder was fused in the ProX300 Laser Powder Bed Fusion to build successive and insulated layer by layer of high Si steel. The study highlights the need for extensive optimisation of coating compositions, thicknesses, and scanning strategies to refine the process. While *in-situ* lamination was successfully achieved, the coating layers were non-uniform and discontinuous. Preliminary results suggest that coating 6.5% Si electrical steel with $(Mn_{0.8},Zn_{0.2})\ Fe_2O_4$ improved its magnetic properties compared to conventionally printed 6.5% Si steel.

Additive manufacturing of G91 alloy by LPBF: parameter optimization, microstructural and mechanical characterization. E. E. Alvarado[1,2], Roger Castellote-Alvarez[1], Isaac Toda-Caraballo[1], Carlos Capdevila[1], Pilar Rey[3], Rebeca Hernández-Pascual[4], Antonio Fernández-Viña[4], Marta Serrano[4], David San-Martin[1].

[1]National Centre for Metallurgical Research, Madrid, Spain.

[2]Faculty of Chemistry of Complutense University of Madrid, Madrid, Spain.

[3]AIMEN Centro Tecnológico, Pontevedra, Spain.

[4]Centro de Investigaciones Energéticas, Medioambientales y Tecnológicas (CIEMAT), Madrid, Spain.

G91 steel is commonly employed in the manufacture of components for high-temperature applications in the energy sector, due to its excellent mechanical and thermal properties. As a result, it is also considered a candidate material for the fabrication of structural components in the next-generation of power plants. However, the conventional manufacturing processes typically used to produce these components limit the fabrication of complex geometries. Laser Powder Bed Fusion (LPBF) is an Additive Manufacturing (AM) technique that has been used to fabricate components in various alloys. Nevertheless, its viability for producing G91 steel components is still being investigated. This study investigates the fabrication of G91 steel samples via LPBF additive manufacturing. A comprehensive characterization of the G91 steel powders was conducted, assessing the flowability, microstructure and composition through a suite of complementary experimental techniques including X-ray fluorescence (XRF), inductively coupled plasma optical emission spectroscopy (ICP-OES), X-ray diffraction (XRD), scanning electron microscopy with energy dispersive spectroscopy (SEM/EDS), and electron probe microanalysis (EPMA). Following an in-depth optimization process aimed at minimizing porosity, the optimal printing parameters were identified: 150-200 W, 750-1000 mms^{-1}, 0.05 mm for hatch distance and 0.03 mm for layer thickness. The resulting printed microstructures were examined in both as-built and normalized conditions using optical microscopy (OM), SEM and XRD. The mechanical performance was evaluated through by microhardness and small-punch testing, providing insight into the properties of the material under these conditions.

M2a.1-4: Ferrite formation in steels (II).

Linking the Avrami model parameters for diffusional phase transformation kinetics for Fe-C-Mn alloys to composition, thermodynamic input, cooling conditions and 3D microstructural input.

Hussein Farahani[1, 2], Sybrand Zwaag[2].

[1] Tata Steel Research & Development, IJmuiden, The Netherlands.

[2] Delft University of Technology, Delft, The Netherlands.

The Avrami model, going back to 1942, is one of the oldest kinetics models to describe solid state reactions in metals, such as recrystallisation, precipitation and diffusional phase transformations. The model itself assumes a homogenous continuum as the starting conditions and makes prior assumptions regarding the nucleation behaviour and the shape of the new phases to form. While an elegant and simple model, the parameters of the Avrami model cannot a-priori be linked to the chemical composition, partitioning processes taking place at the moving ferrite-austenite interface, the cooling conditions, or features of the 3D starting microstructure, hence holds little to no predictive power. This not withstanding experimentally determined Avrami expressions have been used in the past as the key kinetic expression in the control of run-out table cooling installations. In the present work we use a recently published 3D mixed-mode multigrain model with efficient implementation of solute drag applied to austenite-ferrite phase transformations in Fe-C-Mn alloys (Acta Materialia 2021) to calculate the transformation kinetics for isochronal and isothermal conditions, for alloys with C concentrations ranging from 0 to 0.25 wt% and Mn concentrations ranging from 0 to 2.5% wt% and prior austenite grain sizes ranging from 10 to 300 micrometer. The kinetic curves are then fitted to a common variant of the Avrami expression. The changes in parameter values with composition, cooling conditions and starting microstructure are analysed and rationalised.

Coupled solute-drag effect in Fe-C-Mn V alloy. M.G. Mecozzi , S.E. Offerman.

Delft University of Technology, Delft, the Netherlands.

Different phenomena occur simultaneously during the austenite-to-ferrite transformation: the crystallographic lattice change, the partitioning of the alloying elements between the parent and the product phase and the segregation of the solute elements at the moving interface (called solute drag). In a multi-component system, more than one solute element may segregate at the interface. If the interaction with the interface of a solute component interferes with the segregation behaviour of the others, the Gibbs free energy dissipation resulting from the overall solute-drag may differ from the sum of the contributions of each solute element when it is present at the interface separately from the others. This work aims to study the “coupled” solute drag effect that results from the mutual interaction with the interface of manganese and vanadium in a quaternary Fe-C-Mn-V system. A solute-drag model, already applied in literature for a ternary system is modified and extended to a quaternary system. It was found that the Mn addition to the Fe-C-V system reduces the vanadium concentration at the interface and increases the overall Gibbs free energy dissipation. Moreover, the Mn segregation at the interface seems unaffected by the presence of vanadium. The effect of different values of the input parameters of the model on the co-segregation of manganese and vanadium at the interface is analysed and the possible impact on the VC precipitation at the interface is discussed.

Formation of nodular ferrite with interphase precipitation in vanadium-bearing Steels. Zhenqiang Wang[1], Yunxuan Wei[1], Yongjie Zhang[2], Goro Miyamoto[2], Tadashi Furuhara[2].

[1]Harbin Engineering University, Harbin, China.

[2]Tohoku University, Sendai, Japan.

Abnormal nodular ferrite (NF) characterized by a high density of low-angle boundaries was observed in vanadium-microalloyed low carbon steels, which is formed accompanied by interphase precipitation of VC after isothermal transformation at 600℃~690℃. Optical microscope (OM), electron backscattered diffraction (EBSD), transmission electron microscope (TEM), three-dimensional atom probe (3DAP) and nanoindentation were employed to systematically investigate the transformation behaviors of nodular ferrite, and the effects of isothermal temperature and chemical composition. NF formed in different alloys always has an irrational ferrite/austenite orientation relationship (OR) with angular deviation of 15-30 ° from the exact Kurdjumov-Sachs OR with its neighboring austenite grain into which it grows. Although there is no significant difference in number density of VC precipitates and nanohardness between NF and normal grain boundary ferrite, the growth of NF is substantially faster than the latter when compared in the same alloy. A single NF contains several ferrite regions, each of which was bordered by low-angle boundaries and contains a specific variant of VC formed by interphase precipitation. Decreasing the transformation temperature or increasing the V and C contents (i.e. increase in volume fraction of VC) promotes the formation of NF, indicating the strong influence of VC interphase precipitation on the ferrite morphology.

Quantitative evaluation of energy dissipation at migrating interface during ferrite transformation in Fe-C-Mn and Fe-C-Ni alloys. Kanon Sato[1], Yongjie Zhang[2], Hidenori Nako[3], Goro Miyamoto[2], Tadashi Furuhara[2].

[1] Tohoku University, Sendai, Japan.

[2] Institute for Materials Research, Tohoku University, Sendai, Japan.

[3] Kobe Steel, LTD. Kobe, Japan.

Understanding the ferrite growth kinetics is important for controlling microstructure of multi-phase steels. Driving force for ferrite growth is partially dissipated by local partitioning/segregation of alloying elements at migrating interface. In this study, ferrite growth behaviors with incoherent interface were quantitatively evaluated by applying decarburization treatment. Fe-0.77C-2.0Mn and Fe-0.62C-3.0Ni (mass%) alloys were decarburized at 973 K for various holding times up to 172.8 ks to induce one-dimensional ferrite growth from the surface. C concentration profiles across the ferrite/austenite interface were measured by FE-EPMA. The deviation of interfacial C content in austenite from paraequilibrium was used to evaluate the amount of energy dissipation. Macroscopic partitioning behaviors and interfacial local enrichment of substitutional alloying elements were analyzed by using FE-EPMA and 3D atom probe, respectively. In both alloys, ferrite grows without macroscopic partitioning of substitutional elements. In Fe-C-Mn alloy, the interfacial C content was almost constant at NPLE/PLE transition boundary and energy dissipation appeared to be independent of interface velocity within the observed range. A solute drag model suggests that reduction of solute drag effect (SDE) of Mn and an increase of the dissipation from local partitioning counterbalance each other, resulting in constant energy dissipation. On the other hand, in Fe-C-Ni alloy, the interfacial C content was always in between those predicted by paraequilibrium and NPLE even at later stages, indicating smaller SDE and slower evolution of Ni local partitioning compared to Mn. Furthermore, the energy dissipation was larger in the early stage with higher velocity, suggesting the influence of interface friction.

M2b.1-4: Ti alloys (II).

Novel shuffle transformations in metastable beta titanium alloys. Yufeng Zheng[1], Deepak Pillai[1], Rajarshi Banerjee[1], Dipankar Banerjee[2], Yunzhi Wang[3], Hamish Fraser[3].

[1] University of North Texas, Denton, United States.

[2] Indian Institute of Science, Bangalore, India.

[3] Ohio State University, Columbus, United States.

Shuffle transformation is a unique class of displacive solid-solid state phase transformation, involving the atom rearrangement within the unit cell, with little or no pure strain. An example is the bcc beta phase to hexagonal athermal omega phase transformation in metastable beta titanium alloys. During rapid cooling, this transformation occurs via a pure atom shuffle, every two of three adjacent {111} planes in the bcc lattice shifting towards their intermediate plane forming the hexagonal structure without atom diffusion. In this presentation, we will introduce our recent studies regarding two new shuffle transformations in metastable beta titanium alloys, named as beta to O' phase transformation and beta to incommensurate structure transformation, using conventional diffraction contrast transmission electron microscopy and z-contrast aberration-corrected scanning transmission electron microscopy. The mechanisms and the influences the solute concentration on these shuffle transformations will be introduced. Isomorphous stabilizers like Mo and Nb suppress the beta to omega transformation, instead promoting beta to O' phase transformation during rapid quenching, involving the shuffle of alternating {110} planes in the bcc lattice along the <1-10> direction, without solute diffusion. In contrast, eutectoid stabilizers like Fe induce an incommensurate structure through random atom shuffling, deviating from bcc lattice sites. The effects of thermomechanical treatments, including the isothermal aging and cold

rolling, on these transformations will be also discussed, highlighting their role in tuning the phase stability and microstructure evolution in metastable beta titanium alloys.

Effect of mechanical loading and temperature on the formation of stress-induced martensitic transformation in Ti-6242 titanium alloy. Muritala Arowolo[1,2], Vincent Velay[2], Vanessa Vidal[2], Moukrane Dehmas[3].

[1]CIRIMAT, Toulouse INP, Université de Toulouse, CNRS Toulouse 31030, France.

[2]Institut Clément Ader (ICA), Université de Toulouse, CNRS UMR 5312 IMT Mines Albi, INSA, ISAE-Supaéro, UPS France.

[3]CIRIMAT, Toulouse INP, Université de Toulouse, CNRS, Toulouse 31030, France Toulouse 31030, France.

Stress induced martensitic transformation (SIMT) is commonly reported in β metastable titanium alloy [1], however rarely reported in α+β titanium alloy [2]. The SIMT reported in the Ti-6246 loaded at room temperature up to 12% uniaxial strain was attributed to its high molybdenum content in the b phase. However, SIMT is hereby reported in Ti-6Al-2Sn-5Cr-2Mo (Ti-6242), a α+β titanium alloy characterized with low Mo of one-fifth of its critical content [1] subjected to uniaxial strain at 730°C. Consequently, the study aims to investigate the mechanisms underlying the formation of the a'' orthorhombic phase under thermomechanical loading. The microstructure evolution was monitored using in situ High Energy X-ray Diffraction (HEXRD), along with postmortem characterization thought SEM observation and EBSD analysis. Two different holding temperatures (730°C and 920°C) for a constant uniaxial strain rate were considered. The same heat treatment conditions without mechanical loading were also repeated for comparison. The combined analysis of Full Width at Half Maximum (FWHM) and lattice parameter revealed more pronounced variations in the b phase at 730°C under mechanical loading compared to 920°C. In addition, anisotropic elastic behaviour of the α phase during mechanical loading at 730°C was clearly observed. The strain induced by the mechanical loading in the b phase caused the decomposition of the b phase upon rapid cooling from 730°C, leading to the precipitation of a'' orthorhombic phase. In the absence of mechanical loading, the a'' orthorhombic phase was not detected.

[1] Kolli, R.P., Devaraj, A.: https://doi.org/10.3390/met8070506

[2] Kapoor, K., et al, 2020 https://doi.org/10.1016/J.MATCHAR.2020.110410

Phase transformation kinetics during rapid heating of Ti-5553 titanium alloy with different initial microstructures. Dehmas[1], Chanfeau[1], Poquillon[1], Strak[2], Maawad[2].

[1] CIRIMAT, Toulouse, France.

[2] Helmholtz-Zentrum Hereon, Geesthacht, Germany.

Production and machining of titanium alloy are difficult as it involves a complex combination of high loading and rapid temperature evolution. To enhance the machinability of titanium alloys, it is essential to study the phase transformation involved under rapid heating across various initial microstructures. These initial microstructures exhibit α-phase ratios, varied morphologies and characteristic precipitate sizes ranging from tens of nanometers to several micrometers. Phase transformation on heating was tracked in situ with high energy synchrotron diffraction (PETRA III, DESY). Rapid heating at 10, 50 and 100 °C.s^{-1} from room temperature to 1050 °C were considered. Phase transformation during heating was studied by a combined analysis of the microstructural features that are: mass fractions, mean lattice parameters and full width at half maximum (FWHM) of the two phases, which were determined by Rietveld refinement. The monitoring of mass fractions compared to equilibrium calculations (ThermoCalc) revealed a shift of the transformation domain towards high temperatures when the heating rate increased. Furthermore, a change in the transformation kinetics was evidenced whose origin was discussed in terms of differences between the nodular and lamellar morphologies of the α phase. The combined analysis of mean lattice parameters and full width at half maximum suggested that the α+β→β phase transformation on heating was controlled by the diffusion of molybdenum with the β phase inheriting the solute content of the adjacent parent α phase, leading to chemical heterogeneities in the β phase field regardless of the considered heating rate.

Alloy design of α +β titanium alloys to achieve high damage tolerance through increased the work-hardening. Harena Rakotozafy[1,2], Loïc Malet[1], Astrid LEenain[3], Frédéric Prima[2], Stéphane Godet[1].

[1] Université Libre de Bruxelles, Brussels, Belgium.

[2] Université Paris Sciences et Lettres (PSL), Paris, France.

[3] SAFRAN, Milmort, Belgium.

α + β titanium alloys are frequently chosen in the aerospace industry due to their high specific strength; however, they exhibit a low work-hardening capacity. This suggests that the capacity of these alloys to tolerate damage is limited. However, these alloys are anticipated to be produced by additive manufacturing, in order to reduce production costs, which are usually associated with the formation of defects arising during the manufacturing process. This study demonstrates that the generation of either a full hexagonal α' or α + α' dual-phase microstructure, obtained by rapidly cooling several α + β titanium alloys, enables the achievement of high strength and high work-hardening. Therefore, high damage tolerance is obtained through increased work-hardening. This is made possible by the triggering of Reorientation Induced Plasticity (RIP) α' martensite in both microstructures during the deformation process. Specifically, the expansion of one lath of martensite is achieved at the expense of the others under stress. This mechanism is enabled by the presence of the intervariant [4 -5 1 -3]α' Type II twin, which ensures a high level of strain hardening. However, the mobility of this twin is contingent upon the Molybdenum equivalent (Moeq) value of the α'. Consequently, it is possible to produce a heterogeneous microstructure with a varying composition of β-stabiliser, thereby enhancing the yield strength. This permits the design of new α + β titanium alloys in which the effect of grain size, phase proportions and chemical compositions on the mechanical properties can be evaluated.

M2c.1-2: Additive manufacturing (II).

AlCrFeMnNi: the next-generation FCC high-entropy alloys processed by additive manufacturing for nuclear structural applications. Castellote-Alvarez[1, 2], Toda-Caraballo[1], Fernández-Jiménez[1, 2], Petersson[3], Szakalos[3], Molina-Aldareguia[4, 5], San-Martin[1].

[1] National Center for Metallurgical Research (CENIM-CSIC), Madrid, Spain.

[2] Complutense University of Madrid (UCM), Madrid, Spain.

[3] Royal Institute of Technology (KTH), Stockholm, Sweden.

[4]IMDEA Materials Institute, Getafe, Spain.

[5]Technical University of Madrid (UPM), Madrid, Spain.

A Co-Free AlCrFeMnNi High Entropy Alloy (HEA) was designed to obtain an FCC crystalline structure and withstand the extreme environments found in Gen IV nuclear reactors, including exposure to molten lead, lead-bismuth eutectic (LBE), and molten salts. The addition of aluminum in relatively low amounts contributes to the solid solution strengthening, without altering its FCC structure in a wide range of temperatures (720-1350 °C), but more importantly, to promote the formation of a stable, protective alumina scale at high temperatures, enhancing the corrosion resistance of the alloy. Additionally, this HEA was optimized to minimize the hot cracking characteristic of FCC alloys processed through Laser Powder Bed Fusion (LPBF). This work outlines the computational methodology employed in the alloy design, with the assistance of high-throughput thermodynamic calculations, to fulfil the designing criteria. It also describes microstructural characterization (SEM, XRD, EBSD), mechanical characterization (compression tests) and elemental distribution (EPMA) in the as-built condition using the most adequate printing parameters for which porosity and crack formation was avoided. Besides, to test the ability of the alloy to form an alumina scale and its stability during exposure to Heavy Liquid Metals (HLM), the alloy was also exposed to oxygen-containing molten Pb up to 1128 h at 550 and 650 °C inside a controlled chamber. This way the self-healing properties of the alumina scale and the embrittlement resistance of the alloy were evaluated under operating conditions of Liquid Metal Cooled Reactors (LMR).

Role of massive precipitation on multiple deformation mechanisms of additively manufactured FeCrNiAlTi alloy. Xiaopei Wang[1], Wenhua Wu[2], Hao Chen[2].

[1] University of Science and Technology Beijing, Beijing, China.

[2] Tsinghua University, Beijing, China.

Massive precipitation is commonly employed in FCC alloy to enhance their strength across a broad temperature spectrum, while this often results in a reduction in ductility. Nevertheless, this outcome is not inevitable, as the characteristic deformation mechanisms in FCC alloys, namely the formation of stacking faults (SFs) and twinning, can be promoted by massive precipitation. In this study, we developed an FeCrNiAlTi FCC alloy via laser additive manufacturing, demonstrating superior performance from room to cryogenic temperatures. This enhancement is achieved by the introduction of a high density of both incoherent and coherent precipitates within the grains and facilitating the generation of numerous nano-scale SFs/twins during deformation. It is found that massive precipitation reduces the stacking fault energy of matrix by altering its composition, thereby fostering the creation of SFs/twins. Moreover, the local strain heterogeneity significantly influences the formation of SFs/twins. As the precipitates size and spacing increase, the local strain heterogeneity intensifies, which in turn enhances the ductility by generating more nano-scale SFs/twins. On the other hand, the interfacial misfit of the precipitates mitigates the local strain heterogeneity, which exerts a negative effect on the formation of SFs/twins. However, due to the minimal interfacial misfit between $L1_2$ phase and FCC matrix, the impact of interfacial misfit remains marginal, while the size and spacing of precipitates predominantly govern the local strain heterogeneity. By judiciously modulating the extent of precipitation within FCC grains, the strength and ductility can be elevated concurrently across a broad temperature span.

M3a.1-4: Ferrite formation in steels (III).

In-situ investigations on the dynamic transformation in steel near the Ae3. Arina DeBoer[1], Imed-Eddine Benrabah[2], Cecile Rampelberg[1,3], Guillaume Geandier[2], Hatem Zurob[1].

[1] McMaster University, Hamilton, Canada.

[2] Université de Lorraine, Nancy, France.

[3] CanmetMATERIALS, Natural Resources Canada, Hamilton, Canada.

Thermomechanical processing uses controlled deformation at high temperatures to refine the microstructure of ferrous alloys. Deformation at high temperatures incurs dynamic recrystallization and dynamic recovery, but in the 1980s, Matsumura and Yada [1] noticed significant grain refinement for rolling passes near the ferrite transformation temperatures and attributed this to a new phenomenon, called dynamic transformation (DT): the austenite to ferrite transformation during deformation. Few direct observations of DT have been reported above the para-equilibrium temperature (Ap3) [2,3] and it is difficult to distinguish between this dynamic ferrite and ferrite which transforms during cooling, deformation-induced ferrite transformation (DIFT), by traditional methods. In-situ high energy x-ray diffraction (HEXRD) experiments were carried out to directly observe DT near the ortho-equilibrium transformation temperature (Ae3). The results of tests for a Fe-0.1C-6Ni (wt%) model alloy show, contrary to reports from the literature, that there is no DT above the Ae3 temperature. At temperatures near the Ap3, there is DT at low strain rates and ferrite is detected after the end of deformation for high strain rates (DIFT). Discrepancies between ferrite fractions observed during high temperature deformation and those observed at room temperature are attributed to accelerated ferrite precipitation during cooling.

[1] Y.M. Matsumura, H. Yada, Trans. Iron Steel Inst. Jpn. 27 (1987) 492–498.

[2] H. Yada, C.-M. Li, H. Yamagata, ISIJ Int. 40 (2000) 7.

[3] C. Aranas, S. Rodrigues, F. Siciliano, J. Jonas, Scr. Mater. 177 (2020) 86–90.

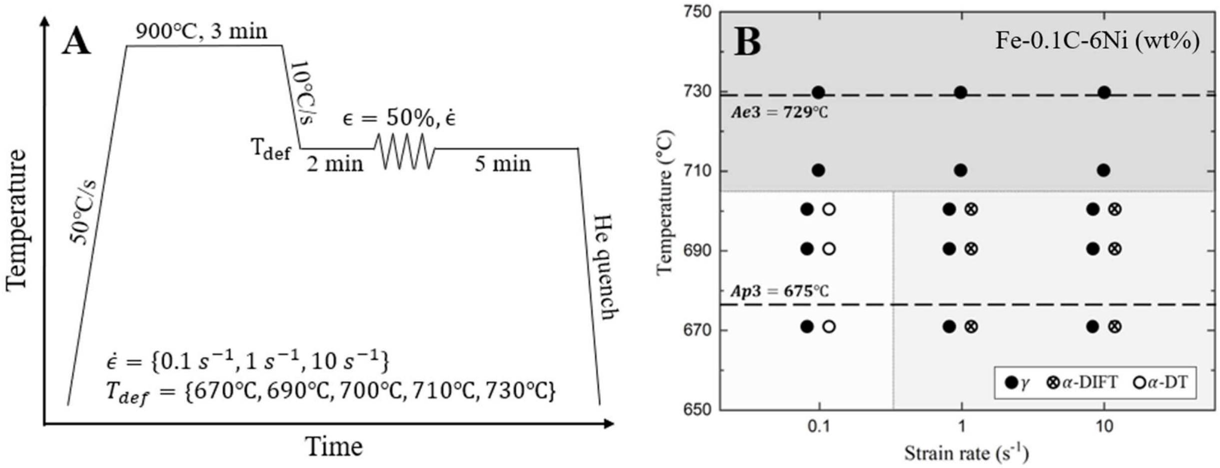

Figure 1: (a) HEXRD experimental parameters and (b) phase portraits observed for each condition.

Development of a machine learning model to predict phase transformation(s) from dilatometer data for application to laminar cooling of hot rolled steel. Jarrod Angove[1], J. Barry Wiskel[1], Chad Cathcart[2], Tihe Zhou[2], Azin Mehrabi[2], Hani Henein[1].

[1]University of Alberta, Edmonton, Canada.

[2]Stelco, Hamilton, Canada.

The austenite to ferrite transformation during laminar cooling has a significant impact on both the strength and toughness of hot rolled steel via its effect on the amount and type/morphology of phase(s) that can form during the transformation. Quantitative transformation information is generally obtained from dilatometer testing. A limitation of this method is the relatively low number of cooling rates that are typically tested for a single composition of steel. The objective of this work will be to develop a Machine Learning Model (MLM) capable of predicting austenite decomposition for any cooling rate encountered during laminar cooling and for any composition within the range of the training data. The MLM proposed in this work is a modified Gaussian Process model that utilises a similarity metric between thermal histories. The initial scope of the work will focus on predicting the amount and type of phase(s) formed for a single composition of steel subjected to the complex temperature profile encountered during laminar cooling.

Phase field modelling of α/γ interface migration under non-equilibrium conditions in Fe-C-Mn alloy. Luyao Fan[1,2], Yongjie Zhang[1], Goro Miyamoto[1], Tadashi Furuhara[1], Hao Chen[2].

[1] Tohoku University, Sendai, Japan.

[2] Tsinghua University, Beijing, China.

A phase field model (PFM) considering the diffusion of both C and Mn is developed to simulate the α/γ interface migration in Fe-C-Mn alloy. When compared with DICTRA simulation using same thermo-kinetic data, the two methods are consistent in the predictions of γ growth in binary Fe-C and Fe-Mn alloys except that PFM predicts a partitionless (massive) growth while DICTRA simulation predicts partitioning one in Fe-Mn alloy under high supersaturation. For ternary alloy, Mn-partitionless growth can be reproduced by both methods but the predictions of Mn spike are different. For DICTRA simulation, the instant establishment of equal chemical potential at interface is the first principle. As for PFM, since the reduction of system energy is the first priority without restriction on interfacial composition, that high Mn spike predicted by DICTRA simulation is not preferred. Therefore, PFM predicts postponed transition from Mn-partitionless to Mn-partitioning growth compared with DICTRA simulation. The kinetic transition predicted by PFM is shown to occur when Mn partitioning begins to reduce the system energy more efficiently than C partitioning. PFM is then applied to γ to α transformation where kinetic transition plays a crucial role in determining α fraction with further consideration of solute drag effect (SDE). SDE appears to promote the kinetic transition and cause the final α fraction to deviate from the PE prediction, but SDE retarding interface migration kinetics is not so significant as expected (Fig.1(a)). This is because kinetic transition can occur suddenly before SDE starts to play a significant role (Fig.1(b)).

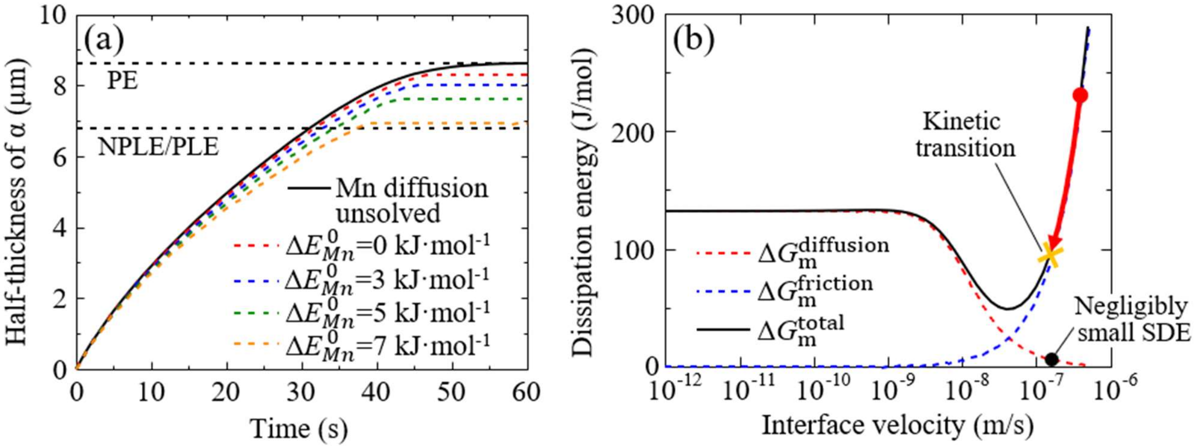

Fig. 1 (a) Simulated growth kinetics of α in Fe-0.1C-1.5Mn alloy (mass%) at 973 K and (b) the calculated dissipation energies.

So long and thanks for the memory: non-diffusive interface behaviour in the presence of solute. Chad Sinclair.

University of British Columbia, Vancouver, Canada.

Traditionally the motion of interfaces assumes linear response theory, where driving force is proportional to force via mobility. The detailed atomic processes involved in the motion of the mean interface position are coarse grained allowing for predictions on practically relevant length and timescales. This process of coarse graining, however, can introduce a time dependent memory effect that appears on short timescales - timescales that are achieved, for example, in molecular dynamics (MD) simulations. This appears as transient sub-diffusive behaviour where one would otherwise expect purely diffusive kinetics. Here we introduce the idea of a generalized master equation approach to quantify this memory and to extrapolate short MD trajectories to get at the long time diffusive behaviour required for linear response. Here we illustrate this method using solute-grain boundary effects described via a simplified kMC model and Fe-C MD simulations.

M3b.1-5. Ti alloys (III).

In situ observation of microstructure evolution in Ti-6Al-4V fabricated by micro-laser powder bed fusion upon annealing. Dayong An.

Shanghai Jiao Tong University, Shanghai, China.

As one of the most widely used titanium alloy, extensive investigations have been performed to reveal the microstructure and mechanical properties of Ti-6Al-4V alloy manufactured via additive manufacturing (AM) techniques. The rapid cooling rate and complex thermal history of AM process lead to a characteristic microstructure dominated by acicular α’ structure associated with dislocations or/and twins and columnar grains. This results ine AMed Ti-6Al-4V exhibiting higher strength but reduced ductility compared to their counterparts. Post-process annealing is a common approach to tailor these mechanical properties, making it critical to understand the mechanisms of microstructure evolution during annealing and their influence on performance. In this study, quasi in-situ characterizations, including electron channeling contrast imaging (ECCI) and electron backscatter diffraction (EBSD), were performed to track the evolution of non-equilibrium solidification microstructures in Ti-6Al-4V manufactured via micro laser powder bed fusion. The as-built microstructure revealed extensive twins and dislocations. Upon annealing, α' martensite decomposed into α and β phases, with β preferentially nucleating at twin and grain boundary intersections. Annealing at 900℃ resulted in the formation of secondary α within grains and grain boundary α at triple junctions. Furthermore, the orientation relationships of the phase transformations during annealing were elucidated. These findings provide valuable insights into tailoring the microstructure and mechanical properties of AM-produced Ti-6Al-4V through thermal treatments.

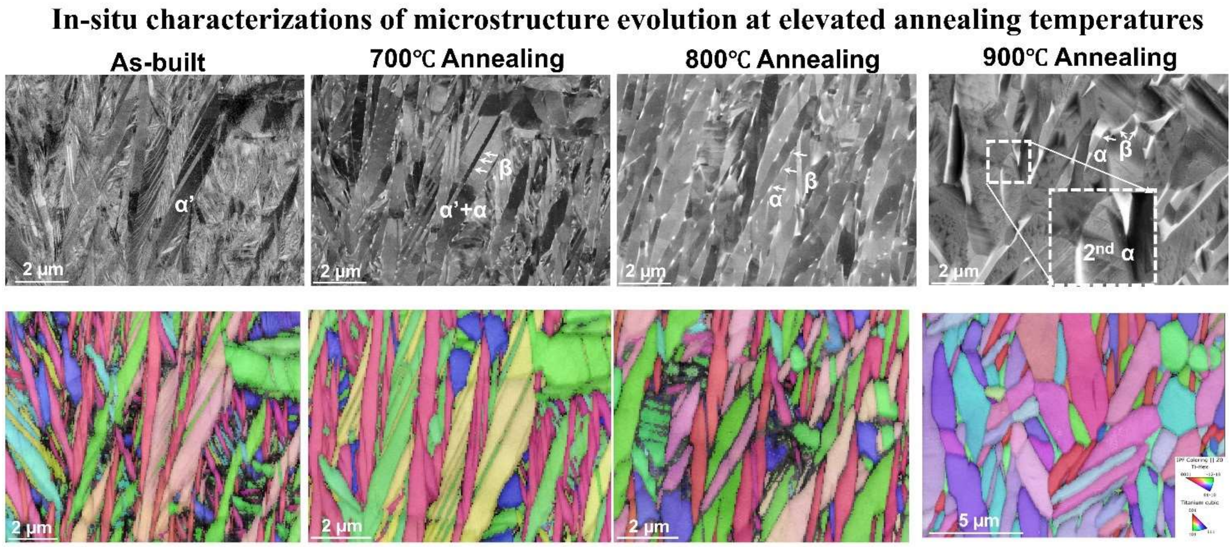

New phase transition mechanism for the multiscale precipitation design in titanium alloys and performance enhancement. Dong Wang[1], Mengyuan Hao[1], Yufeng Zheng[2], Yunzhi Wang[3].

[1]Xi'an Jiaotong University, Xi'an, China.

[2]University of North Texas, Denton, United States.

[3]The Ohio state University, Columbus, United States.

The precipitation and its corresponding microstructure in titanium alloys have a significant impact on comprehensive mechanical performance. Alloying and heat treatment processes are the primary means of regulating titanium alloy microstructures and optimizing mechanical properties. The presenter conducted research using coupled thermodynamic databases, phase-field dynamic simulations, and experimental characterization to investigate the influence of alloy composition, heat treatment temperature, and cooling rate on the microstructure of titanium alloys. At low-temperature aging and near the critical alloy composition, a novel phase transition mechanism with high nucleation density and fine precipitate size, termed pseudoquenching decomposition, was discovered. By designing multi-step aging, primary precipitate phase dissolution, and controlling the cooling rate, an effective approach based on the pseudoquenching decomposition mechanism was proposed for designing multi-scale microstructures in titanium alloys. This approach further guided experimental design to achieve corresponding multi-scale microstructures in titanium alloys and improve their strength and toughness.

Nanotwinned α precipitates in metastable β titanium alloys induced by variant assembly during β to α phase transformation. Jiaqiang Chang, Yingna Wu, Zhenbo Zhang.

Centre for Adaptive System Engineering, Shanghai, China.

Nanotwinned microstructures are expected to break the strength-ductility trade-off. However, the fabrication of nanotwinned microstructures in duplex titanium alloys without the introduction of detrimental residual stress presents a considerable challenge. Here we introduce the mechanism of a novel nanotwinned α precipitation that occurs during the β to α-phase transformation in aging treatment. High-resolution transmission electron microscopy reveals that serpentine α-laths form through β-phase separation (β → β' + β), with α-phase nucleation initiating at zigzag interfaces of metastable β' domains enriched in α-phase stabilizing elements. Three α-phase variants, oriented at <11-20> /60° axis-angle pairs, coalesce into {10-11} nanotwins in size of proximately 8 nm. These α-laths assemble brick-by-brick, with twin lamellae directionally stacking along β' precursors. The β' phase templating effect provides preferential nucleation sites and growth pathways for α-variants, suppressing conventional self-assembly effects that promote 3-variant cluster and impede continuous twin formation. Our works establish a foundation for developing structural materials with unique microstructures and exceptional properties.

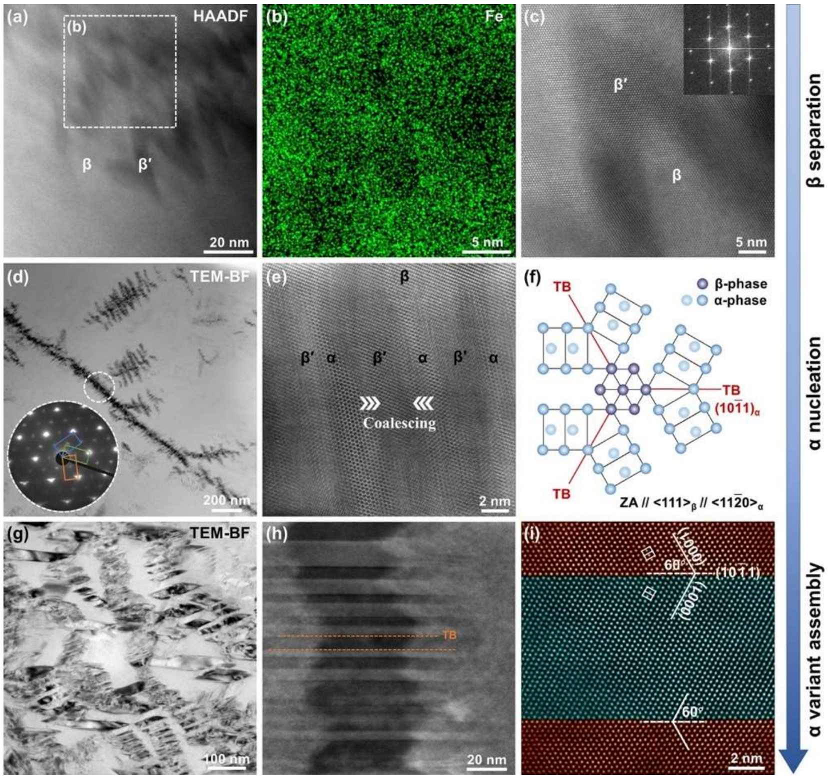

Phase transformation during aging treatment: (a-c) β phase separation; (d-f) α precipitate nucleation; (g-i) α variants coalescing to form nanotwins.

Novel high-temperature Ti-alloy for enhanced wire-based directed energy deposition applications.

Ehsan Farabi[1], David Obersteiner[2], Michael Musi[2], José Neves[3], Thomas Klein[3], Sophie Primig[1].

[1]UNSW Sydney, Sydney, Australia.

[2]Montanuniversität Leoben, Leoben. Austria.

[3]AIT Austrian Institute of Technology, Ranshofen, Austria.

This study presents a novel high-temperature Ti-alloy designed for wire-based directed energy deposition (waDED) processes for various applications in the aerospace and energy industries. While high-strength Ti-alloys for waDED have been extensively researched, high-temperature variants are yet to be designed, even though aerospace and energy components commonly operate at elevated temperatures. Current waDED techniques often introduce significant heterogeneity and anisotropy in mechanical properties, as seen in existing alloys like Ti-6Al-2Sn-4Zr-2Mo. Our novel alloy combines additions of Si, Cu, Nb, and Y. It seeks to improve high-temperature performance by leveraging phase transformations and precipitation to achieve fine, homogeneous microstructures during additive manufacturing. We investigate the microstructural evolution during simulated waDED solidification and various heat treatments associated with cyclic reheating. Our developed alloy exhibits refined, equiaxed β grains post-heat treatment. Y inhibits β grain growth, transforming the microstructure from a fine lath-like colony α-phase to a coarse lamellar structure. High-resolution atom probe microscopy reveals very fine (15–20 nm) core-shell Ti_2Cu precipitates with Y cores, significantly enhancing mechanical performance despite microstructure coarsening during the heat treatment. Our developed alloy shows substantial promise for high-deposition-rate waDED processes, offering improved high-temperature capabilities.

Unveil the kinetics of eutectoid decomposition in additively manufactured Ti-8.5Cu alloy using in situ synchrotron X-ray diffraction. Dong Qiu[1], Zherui Tong[1], Yunhui Chen[1], Jayshri Dumbre[1], Nathalie Isac[2], Mark Easton[1], Manas Upadhyay[2].

[1]RMIT University, Melbourne, Australia.

[2]Institut Polytechnique de Paris, Paris, France.

Tracking phase transformations and microstructure evolution during the rapid heating and cooling cycles of metal additive manufacturing (AM) processes remains a significant challenge. This difficulty is compounded when continuous cooling transformation (CCT) curves are unavailable, as seen in the case of eutectoid decomposition in Ti-Cu alloys (β-Ti → α-Ti + Ti_2Cu). This eutectoid decomposition occurs so rapidly that it cannot be suppressed even by water quenching. Conventional volume dilatometry, with cooling rates usually limited to 0.1–10 K/s, is inadequate for capturing the fast kinetics of this process. To overcome this limitation, in this study, we utilized synchrotron X-ray diffraction (SXRD) to monitor phase evolution *in situ* during the laser direct-energy deposition (L-DED) of Ti-8.5Cu alloy. With its high time resolution (0.01 s), angular resolution (0.01°), and spatial resolution (~100 μm), SXRD provides an ideal platform for experimentally determining the CCT curves of eutectoid decomposition in the L-DED Ti-8.5Cu alloy (Figure 1). Furthermore, the kinetics of eutectoid dissolution (α-Ti + Ti_2Cu → β-Ti) were also characterized during rapid heating cycles. Additional insights, including the evolution of texture, the prior b-Ti grain size, and total dislocation density during the intrinsic thermal cycles are also investigated using the Williamson-Hall approach.

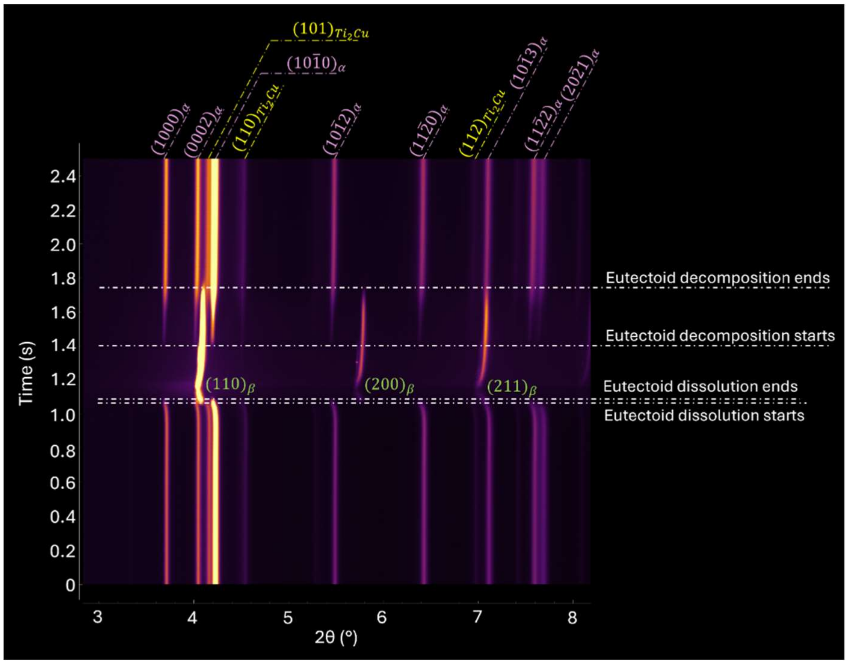

The Synchrotron XRD spectrum showing the evolution of phase constituents through a typical thermal cycle of L-DED Ti-8.5Cu alloy.

M3c.1-5: Additive manufacturing (III).

Refining the microstructure of a layered stainless steel by selective laser. Lucia Morales-Rivas.

National Center for Metallurgical Research (CENIM-CSIC), Madrid, Spain.

Additive manufacturing (AM) is driving metallurgists to design new alloys and complex microstructures. One of the main restrictions of AM is that, in general, it is not intended for a subsequent thermomechanical process. This motivates the study of alternative hardening methods based on pure heat treatments. This work proposes the design and manufacturing of new stainless steels by selective laser melting, in line with the following alloying and microstructural strategies: reduction of nickel content and mechanical composite behavior conferred by a layered structure. The intrinsic heat treatments during the manufacturing process will be explored in order to achieve a controlled microstructural refinement, and, consequently, improved mechanical properties. This work has been funded by the "ComFuturo Third Edition" Programme, supported by the MSCA-COFUND Agreement No. 101034263.

Phase field simulations to elucidate residual ferrite fractions in wire-based additive manufacturing of 316L. Markus Apel, Oleg Stryzhyboroda.

Access e.V. Aachen, Germany.

The austenitic stainless steel 316L is being widely investigated as a material for additive manufacturing. Compared to powder-based processes, wire-based additive manufacturing, e.g. wire arc (WAAM) or wire laser (WLAM) offer higher build rates and are therefore promising for the production of larger parts. The local thermal conditions around the solidifying melt pool, i.e. cooling rate and thermal gradient, vary by several orders of magnitude for the different processes. In addition, the local cooling path also depends on the part geometry and printing position, i.e. is also not constant throughout a single build process. Eventually, the variations in temperature history pose a severe challenge to the control of material properties. The microstructure of AM build 316L is determined by dendritic solidification and subsequent solid-state transformation, both of which occur under conditions far from equilibrium. According to CALPHAD thermodynamic calculations using the TCFE13 database from Thermo-Calc, 316L solidifies by peritectic solidification, starting with primary delta-ferrite followed by austenite. Gulliver-Scheil calculations predict approximately 55% primary delta-ferrite at the end of solidification. Experimentally, it has been found that for WAAM or WLAM processing, the ferrite fraction in as-built samples varies between 5% and 16%, correlating with the estimated cooling rate. We have visualized the microstructure formation by CALPHAD coupled phase field simulations using the MICRESS software and rationalize that the resulting ferrite fraction is determined by the ferrite-austenite solid state transformation and the temperature dependent interfacial mobility is the critical open material parameter to match the simulation results with experimental findings.

Delta-ferrite to austenite phase transformation pathways and mechanical properties in 2205 duplex stainless steels manufactured via laser powder bed fusion. Xinyi He[1], Zipeng Xu[2], Charlie Kong[3], Hao Wang[4], Xiaozhou Liao[5], Gregory Rohrer[2], Simon Ringer[5], Nima Haghdadi[6], Sophie Primig[1].

[1]School of Materials Science & Engineering, UNSW Sydney NSW 2025, Australia.

[2]Department of Materials Science and Engineering, Carnegie Mellon University, Pittsburgh, PA 15213-3890 United States.

[3]Electron Microscope Unit, Mark Wainwright Analytical Centre, UNSW, Sydney NSW 2052 Australia.

[4]Department of Materials Science and Engineering, Monash University, Victoria 3800, Australia.

[5]The University of Sydney, NSW 2006, Australia.

[6]Department of Materials, Imperial College London, London SW7 2AZ, United Kingdom.

Recent advancements in metal additive manufacturing (AM), such as laser powder bed fusion (LPBF), enable the net-shaped production of complex engineering components from multi-phase alloys such as duplex stainless steels (DSSs). DSSs are known for their mechanical properties and corrosion resistance, attributed to their equilibrium delta-ferrite and austenite microstructures. However, the rapid cooling during LPBF leads to a predominantly delta-ferritic, non-equilibrium microstructure with reduced ductility due to high densities of dislocations and Cr_2N precipitates. A short heat treatment induces various types of austenite (intergranular, instability-induced, sympathetic, and intragranular), refining the microstructure and achieving enhanced ductility. Through 3D EBSD, we study the delta-ferrite to austenite phase transformation mechanisms and interphase boundaries. We observe that the higher-energy (crystallographically irrational) interfaces have lower grain boundary curvatures, deviating from the expected inverse correlation between grain boundary energy and curvature. This may be caused by the interplay between strain energy minimization and interfacial energy minimization during the phase transformation. Multi-scale characterization reveals a combination of deformation mechanisms, including deformation induced nano-twinning and martensitic transformation, contributing to improved ductility and work-hardening. These findings demonstrate the potential of AM and post-processing to tailor duplex microstructures with desired properties via leveraging the microstructural complexities and solid-state phase transformations.

Multiscale microstructure of an AlxFe1-x alloy manufactured by the L-PBF process. Yann Le Bouar[1], Louise Toualbi[2], Frédéric Fossard[1], Jean-Sébastien Mérot[1], Pauline Stricot[2], Simon Fritz[2], Eric Grévin[1], Agnès Bachelier-Locq[2], Nicolas Horezan[2], Quentin Barres[2], Yves Renollet[2], Aidar Zakirov[3], Williams Lefebvre[3]

[1]Université Paris-Saclay, ONERA, CNRS, Laboratoire d'Etude des Microstructures, Châtillon, France.

[2]Université Paris-Saclay, ONERA, DMAS Châtillon, France.

[3]University of Rouen, CNRS UMR 6634, Groupe de Physique des Matériaux, Saint-Etienne du Rouvray, France.

The recent development of Additive Manufacturing (AM) processes has made it possible to produce parts with complex geometries that are difficult to manufacture using conventional manufacturing methods. However, AM results in microstructures and metallurgical states that are different from those achieved with traditional processes. There is therefore a need to develop new alloy grades specifically for AM to exploit the unique characteristics of these manufacturing processes. We are interested in lightweight aluminum-based alloys, and in particular in the use of iron solute to harden the alloy, which is made possible by the very rapid solidification of the Laser-Powder Bed Fusion (L-PBF) process. More specifically, we have considered model binary Al_x-Fe_{1-x} alloys, which exhibit a remarkable hardening in the as-built state. To explain this behavior, we have carried out a detailed characterization of the multiscale microstructure (Figure 1) using optical microscopy, scanning electron microscopy (SEM), transmission electron microscopy and tomographic atom probe. In particular, extensive experimental characterization of the solidification cell has been carried out as a function of the position within the melt pools. We have thus determined the size of the cells and the composition of the cell interior, two characteristics that largely control the yield strength of the material. We also used the recent STEM-4D technique, which enabled us to show that cell edges have an unexpected structure, formed of a polycrystalline metastable phase with nanometric grains. Finally, the heterogeneity of the mechanical behavior is highlighted by performing nano-indentation tests as well as in-situ SEM tensile tests.

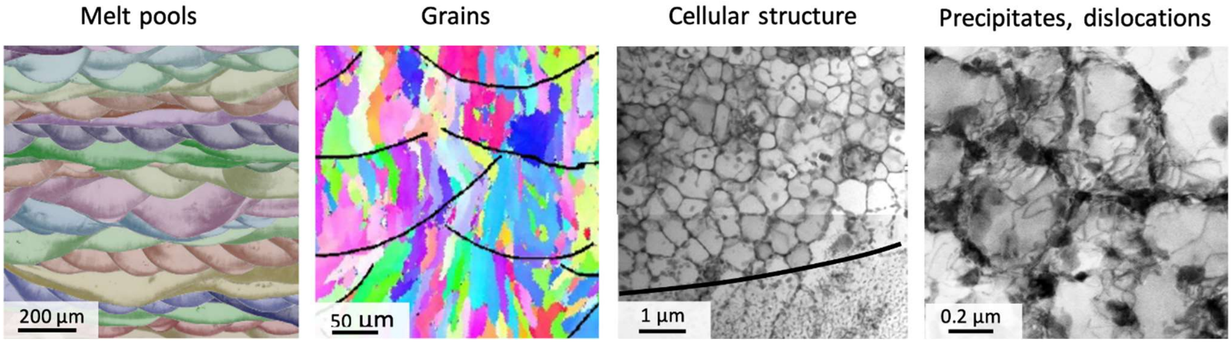

Enhancing additive manufacturing of recycled AA7075: titanium-coated powders for crack-free aerospace components. Romain Giaux[1], Loïc Malet[1], Thomas Kairet[2], Thomas Godfroid[3], Stéphane Godet[1].

[1]Université Libre de Bruxelles, Brussels, Belgium.

[2]Sirris, Seraing, Belgium.

[3]Materia Nova, Mons, Belgium.

Aluminium alloys such as AA7075 are widely employed in aerospace applications due to their elevated strength-to-weight ratio, robust resistance to crack initiation and propagation, minimal operating costs, and commendable corrosion resistance. As an increasing number of aircraft reach the end of their operational lives each year, the aerospace industry is presented with a significant opportunity to recycle and reuse AA7075 in the construction of new-generation aircraft. Additive manufacturing (AM) techniques, in particular selective laser melting (SLM), have been the subject of extensive investigation with a view to establishing their capacity to produce intricate three-dimensional components with exceptional mechanical properties. It would be optimal if retired AA7075 parts could be gas vaporised into a fine powder for use in SLM to fabricate new components. However, the high cracking tendencies of AA7075 present a significant challenge for SLM processing, rendering the parts unsuitable for aerospace applications. A novel strategy combining substrate modification and inoculation treatment has been proposed as a means of producing crack-free, dense, high-strength AA7075 via SLM. This strategy involves coating the alloy powder with titanium, which substantially refines the Al grains during the printing process, effectively increasing the cracking resistance. The refining mechanism, as well as the influence of different solution heat treatments on the microstructure and mechanical properties, will be presented here. Additionally, novel observations about the formation of the refining Ti particles, as well as the corrosion behaviour of this material, will be discussed.

Plenary 2. Phase transformations in chemically heterogenous steels. Hao Chen.

Tsinghua university, Beijing, China.

Steels are inherently chemically heterogeneous materials, exhibiting multi-scale chemical heterogeneities that arise from processes such as solidification segregation, spinodal decomposition, and alloying element partitioning during solid-state phase transformations. Recent advancements have demonstrated the potential to harness this chemical heterogeneity to manipulate phase transformation behavior and tailor microstructures in various types of steels, leading to substantial improvements in mechanical properties. In this presentation, we will present several examples where chemical heterogeneity has been strategically employed to achieve tailored phase transformations and microstructural optimization in steels. Additionally, we will delve into a detailed discussion on the mechanistic role of chemical heterogeneity in phase transformation behavior.

Tuesday, July 8

Plenary 3. Science-based advanced manufacturing of metals and alloys. Amy Clarke[1,2].

[1] Los Alamos National Laboratory, Sigma Manufacturing Science Division Los Alamos United States.

[2] Colorado School of Mines, Department of Metallurgical and Materials Engineering Golden United States

Solidification is the first step encountered during the processing of metals and alloys. Significant opportunity exists to not only employ conventional processes like metal casting, but also emerging processes like additive manufacturing (AM) that typically produce large temperature gradients, high solidification rates, and repeated cycles of heating and cooling. The local conditions experienced during solidification processes (e.g., thermal gradients and solid-liquid interface velocities) dictate microscopic structure (i.e., microstructure) evolution. Here we visualize solidification dynamics during metal casting, directional solidification, and simulated AM by real-time imaging with protons, synchrotron x-rays, and electrons and computational modeling to link processing conditions to microstructure development. We also explore the role of subsequent solid state phase transitions on final microstructural state. A deeper understanding of phase transitions is needed to optimize processing conditions, predict and control microstructure evolution, and achieve advanced manufacturing of metals and alloys.

Tu1a.1-4: Martensite (I)

Invited. **Thermally activated martensite formation: an exception or the rule?** Matteo Villa[2], Marcel Somers[1].

[1]Technical University of Denmark, Kongens Lyngby, Denmark.

[2]Politecnico di Bari, Bari, Italy.

Generally, the formation of martensite in steel is represented by horizontal lines in the CCT and TTT diagrams implying that martensite formation is athermal, i.e., independent of time. Nevertheless, hardening of precipitation hardening stainless steels that contain a significant fraction of austenite after cooling to room temperature is achieved by isothermal treatment in the sub-zero Celsius temperature regime. In the last 15 years, we investigated the kinetics of martensite formation with in-situ magnetometry, complemented by electron microscopy and X-ray diffraction studies. Our investigations revealed that thermally activated formation of martensite in a wide variety of steels and model alloys is the rule rather than the exception. For all the investigated steels and model alloys it was observed that martensite can form during cooling, isothermally as well as during heating. The kinetics of martensite formation depends on the steel chemistry and relates intimately to martensite's internal structure. In this overview of our work, the data is put into perspective and it is demonstrated that Zhao & Notis' presentation of lath and plate martensite as individual C-shaped curves can be extrapolated to the sub-zero Celsius regime to provide a comprehensive understanding. This paves the way for development of new steel compositions.

Kinetics of athermal martensite formation studied by in situ high-energy synchrotron X-ray diffraction. Daniel Dos Santos Avila[1], Pablo Martin[1], Pere Barriobero-Vila[2,3], Sven Erik Offerman[1], María J. Santofimia[1].

[1]Delft University of Technology, Delft, Netherlands.

[2]Technical University of Catalonia (UPC), Barcelona, Spain.

[3]CIM, UPC, Barcelona, Spain.

The kinetics of athermal martensite formation during the quenching of steels is commonly represented by the Koinstinen-Marbuger (KM) equation. The KM equation considers that the fraction of available austenite that is decomposed by a 1 K increase in undercooling is a composition-dependent constant, usually referred to as alpha or KM coefficient. Such an approach ignores the autocatalysis in martensite formation and hence cannot represent the slow-start and slow-finish of martensite formation. In this work, we discuss possible paths to include autocatalysis in the KM equation such that both the slow-start and slow-end are represented. We compare the proposed equations to an accurate measurement of the kinetics of martensite formation in low and high carbon steels using *in situ* high-energy synchrotron X-ray diffraction (HEXRD) at the P07 beamline at DESY, Germany. The kinetics of martensite formation measured by HEXRD is compared to that measured by dilatometry using both the tangent line and thermal expansion coefficient methods. The results and theoretical considerations presented in this work might help to improve our understanding of the kinetics of martensite formation in steels and how it is affected by chemical composition and microstructural features such as prior austenite grain size.

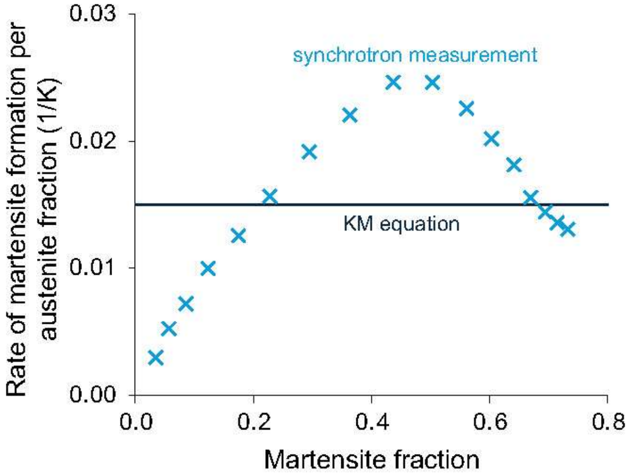

Bragg-edge neutron imaging and FEM simulation of martensite phase fraction of case hardened steel. Clas Dahlin, Carl Dahlberg, Henrik Larsson.

Royal Institute of Technology, Stockholm, Sweden.

Case hardening is an important process to enhance surface hardness and wear resistance of steel components. This study combines experimental techniques with numerical simulations to investigate the microstructural and mechanical gradients introduced by case hardening. Two different heat treatments were used to case-harden cylindrical steel samples. Bragg-edge neutron imaging was used to analyse the crystal structure and residual stress distribution along the radial direction, while Vickers hardness testing provided detailed hardness profiles. These experimental studies were complemented by a numerical model based on CALPHAD for solid-solid phase transformations, combined with thermal and mechanical calculations within a finite element framework. The results revealed good agreement between the numerical predictions and experimental measurements, particularly in capturing the transition zone between the hardened surface layer and the core. Discrepancies in the phase fraction estimation of the numerical model highlights areas where further refinement of the phase transformation models are needed. This approach of using Bragg-edge neutron imaging combined with numerical simulations opens the possibility to non-destructively investigate microstructure and mechanical behaviour on the macro-scale directly applicable to real engineering components. The methodology can offer valuable insights for designing materials and heat treatments for tailored mechanical properties.

Three-dimensional shape metrics for martensite from two-dimensional orientation maps. Tuomo Nyyssönen, Adam Ståhlkrantz.

Swerim AB, Stockholm, Sweden.

A martensite lath has a distinct three-dimensional shape intrinsically related to its formation mechanism by shear-assisted transformation from austenite. It can roughly be described as a flattened, elongated ellipsoid resting on a specific habit plane in the austenite (or martensite) reference frame. Characterizing this three-dimensional shape from two-dimensional orientation maps (such as those readily obtained by electron backscatter diffraction) is difficult to do directly. However, if the parent austenite crystallographic orientation and the corresponding martensite orientation are known, it is possible to eliminate symmetry issues when rotating shape metrics measured on a two-dimensional imaging plane to either the austenite or martensite reference frame. We show that with a sufficient number of data points, it becomes possible to extract three-dimensional information on the martensite habit plane, the long axis of the lath, as well as the aspect ratios between width, length and thickness in the martensite lath from two-dimensional orientation maps. This information can then be applied to the extraction of relevant data for phenomenological or more advanced models describing the martensitic transformation.

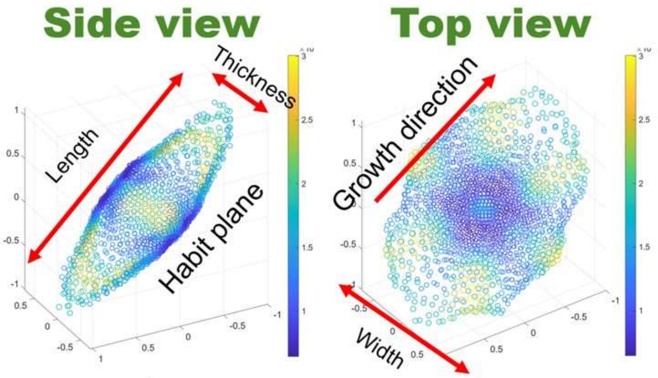

$$\vec{t}_P = C_i^{-1} O_{\gamma,i}^{-1} \vec{t}_X$$

Tu1b.1-4: Al alloys (I)

Invited. **Understanding Impurity-Driven Precipitation Kinetics in Al-Sc-Zr Core-Shell Precipitates.** Thomas Dorin.

Deakin University, Waurn Ponds, Australia.

Scandium (Sc) additions to aluminium (Al) alloys provide exceptional strengthening through the formation of nanoscale spherical Al_3Sc $L1_2$ precipitates. A notable feature of these precipitates is their core-shell morphology when other $L1_2$-forming elements, such as Zr, are added. Although, solute diffusivity differences drive this thermally stable core-shell structure, their detailed formation kinetics is not fully understood. This study combines advanced characterisation techniques and modelling to develop a comprehensive understanding of precipitation kinetics in Al-Sc-Zr alloys. Using anomalous small-angle X-ray scattering (ASAXS), atom probe tomography (APT), and diffusion couples, we investigate the formation mechanisms, impurity effects, and compositional evolution of $Al_3(Sc,Zr)$ core-shell precipitates. ASAXS was conducted near the Zr absorption edge to vary the scattering contrast of $Al_3(Sc,Zr)$ particles, capturing the formation of the core-shell structure during in-situ heat treatments. APT complemented the SAXS data and revealed the presence of Si and Fe impurities at early clustering stages. Diffusion couples, with composition gradients in Si and Fe at constant Sc and Zr levels, revealed that Si accelerates precipitation kinetics, while Fe forms novel nanoscale pseudo-icosahedral structures with Sc. These experimental results were used to develop a novel precipitation kinetics model for $Al_3(Sc,Zr)$

core-shell precipitates. The model accounts for impurity-driven nucleation and the multi-layered chemistry of the precipitates. The precipitation kinetics model was paired with a precipitation strengthening model, providing a framework to optimise heat treatment strategies for these alloys. The exceptional performance of Al-Sc alloys can enable lighter and more efficient components reducing emission and contributing to a more sustainable future.

Understanding the competition between dynamic precipitation and dynamic dissolution in Aluminium alloys. Guillaume Crowin[1], Adam Bouayoune[2], Fredéric De Geuser[1], Arthur Després[3], Jean-Yves Buffière[2], Michel Perez[2], Alexis Deschamps[3].

[1] CNRS-SIMaP, Grenoble, France.

[2] MateIS-INSA, Lyon, Villeurbanne, France.

[3] Grenoble-INP SIMaP, Grenoble, France.

Dynamic precipitation occurs in Aluminium alloys when an evolution of the precipitate microstructure is caused by straining. Recent work, particularly in Al-Zn-Mg-Cu alloys, has shown that the kinetics of dynamic precipitation is largely controlled by the production and annihilation of excess vacancies due to non-conservative dislocation motion, which accelerates the diffusion-controlled growth and coarsening processes. However, depending on the initial state and straining conditions, precipitate dissolution may also occur, whose mechanisms have been little studied yet. In this work we study the competition between this dynamic dissolution and more classical dynamic precipitation, for an initial Al-Zn-Mg-Cu alloy in the T6 state, submitted to straining temperatures from room temperature to 120°C, at different strain rates. *In situ* straining Small-Angle X-ray Scattering (SAXS) experiments show that during room temperature straining a clear precipitate dissolution occurs (fig 1a), while at 120°C an initial dynamic dissolution is followed by dynamic precipitation (fig. 1b), the transition being strongly strain-rate dependent. Applying a model-free determination by Monte Carlo methods of the precipitate size distribution from SAXS data allows to determine *in situ* the evolution of the critical radius for dissolution (fig. 1c), which is observed to strongly increase in the initial stage of straining. We hypothesize that this increase in critical radius is caused by the continuous precipitate shearing which increases the effective precipitate interface energy, and including this effect in a mean field class model of precipitation allows to successfully describe the dissolution stage and the transition to further dynamic growth and coarsening (fig. 1d).

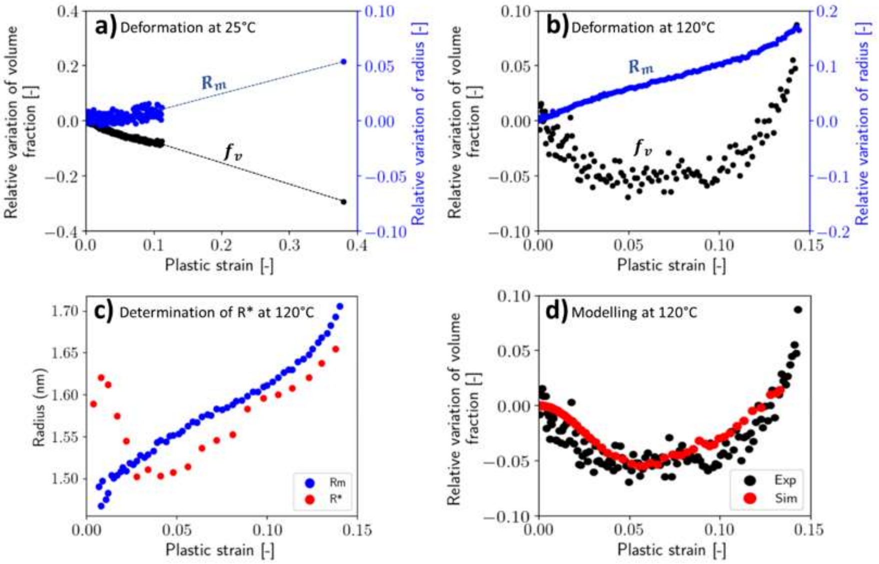

Fig. 1 : Evolution of the volume fraction and the mean radius of precipitates for a Al-Zn-Mg-Cu alloy in the T6 state a) during room temperature straining (at 4.10^{-5} s^{-1} for low plastic strain and after cold rolling for large plastic strain), and b) during straining at 120°C (at 1.10^{-3} s^{-1}). For the straining at 120°C, c) comparison of R to the mean radius, and d) modelling of the volume fraction by including dynamic precipitation and dynamic dissolution in a mean field class model of precipitation.*

A pragmatic and robust approach for modelling mean-field precipitation kinetics in aluminium alloys during cooling and heating at moderate rates. Robert Kahlenberg[1,2], Georg Falkinger[3], Roman Schuster[1], Bernhard Miesenberger[1], Nicolás García Arango[1], Emad Mawaad[4], Benjamin Milkereit[5,6], Ernst Kozeschnik[1].

[1]TUWien / Institute of Materials Science and Technology, Vienna, Austria.

[2]Materials Center Leoben Forschung GmbH, Leoben, Austria.

[3]AMAG rolling GmbH, Ranshofen, Austria.

[4]Helmholtz-Zentrum Hereon / Institute of Materials Physics, Geesthacht, Germany.

[5]University of Rostock / Chair of Materials Science, Rostock, Germany.

[6]University of Rostock / Competence Centre °CALOR, Rostock, Germany.

Mean-field modelling of solid-state precipitation kinetics in aluminium alloys is both a well-established and yet somewhat controversial field. The latter is, among other things, because of classical nucleation theory. Specifically, due to the uncertainties in some of its input quantities (e.g. interfacial energies of nuclei) and the difficulties regarding the verifiability of the main output quantity, that is, the nucleation rate. This can make it difficult to adjust the nucleation conditions in a manner that is robust enough for, e.g., process simulations that aim to include microstructural interdependencies and predict the effect of composition changes without prior calibration based on experimental data. The present work suggests a fairly simple, but robust approach to treat precipitation of non-hardening phases during cooling and heating in aluminium alloys. We use data obtained from differential scanning calorimetry (DSC), high energy x-ray diffraction (HEXRD) and electron microscopy to validate our simulations. We show that by considering two precipitate populations of the stable phase many essential features of heating DSC curves can be accurately reproduced. Furthermore, this combination of data can be quite effective to reduce uncertainties regarding thermodynamic descriptions of metastable phases, which is another common bottleneck for CALPHAD-based precipitation models.

Phase field modelling of nucleation and growth of T1 phase in Al-Cu-Li alloys. Ali Reza Safi, Elizabeth Mathew, Rupesh Chafle, Benjamin Klusemann.

Helmholtz Zentrum Hereon, Geesthacht, Germany.

Aluminium (Al) alloys are excellent candidates for lightweight applications due to their outstanding strength-to-weight ratio. Age-hardenable Al alloys benefit from precipitation strengthening through complex mechanisms that impede the motion of dislocations. The addition of copper (Cu) and lithium (Li) to pure Al enables the formation of a range of precipitates, out of which the stoichiometric T_1 precipitate contributes the most to the strengthening in Al-Cu-Li alloys. The crystal structure of T_1 is hexagonal and it forms as plates on the {111} Al matrix planes. In this work, we aim to study the role of elastic energy, interface energy, and interface mobilities in the equilibrium shape of T_1 precipitates in Al-Cu-Li alloys. Phase-field modelling is a powerful method that allows quantifying competing thermodynamic, kinetic, and elastic effects in the precipitate evolution of alloys in a thermodynamically consistent manner. Experimental studies have shown that T_1nucleation can be enhanced by microalloying with silver (Ag) and magnesium (Mg) or by increasing the density of nucleation sites through pre-deformation. In this way, it is possible to suppress the formation of other phases, such as θ’, and significantly increase the strengthening effect. Here, we study the impact of pre-deformation by implementing classical nucleation theory to account for both homogeneous and heterogeneous nucleation. Elastic properties and interfacial energies computed from DFT calculations serve as inputs to the total free energy of the system. The chemical free energies and diffusion coefficients are extracted from CALPHAD and diffusion databases, respectively.

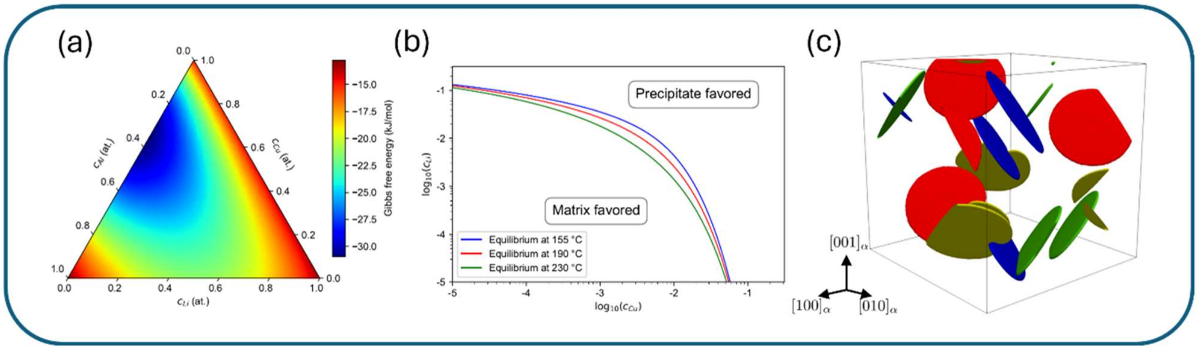

(a) Gibbs free energy of Al at 155°C, (b) reaction equilibria and (c) multiparticle simulation of T1 variants.

Tu1c.1-3: Plasticity

Invited. **Characterization and quantification of transformation / deformation-induced disclinations in BCC and HCP metals.** Yipeng Gao[1,2]

[1]Jilin University Changchun, China.

[2]Max-Planck-Institute for Sustainable Materials, Dusseldorf, Germany.

Disclinations, alongside dislocations, are fundamental topological defects that govern the deformation behavior of metals. While the role of dislocations is well understood, the influence of disclinations remains less explored due to difficulties in capturing their rotational nature. In this study, a Lie-algebra-based method is employed to quantify disclinations from electron backscatter diffraction (EBSD) data, enabling precise identification of their density and distribution. Using body-centered cubic (BCC) and hexagonal close-packed (HCP) metals (e.g., Ti, Mg) as examples, we show that disclinations can emerge from various defect reaction mechanisms during phase transformation and mechanical deformation, including multiple types of interactions and reactions among dislocations, twins, grain boundaries, and interfaces, significantly impacting stress localization and strain accommodation. These findings provide a robust framework for understanding disclination behavior and its role in microstructural evolution, offering valuable insights for enhancing the mechanical performance of metals and alloys.

Designing ultrasonic sonotrodes based on Laves phase machine learning to enhance the ultrasonic forming capability of CoNiFeCuTa high-entropy alloys. Yuan Zheng.

Beijing Jiaotong university, Beijing, China.

This study presents a machine learning approach centered on Laves phase prediction for designing ultrasonic sonotrodes to enhance the ultrasonic forming capability of CoNiFeCuTa high-entropy alloys. By developing a machine learning model that predicts the formation of Laves phases and their impact on mechanical properties and microstructural features, we optimized the structural parameters of the ultrasonic sonotrodes. Experimental results demonstrate that the optimized sonotrodes significantly reduce surface roughness by 30%, decrease flow stress by 100 MPa, and increase ductility by over 20% during ultrasonic forming processes. This methodology offers a new technical pathway for the plastic forming of high-entropy alloys and holds promise for advancing their application in the field of advanced manufacturing.

Expanded austenite in 316L stainless steel: characterization and modelling of plastic anisotropy. Matthew Bolan, Saeed Jafarpour, Stefan Martin, Anke Dalke, Horst Biermann, Andreas Leineweber.

TU Bergakademie Freiberg, Freiberg, Germany.

Austenitic stainless steels demonstrate excellent corrosion resistance, making them suitable for maritime, chemical, and nuclear applications, but suffer from poor hardness and tribological properties. This poor performance can be mitigated by generating a hardened outer layer via a thermochemical diffusion treatment, introducing N, C, or N+C into the surface. Under suitable conditions the N and C atoms will occupy interstitial sites in the austenite matrix, increasing its volume into so-called expanded austenite. It may appear as a single layer as a result of relatively pure nitrogen or carbon diffusion (γ_N and γ_C), or it may exhibit a compositionally distinct duplex structure (γ_N/γ_C). The volumetric expansion of the fcc lattice is, however, geometrically confined by the substrate, leading to compressive residual stresses. These stresses exceed the yield limit and thus induce plastic slip, in turn causing reorientation of the expanded austenite relative to substrate, and, in particular, to severe lattice curvature. This study investigates the observed cross-sectional lattice curvature in nitrocarburized AISI316L stainless steel in view of known crystal plasticity models, namely the Taylor-Bishop-Hill polycrystal model and more advanced ones. Crystallographic characterization was conducted using x-ray diffraction and electron backscatter diffraction. Composition-depth data was extracted through glow-discharge optical emission spectroscopy and energy dispersive x-ray spectroscopy. Correlative visual observations were made through light optical microscopy of etched samples and backscattered electron imaging of un-etched samples. A plastic slip model for expanded austenite is thereby presented, describing both the single and duplex layers, corroborating microstructural characterization of the plasma-assisted nitrocarburized lattice distortion.

Tu2a.1-5: Martensite (II)

Invited. **Kinetics of ordering transitions and Bain variant selection in Fe-C martensite.** Philippe Maugis, Liangzhao Huang.

Aix-Marseille University, Marseille, France.

It is well established that the displacive martensitic transformation of austenite during quenching leads to a state of carbon order in the body-centered structure of martensite. This so-called Zener order is the origin of the tetragonality of the martensite unit cell, which can occur along 3 possible directions of the lattice, giving rise to 3 Bain variants. The size, shape, and carbon content of these variants are difficult to investigate experimentally due to the nanoscale character of these microstructural constituents, although their properties are expected to affect both the hierarchical microstructure of martensite and its mechanical properties. We developed a multi-scale model of carbon ordering in body-centered iron, based on a unified description of ferrite and martensite phases in terms of alloy thermodynamics and carbon diffusion. This approach allowed to investigate the alloy thermodynamics, elasto-diffusion of carbon and thermo-elastic response of ferrite and of martensite variants [1]. On this basis, we built an atomic-scale kinetic Monte Carlo framework able to simulate the kinetics of diffusion-controlled ordering transitions in ferrite and martensite [2]. The results presented will include the effects of carbon content and thermal treatment on the nucleation, growth, and/or recession of Bain variants in a Fe-C martensite crystal. Our findings highlight the key influence of the local stress state on the final nanostructure of martensite.

[1] Maugis, P., Proceedings of International Symposia on Steel Science 2024, 103–112.

[2] Huang, L., Maugis, P., Acta Materialia 249 (2023) 118846.

The hidden austenite symmetries behind the type I and type II twins of martensite variants. Cyril Cayron.

Ecole Polytechique Fédérale de Lausanne, Neuchatel, Switzerland.

Two variants of martensite that are created simultaneously from the same austenite grain constitute a “transformation twin”. This twin can be type I or type II; the variants are linked by a rational mirror symmetry on a rational plane for the formed, and a 180° rotation around a rational axis for the latter. The interface between the variants is called “junction plane”. The phenomenological theory of martensite crystallography (PTMC) introduces some equations that should be solved in order to determine the twin elements and the junction planes. We will show that the mirror plane of the type I twins and the 180° rotation axis of the type II twins can actually be deduced without solving any equation, just from the correspondence matrix and the lost and hidden parent symmetries linking the variants. This approach permits to understand why these twin elements are generic, i.e. independent of the metrics of the daughter and parent phases. Tin addition, the junction plane is the mirror plane of the type I twins. For the type II twins, it can be the invariant irrational plane or a rational plane that is just slightly distorted (“weak plane”). The type of twin (I or II) between a pair of variants depends on the deviation between the "closing-gap" parent-martensite orientation relationship imposed by the twin and an absolute "natural" one (Fig. 1). Examples will be given with NiTi shape memory alloys and Fe martensitic steels. The predictions will be compared to EBSD and TKD maps.

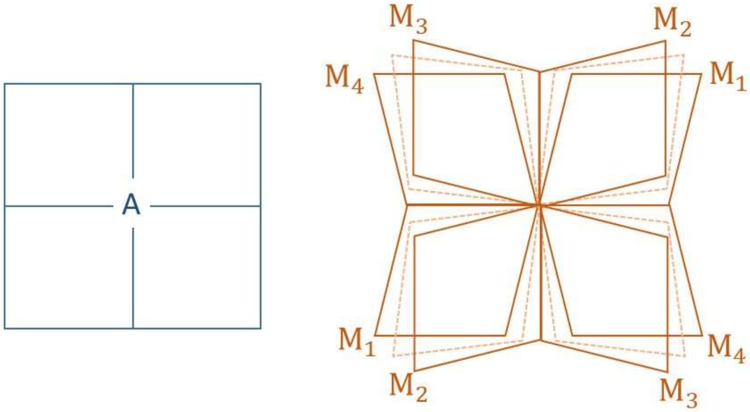

Closing-gap orientations of four rhombic martensite variants generated from a square austenite parent with a natural aM // aA orientation relationship.

Effect of different quenching methods on the microstructure and mechanical properties of 30MnB5NbTi. Xinwei Wang, Renbo Song, Shuai Zhao.

University of Science and Technology Beijing, Beijing, China.

The effects of different quenching methods on the microstructure and mechanical properties of 30MnB5NbTi hot stamping steel were investigated, and the quenched microstructure was characterized by SEM, EBSD and TEM. The mechanical properties were evaluated by uniaxial tensile test. The results showed that compared with die quenching, oil quenching or air cooling, the ultimate tensile strength (UTS) and yield strength (YS) of water-quenched samples were the highest, reaching the UTS of 2052MPa, the YS of 1422MPa. Through different quenching methods, the multi-level strength control of the same steel grade was achieved, and the strength control range was about 1000MPa. The microstructure of samples quenched by water, die and oil was fully martensite, and martensite exhibited block and lath morphology. With the increase of cooling rate, martensite laths became finer and the prior austenite size decreased. The microstructure of air-cooled samples was martensite, ferrite and retained austenite. The strengthening mechanisms of different quenched samples were calculated. The results showed that dislocation strengthening and precipitation strengthening were the two dominant strengthening mechanisms in 30MnB5NbTi hot stamping steel. Therefore, the properties of hot stamping steel can be improved by designing physical dies.

A discovery of new metastable Omega phase formed in coarse-grained medium manganese steel during quenching. Haiwen Luo, Ru Ge.

University of Science and Technology Beijing, Beijing, China.

The rapid quenching of carbon steel leads to the formation of martensite, known for its exceptional hardness due to the supersaturated carbon atoms in bcc or bct structure formed by a diffusionless martensitic transformation. More than half a century ago, the ω phase was discovered in the bcc phase of Ti, Zr, and Hf-based alloys and has been known to influence mechanical properties. Here we report a similar phase found in a water-quenched medium manganese steel after the long homogenization at

1200 °C for 20h by using both high-resolution transmission electron microscopy and atom probe tomography. This is a transition phase having a hexagonal structure. It was formed at the martensite lath boundaries, the latter has the distinctive feature of double edges. We suggest that such a ω phase may be formed when the segregated C concentration at lath boundaries exceeds 1.6 wt%. Our study also indicates that the ω phase may act as an intermediate for the austenitic reversion during heating.

Cooperative interfaces migration during hcp<->fcc transformation in cobalt. Xinfu Gu.

University of Science and Technology Beijing, Beijing, China.

The phase transformation between fcc (face-centered cubic) and hcp (hexagonal close-packed) structures (fcc<->hcp) is a fundamental yet crucial process observed in materials such as in cobalt alloys, steel, etc. Pure cobalt commonly undergoes an allotropic fcc<->hcp transformation, around 420°C, and the hcp structure is stable at lower temperatures. During the fcc<->hcp transformation, a low-energy interface is established between the fcc and hcp structures to minimize the energy barrier associated with the phase transformation, leading to a reproducible orientation relationship between these two phases. Specifically, this relationship is known as the Shoji-Nishiyama orientation relationship, $\{111\}_f$ // $\{0001\}_h$, $<\text{-}101>_f$ // $<2\text{-}1\text{-}10>_h$, with the interface parallel to $\{111\}_f$ // $\{0001\}_h$ and the subscripts f represent indices in the fcc structure, while h in the hcp structure. It is worth noting that the fcc<->hcp transformation is considered as an athermal process and the transformation proceeds with the movement of partial dislocations, specifically $<112>_f/6$ or $<1\text{-}100>_h/3$. In this study, we will present the cooperative growth of the fcc interface with self-accommodated partials. The partials are identified based on the atomic images obtained during the transformation process. Furthermore, we observe the formation of cooperative partials at the early stages of fcc formation. The results will be discussed in conjunction with atomic simulations conducted via molecular dynamics, emphasizing the athermal nature of the transformation.

Tu2b.1-5: Al alloys (II)

Invited. **Solute clustering and early-stage precipitation in Al-Mg-Si alloys.** Chunan Li[1], Calin Marioara[2], Constantinos Hatzoglou[1], Sigmund Andersen[2], Randi Holmestad[1], Yanjun Li[1]

[1]Norwegian University of Science and Technology, Trondheim, Norway.

[2]SINTEF industry, Trondheim, Norway.

In industrial applications of age-hardenable aluminum alloys, precipitation involves solution heat treatment, pre-aging treatment, natural aging (storage at room temperature), and artificial aging. Precipitation in Al-Mg-Si alloys are well-known to be sensitive to the thermal history at early stage, the mechanism of which is not fully understood. Systematic investigation shows that the pre-aging treatment and natural aging for different amount of times can significantly influence the age-hardening response and peak-aged strength in Al-Mg-Si alloys. Combining results from advanced transmission electron microscopy (TEM) and atom probe tomography (APT), we show that for dense Al-Mg-Si alloys such as the 6082 alloy, GP-zones with a structure different from β" are formed after natural aging. It is difficult for these GP-zones to transform into β" and most of them will have to be dissolved during the following artificial aging. In contrast, pre-aging treatment promotes the formation of GP-zones with the same structral motif as β" strengthening precipitates, which can easily grow into β" needles after the subsequent artificial aging. During the natural aging after pre-aging, more β"-type GP-zones can be formed, and the fraction of non-β" type GP-zones is much lower than direct natural aging. As a result, finer and denser β" can be formed after artifical aging, achieving a higher strength and ductility with a shorter aging time needed to achieve peak strength as compared to direct artifical aging. The findings above shed new light into the long-standing natural aging problem in Al-Mg-Si alloys.

Formation and dissolution of the T-phase in a novel Al-Mg-Zn-(Cu) crossover alloy for automotive sheets.

Georg Falkinger[1], Lukas Stemper[1], Ramona Tosone[1], Stefan Pogatscher[2]

[1]AMAG rolling GmbH, Ranshofen, Austria.

[2]Montanuniversität Leoben, Leoben, Austria.

Recent efforts to combined the ductility of Al-Mg alloys with the strength of Al-Zn-Mg-(Cu) alloys have resulted in the development of an age-hardenable Al-Mg-Zn-(Cu) alloy for automotive sheets. The novel alloy, produced industrially by AMAG under the commercial name crossAlloy®.57 offers a balanced mix of strength, formability and corrosion resistance. The main stable phase in this alloy is the ternary T-phase, written as $(Mg)_{26}(Mg,Al)_6(Al,Zn,Mg)_{48}(Al)_1$ with cubic crystal structure. Few investigations of the evolution of this phase exist during industrial processes, because it is not considered as being relevant in any traditional commercial aluminum alloy system. In the present contribution we analyze the nucleation, growth and dissolution of the T-Phase during slow cooling and subsequent re-heating. To this end we use differential scanning calorimetry and electron microscopy in combination with mean-field models. We show that the T-phase concurrently grows at grain boundaries and in the interior of the grain. The precipitates at the grain boundary however are larger and therefore more critical than the ones in the grain interior. Our findings help to understand the evolution of the T-phase throughout the production process, including casting, homogenization, hot-rolling, intermediate annealing, cold-rolling and solution annealing. We show how the formation of large T-phase precipitates can be suppressed during these steps to improve the formability of the final product.

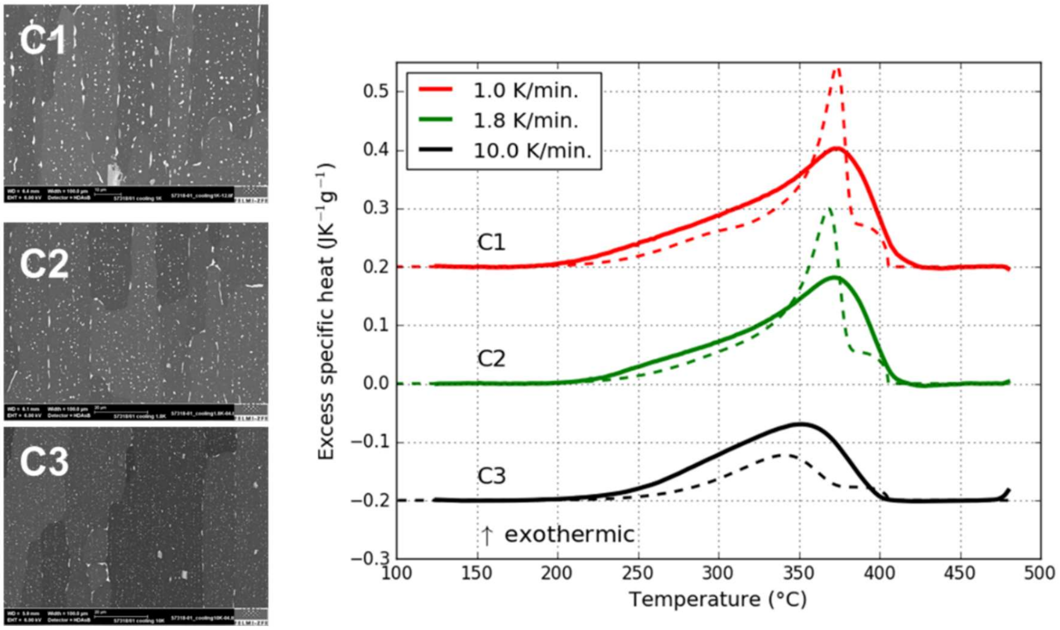

Combined use of DSC, SEM and mean field model to characterize the evolution of the T-phase during slow linear cooling.

Impact of atomic couples and pairs on quenched-in vacancies in Al-Mg-Si-Cu alloys. Ya Li[1], Robert Kahlenberg[2,3], Philipp Retzl[2,4], Yao V. Shan[2], Ernst Kozeschnik[2].

[1]Materials Science and Technology, TU Wien, Wien, Austria.

[2]Institute of Materials Science and Technology, TU Wien, Vienna, Austria.

[3]Materials Center Leoben Forschung GmbH, Leoben, Austria.

[4]MatCalc Engineering GmbH, Vienna, Austria.

After solutionizing and quenching age-hardenable Al-alloys, non-equilibrium excess vacancies are retained in traps such as solute atoms and atomic clusters. These excess vacancies are crucial for precipitation since diffusion rates scale with vacancy concentration. Solid phase precipitation begins with the formation of atomic couples and pairs (C&Ps), which are suggested to bind strongly to vacancies. However, the impact of C&P-vacancy interactions on the quenched-in vacancy concentration is less investigated. For instance, after solutionizing and quenching Al-Mg-Si-Cu alloys with cooling rates differing by a factor of about 200, the quenched-in vacancy concentration difference measured by positron lifetime spectrometry is roughly ~40 times. This is contrary to the expected ~200 times difference predicted by the recently developed *FSAK* model for vacancy generation and annihilation. To address this discrepancy, a combined theoretical framework including C&P formation kinetics and vacancy trapping is developed (as shown in Fig. 1) and applied to an Al-Mg-Si-Cu alloy. The results indicate that C&Ps with Si in Al-Mg-Si-Cu alloys act as primary vacancy traps during quenching, capturing more vacancies than isolated solutes. The simulations explain the experimentally measured ~40 times difference in quenched-in vacancies compared to the large difference predicted in the absence of vacancy trapping on C&Ps. These findings highlight the importance of C&Ps in trapping vacancies, providing valuable insights into controlling ageing behavior and optimizing mechanical properties in Al-alloys.

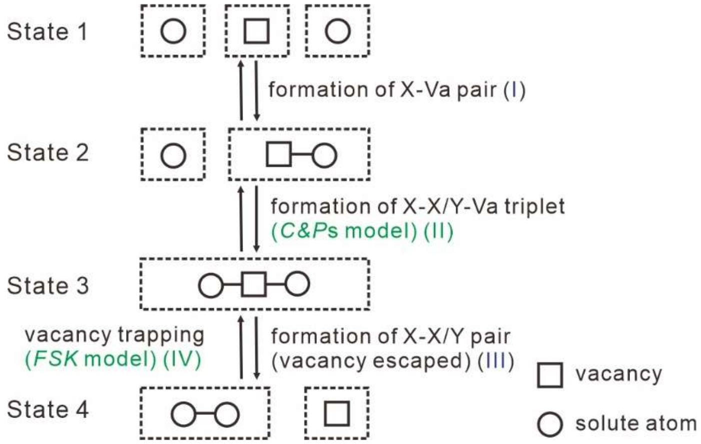

Fig. 1. Mechanisms of solute-solute (X-X/Y) C&P formation and vacancy trapping.

Geometrical analysis of the coherency of η/Al heterointerfaces in Al-Zn-Mg alloy. Seiichiro II, Toru Hara.

National Institute for Materials Science, Tsukuba, Japan.

It is well-known that the typical precipitation process in Al-Zn-Mg alloys with a high Zn/Mg ratio is from the super-saturated solid solution, GP zone, η', and η. Among them, the η phase of Mg_2Zn is one of the typical equilibrium precipitates in Al-Zn-Mg alloy. The η phase and Al matrix exhibit a variety of orientation relationships. To clarify the origin of the various orientation relationships, we discussed the η/Al heterointerface, mainly the habit plane, from the analysis of geometric viewpoints, specifically the near coincidence site lattice (NCSL) analysis and M parameter based on the misfit strain in the interface. In the NCSL analysis, the density of NCS points nearly equal to the Σ value in the grain boundary can be evaluated. Although we evaluated the coherency of the interface for all orientation relationships reported so far, there was no significant tendency or dependence on the NCS density at the interfaces. On the other hand, regarding the M parameter in the interfaces, expressed by $M=\varepsilon_1^2+ \varepsilon_2^2+(2/3)\varepsilon_1\varepsilon_2$ (ε_a: the principal misfit strain along the a-axis), it was found that the lower M parameters, meaning a smaller misfit strain, are obtained at the interfaces with the orientation relationships reported in the early stage of the study on the η phase. Combining the previous experimental observations and our analyses, it is suggested that elastic relaxation may play an important role, as well as atomic matching in the η/Al heterointerface formation and growth of the η phase in Al-Zn-Mg alloy.

Evolution of nanostructures during slow quenching in an Al-Zn-Mg alloy and their effect on age-hardening. Mami Mihara-Narita[1], Hideo Yoshida[2].

[1]Nagoya Institute of Technology, Nagoya, Japan.

[2]ESD Laboratory, Nagoya, Japan.

Generally, age-hardenable aluminum alloys are quenched in water to obtain the required strength. However, recent studies have revealed that furnace cooling (FC) of an Al-Zn-Mg alloy can provide strength comparable to that of water quenched (WQ) material. The reason why higher strength can be obtained by FC has not been clarified. In this study, microstructure observation by using transmission electron microscope with atomic resolution were conducted to elucidate the effects of quenching rate on changes in hardness during aging. As a result, it was confirmed that the hardness of an Al-6Zn-0.8Mg (mass%) alloy could be obtained by FC to be equivalent to that by WQ. The results of DSC analysis suggested that GP zones and clusters were already formed during FC and that they contribute to age hardening. In fact, TEM observation confirmed the structure of spherical GP zones and many clusters in the FC material. Changes in nanostructure during aging process will also be discussed in the presentation.

Tu2c.1-3: Materials for energy (I)

Invited. **TRIP effect in Zirconia: atomistic simulations and in-situ experiments.** Gael Huynh[1], Jin-Yu Zhang[1,2], Marcelo Demetrio de Magalhaes[3], Tristan Albaret[1], David Rodney[1].

[1]Institut Lumière Matière, Villeurbanne, France.

[2]Department of Mechanical Science and Bioengineering, Osaka, Japan.

[3]MATEIS, Villeurbanne, France.

Like steels, zirconia ceramics exhibit transformation-induced plasticity (TRIP) due to a transformation between a tetragonal (t) and a monoclinic (m) phase. This unique feature allows zirconia ceramics to undergo substantial plastic deformation, reaching a remarkable 7% plastic strain. However, this effect is far from fully understood, hindering the development of ceramics with macroscopic deformability exceeding 1%. Additionally, the lack of interatomic potentials capable of accurately describing zirconia complex polymorphism and phase transformations makes understanding the TRIP effect at the atomic scale difficult. In this work, we combine in-situ Laue diffraction on micropillars and atomic-scale simulations to obtain microscopic information on transformation conditions. Specifically, we explore how compression direction influences the transformation. The simulations required the development of a neural network-based interatomic potential to accurately describe zirconia polymorphism. We characterize the deformation processes, critical stress-strain states, and phase transformations both experimentally and numerically across various compression directions, spanning the entire standard triangle. Our simulations challenge the prevailing notion that a limited number of variants govern the TRIP in zirconia. Furthermore, we observe through simulations a complex interplay between competing stable and metastable phases, some of which have not been documented experimentally. An interesting question, which remains to be explored, is why these phases have not been reported experimentally so far: an effect of size, temperature, or strain rate, a lack of realism of the NNP, or have these phases been overlooked experimentally in the past?

Atomistic modeling of microstructure evolution in Cu-Mo nano-multilayers at elevated temperatures. Anastasiia Titova, Renaud Patte, Helena Zapolsky.

Université de Rouen, Normandie Saint-Étienne-du-Rouvray, France.

Nanometric metallic multilayers (NMMs) exhibit exceptional electronic, magnetic, optical, mechanical, and radiation-tolerance properties, stemming from the combination of the unique characteristics of their individual components. For example, Cu-Mo NMMs show great potential as materials for heat spreader applications in integrated circuits and as cladding materials for fabricating fuel rods in nuclear reactors, among other uses. Cu-Mo NMMs are composed of immiscible metals with incoherent FCC/BCC interfaces, offering a combination of the excellent thermal and electrical conductivity of Cu and the low coefficient of thermal expansion of Mo. Despite extensive experimental data, the thermal stability of Cu-Mo nanolaminates remains poorly understood and demands further investigation. The aim of this study is to gain a deeper understanding of microstructure evolution occurring at the nanoscale in Cu-Mo NMMs at elevated temperatures using atomistic scale modelling based on the Quasiparticle Approach. This model is an extension of the atomic density function theory to the continuum case. In particular, we investigate the impact of a grain structure and thickness of layers in Cu-Mo NMMs on their microstructural evolution. Our modeling results show that these two parameters have a significant influence on thermal grooving and layer pinch-off phenomena in NMMs.

Coarse Cr-rich carbides precipitates evolution during consolidation, as consolidated and after thermal ageing in ODS ferritic and ferritic/martensitic steels. Emilien Guy[1], Joël Malaplate[1], Raphaëlle Guillou[1], Jacques Perrin Toinin[1], Xavier Boulnat[2], Michel Perez[2].

[1] Université Paris-Saclay, CEA 91191, Gif-sur-Yvette, France.

[2] Univ. Lyon, INSA-Lyon, UCBL, MATEIS UMR CNRS 5510 69621, Villeurbanne, France.

ODS (Oxide Dispersion Strengthened) steels have been developed as candidate cladding materials for 4th generation nuclear reactors. However, coarse precipitation which can be either oxides, nitrides with Ti, or Cr-rich carbides, is known to have a detrimental effect on impact properties by occurring at grain or prior powder boundaries. Two ODS steels with different Cr contents ($9_{wt}\%$Cr vs $14_{wt}\%$Cr) and high C contents

(1000 ppm vs 700 ppm, respectively) were elaborated using Mechanical Alloying techniques, including ball milling with Y_2O_3 and TiH_2 powders, followed by a final HIP treatment. Coarse precipitation evolution during consolidation was analyzed by *in situ* WAXS on mechanically alloyed powders. Carbides precipitation starts during heating at 650°C and dissolve above 1000°C (Figure 1a) and precipitation kinetics were obtained. This evolution is modelled with the classical nucleation theory using a mean field approach showing consolidation step is governed by nucleation and growth. Combined WAXS, SEM-EDX, APT and selective dissolution analyses have been done on as-consolidated materials. Carbides size were 0.7 µm and 1.0 µm for ODS $9_{wt.}$%Cr and $14_{wt.}$%Cr, respectively, always located at grain boundaries. Stoichiometry is found to be near $Cr_{23}C_6$, with a slight enrichment in W and Fe. APT analysis highlight a segregation of Cr, W and C at grain boundaries, leading to the precipitation of carbides (Figure 1b). Carbide evolution with time has also been investigated via thermal ageing at 650°C for several thousand hours. The coarsening observed by SEM has been modelled with classical nucleation theory.

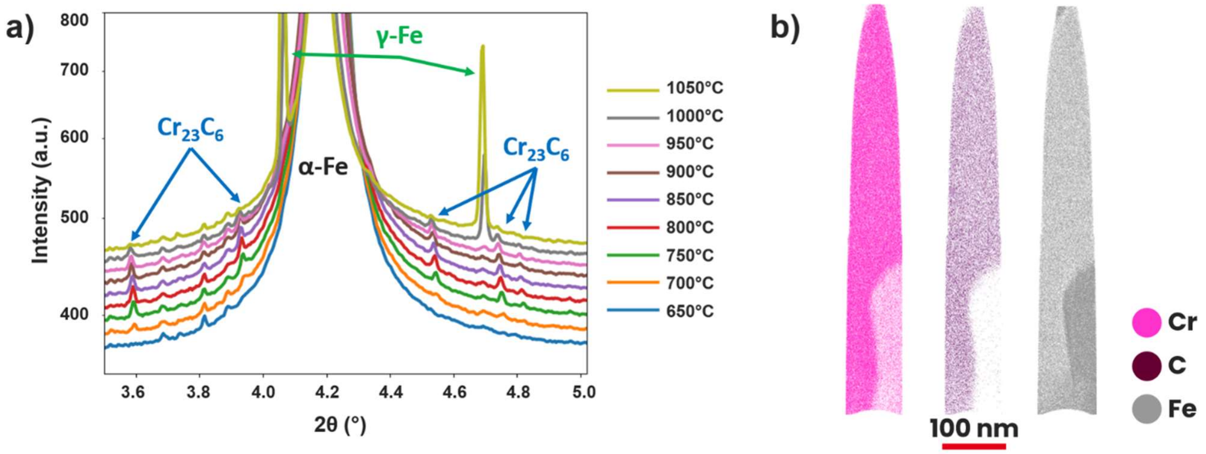

Figure 1 : WAXS patterns evolution during in situ heating (a) and front view of an APT analysis of an interface between Cr23C6 carbide and matrix (b)

Tu3a.1-5: Martensite (III)

Modelling T_0, B_s and M_s temperatures of steels. Stefan Bohemen.

Tata Steel Research and Development, IJmuiden, Netherlands.

Thermodynamic T_0 temperatures have been analysed for various Fe systems with additions of C, Mn, Si, Cr, Mo, Ni and Al. The findings indicate that the additivity rule is inadequate to accurately describe T_0 of ternary and higher order systems. To address this issue, a novel method accounting for the interaction of alloying elements was introduced and validated using 860 data points. A critical assessment of B_s and M_s data from literature was performed, and the values of various error contributions were estimated. Similar to the developed T_0 model, the possible interactions of alloying elements in modelling B_s and M_s temperatures were explored, but no conclusive evidence was found due to high uncertainty in the experimental data. After these unsuccessful initial explorations, models assuming additivity were developed. These newly proposed models can accurately describe B_s and M_s of steels with a very wide range of alloying concentrations, demonstrating a significant improvement compared to benchmark models. It is also worth emphasizing that the proposed B_s model is fully consistent with the diffusionless growth mechanism because $B_s < T_0$ is obeyed up to 0.5 wt.% C, while B_s becomes already lower than A_{cm} beyond 0.4 wt.% C. For temperatures below the A_{cm} line cementite can precipitate in the supersaturated austenite, and subsequently inverse bainite can nucleate and grow in the carbon-depleted austenite regions where the B_s temperature has locally increased compared to the value of the bulk composition. Then the criterion $B_s < T_0$ based on bulk compositions is no longer meaningful.

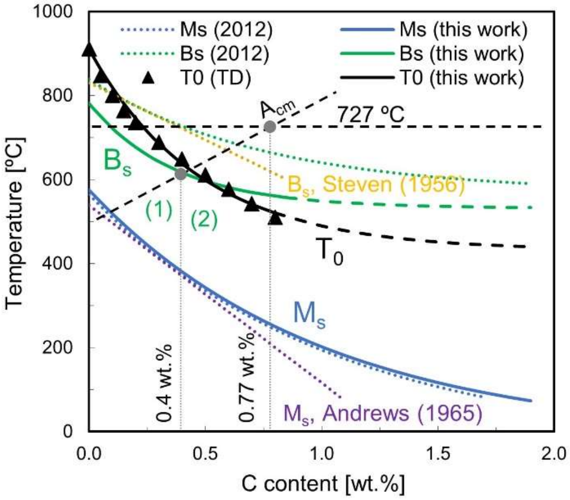

Figure: The calculated dependency of T0, Bs and Ms on the carbon concentration.

Martensitic transformations in 17-4 PH stainless steels at sub-zero celsius temperatures. Basit Ali[1], Matteo Villa[2], Marcel Somers[1].

[1]Technical University of Denmark, Kgs. Lyngby, Denmark.

[2]Polytechnic University of Bari, Bari, Italy.

Martensitic transformations in nitrogen-doped 17-4 PH stainless steels were investigated using in-situ magnetometry, in-situ dark filed X-ray microscopy (DFXM), and electron microscopy. Controlled amounts of nitrogen were added to conventionally manufactured 17-4 PH to stabilize austenite at sub-zero Celsius temperatures and to tailor the martensite start temperature. Our magnetometry investigations clearly revealed that martensite in these systems forms during cooling, isothermal holding, as well as during (re-)heating from cryogenic temperature back to room temperature. For the first time, DFXM was applied to investigate in-situ isothermal martensite formation, enabling the observation of elastic and plastic deformation in austenite during martensite formation. The kinetics of martensite formation were related to martensite morphology, and it was demonstrated that lath and plate martensite form depending on the nitrogen content and cooling rate. These results challenge the traditional view of martensitic transformations as athermal and demonstrate that thermal activation is an essential aspect of martensitic transformations. The results provide insight into tailoring the properties of 17-4 PH steels, such as in relation to additive manufacturing of this steel type. For this reason, martensite formation in 17-4 PH fabricated by laser powder bed fusion (L-PBF) is also included in this presentation.

Strain glass transition — a frustrated martensitic transformation: origin and features studied through multi-scale modeling. Liang Chuanxin[1], Wang Dong[1], Dong Tianjiao[1], Su Yunting[1], Wang Yunzhi[2].

[1]Xi'an Jiaotong University, Xi'an, China.

[2]Ohio State University, Columbus, United States.

Strain glass state in ferroelastic systems is the counterpart of relaxor in ferroelectric systems and cluster spin glass in ferromagnetic systems, all of which are collectively referred to as ferroic glasses. Different from other glasses such as metallic glasses, polymer glasses, glass-ceramics, etc., which show the frozen process into an amorphous state from a liquid state by rapid cooling or pressurizing, a ferroic glass is structurally still in a crystalline state; and it is the corresponding order parameter (e.g., polarization, magnetization or strain) that is “frozen” into a disordered state from a para ferroic state by charge- or stress-carrying defects (including point defect, dislocations, nano-precipitates, etc.). Through an integrated approach combining molecular statics calculations and phase field simulations, we quantitatively mapped the strain/stress fields distribution caused by point defects and its impact on martensitic transformation. Our analysis reveals two significant findings: First, we demonstrated how the strain network created by point defects at critical concentrations regulates nucleation and growth of martensitic domains, transforming the sharp first-order martensitic transformation into a continuous strain glass transition through strain frustration. Second, we identified that a percolation-like metastable suppression field, formed during cooling, serves as the physical origin of β-relaxation in strain glass systems, explaining both the anomalous relaxation behavior and the spontaneous transition from strain glass to martensitic state. These findings provide fundamental insights into both strain glass formation and β-relaxation mechanisms.

A generic model for interface energy in austenite/martensite: a comparative empirical and machine-learning study. Hussein Farahani[1,2], Hassan Shirazi[3], Mahmoud Nili-Ahmadabadi[3].

[1]Tata Steel Research & Development, IJmuiden, the Netherlands.

[2]Delft University of Technology, Delft, the Netherlands.

[3]College of Engineering, University of Tehran. Tehran, Iran.

The prediction of stacking fault energy (SFE) in austenitic steels is a critical aspect of material science and metallurgy, influencing properties such as deformation behavior, in particular, stress induced phase transformation, strength, and corrosion resistance. Traditional physical models often use a fixed value for Austenite/Martensite Interface Energy (IE), which can reduce the accuracy of SFE predictions. This study introduces a new empirical model for calculating IE and compares it with a machine-learning approach to enhance the precision of SFE predictions in Fe-based alloys. A dataset comprising over 100 SFE measurements in Fe-based alloys was utilized. The empirical model incorporates various thermodynamic parameters, including Gibbs energy differences between phases, to predict IE. Additionally, machine-learning models, were employed to model SFE. The results demonstrate that the empirical model and machine-learning approaches provide improved accuracy over traditional methods. The study’s findings highlight the potential of combining empirical and machine-learning models to predict SFE more accurately, offering significant implications for the design and development of advanced austenitic steels.

Two-step B2→R→B19' continuous Transition in NiTi Shape Memory Alloy with Low-fatigue Large Elastocaloric Effect. Qianglong Liang.

Xi'an Jiaotong University, Xi'an, China.

NiTi shape memory alloys (SMAs) are promising candidates as elastocaloric materials owing to their substantial adiabatic temperature change (ΔT_{ad}). However, the simultaneous attainment of large ΔT_{ad} and low fatigue in NiTi poses challenges due to the significant hysteresis and severe functional fatigue associated with the autocatalytic avalanche-like martensitic transformation. This study demonstrates a two-step B2 à R à B19' continuous transition in $Ni_{50.8}Ti_{49.2}$ (at. %), showcasing cyclic stable superelasticity with low Young's modulus (26.2 GPa), large recoverable strain (5.7%), and substantial ΔT_{ad} (19.1 K). *In-situ* loading synchrotron-based X-ray diffraction analysis indicates a stress-induced continuous transition from the B2 parent phase to R phase and subsequently to B19' phase. *In-situ* cooling high-resolution electron microscopic observations reveal continuous formation of R and B19' nanodomains contributing to a wide-temperature-range superelasticity and elastocaloric effect from 329 K to 119 K. Nanoscale lattice analysis exposes a heterogeneous strain network, harboring the metastable state of R phase preceding the B19' phase. Thus, by exploiting differences in critical stress and transformation strain between R and B19' phases, this study demonstrates the possibilities to synergistically integrate the superelastic and functional performances of different martensite in NiTi SMAs into a sequential and continuous two-step transition to provide controlled strain release with unprecedented properties.

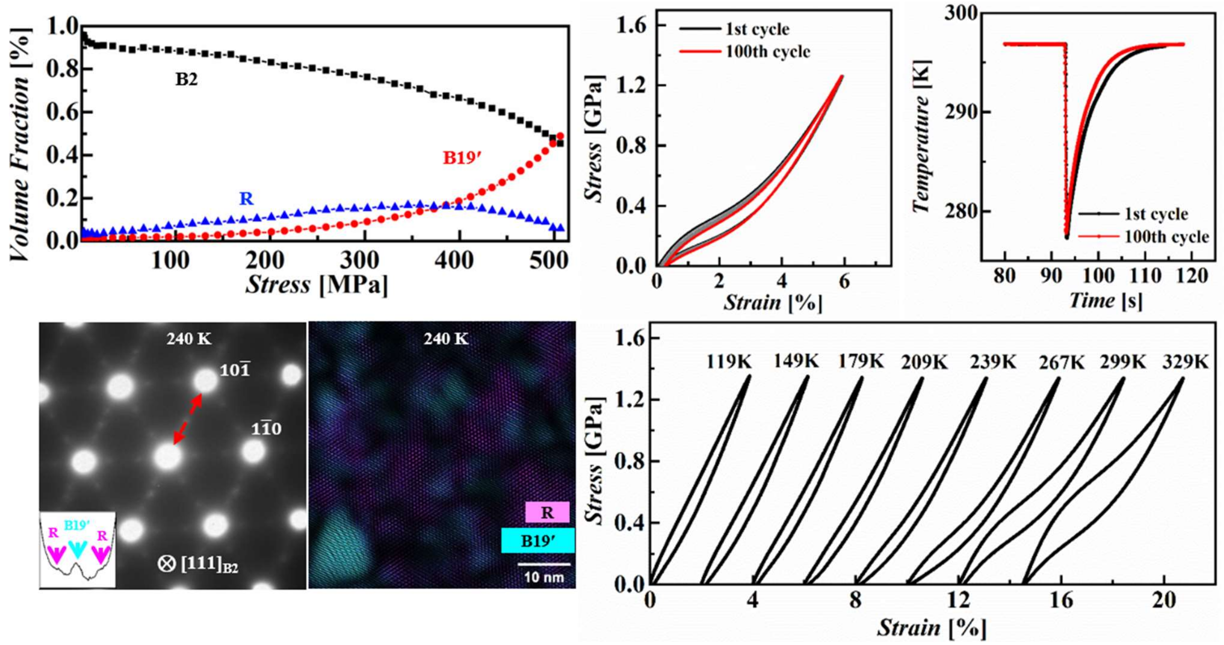

Tu3b.1-5: Al alloys (III)

Process chain-dependent microstructure and strength development of an AlMnFeMgSi(Zr) wrought alloy. Jette Broer, Kevin Oldenburg, Benjamin Milkereit, Olaf Kessler.

University of Rostock, Rostock, Germany.

The properties of age hardening aluminium alloys are essentially controlled by different classes of precipitate particles. The actual precipitation of these different classes of particles typically occurs at different steps of the process chain. In this work two classes of precipitates are in focus: dispersoids and age hardening precipitates. Within the aluminium community particles from relatively high melting alloying elements, which precipitate from the supersaturated as-cast state during a homogenisation treatment are called dispersoids. Those generally are assumed to be affected only little by the later process (heat treatment) steps, while controlling e.g. grain growth. This project aims a direct hardening contribution from dispersoids superimposed to that of the conventional age hardening precipitates. This requires a basic materials science understanding of the temperature-dependent kinetics and types of precipitation formation over the entire process chain. The classical production chain of wrought aluminium alloys consists of casting, homogenisation, hot forming and age hardening. Another goal is to combine different process steps and shorten the process chain. Therefore, four production chains were investigated using an aluminium wrought alloy EN-AW-AlMn0.5Mg0.5(3105) with a significant Si-content. One challenge is that relatively fine dispersoids must first be precipitated while these have to survive a subsequent solution treatment, which is required to bring the major alloying elements into solid solution. The micro- and nano-structure was analysed using electron microscopy. The materials properties are characterised by hardness testing and tensile tests along the process chain. The same strength levels were achieved with considerable savings in process time and energy.

Eutectic spheroidization in AlMg5Si2Mn-type casting alloys containing Lithium. Viktoriya Boyko, Kostiantyn Mykhalenkov, Olaf Kessler.

University of Rostock, Rostock, Germany.

Environmental and consumer demands are driving the use of materials with low density and high mechanical properties. Aluminium alloys, particularly those containing Li, fully meet these requirements. Li-containing alloys are often used as semi-finishes, but their use in foundries is limited. The present study aims to provide structural characterisation of AlMg5Si2Mn-type alloys on a broad scale, including transformations that occur during heat treatment. The experimental alloys contain from 1.0 to 2.0 wt.% Li and were prepared under different conditions of melting and casting. After solidification, the alloys were homogenised at a temperature of 570°C for 1 min-24 hours and the specimens were examined by differential scanning calorimetry, light and electron microscopy and hardness testing. It was established that the addition of the Li affects the eutectic morphology and transforms the shape of the Mg_2Si lamella from plates to fine fibrous, thus specifying the eutectic modification. During homogenisation, the disintegration of the Mg_2Si eutectic starts with lamella cracking. For the base alloy, a fully spheroidised structure was achieved after 15 minutes of soaking, where the average radius of the Mg_2Si particles decreased to 1.0 µm. For Li-containing alloys, where the Mg_2Si was already fibrous, a similar size was achieved after 5 minutes of homogenisation. It has also been found that the AlMnFeSi secondary particles are nucleated at the interface between the Mg_2Si and Al matrix.

Modelling the precipitate transformation of Mg–Si-rich clusters into Mg5Si6 beta" in Al–Mg–Si aluminum alloys. V. Yao Shan[1], Alice Redermeier[2], Ernst Kozeschnik[1], Robert Kahlenberg[3].

[1]TU Wien, Institute of Materials Science and Technology, Wien, Austria.

[2]TGM, Wien, Austria.

[3]Materials Center Leoben GmbH, Leoben, Austria.

A model is presented that describes the kinetics of precipitate transformations in the course of natural and artificial aging of Al alloys containing Mg and Si additions. In our approach, the disordered Mg–Si-rich clusters, which form during natural aging in the highly supersaturated Al matrix, can directly transform into the monoclinic Mg_5Si_6 (beta"), without prior dissolution of the clusters and independent nucleation of beta" in the Al matrix. The transformation rate is evaluated with classical nucleation theory (CNT), assuming that the clusters represent an infinitely large matrix phase in which the beta” precipitates can nucleate. The adapted CNT model is described, and the basic features of the precipitate transformation are discussed in a parameter study. The model can also account for the observation that, during natural aging, the parent clusters occur in a variety of Mg to Si ratios, all of which have a characteristic probability of either transforming into the beta” phase or dissolving.

High-throughput characterization of composition-dependent precipitation kinetics studied in graded Al-Zn-Mg-Cu alloys. Thomas Pejot[1,2], Julien Barlier[2], Frédéric De Geuser[1], Alexis Deschamps[1].

[1]SIMaP University of Grenoble, Alpes Grenoble, France.

[2]Transvalor SA,Biot, France.

The high specific strength of Al-Zn-Mg-Cu alloys is due to the nanometric precipitation of h- and its metastable precursors. Precipitation kinetics critically depend on alloy composition and processing, which influences the thermodynamic driving force, diffusion kinetics, and transition between metastable precursors. Exploring extensively the composition and processing space is extremely time consuming, requiring the development of high throughput methodology. In this work, graded specimens are developed in the Al-Zn-Mg-Cu system, with variations of alloy composition, quenching rate and plastic deformation. These gradients are designed to span over several cm, allowing spatially-resolved precipitate characterization. Precipitate quantification (size, size distribution & volume fraction) is carried out by in-situ small-angle X-ray Scattering (SAXS) while translating continuously the gradients with respect to the beam resulting in maps of precipitation kinetics in the space of alloy composition or processing parameters are obtained. An example of the measurements obtained is shown in Figure 1.a and 1.b, which presents the evolution of the mean precipitate radius with ageing time at 120°C in a sample with a composition gradient in Zn from 5.6 to 9.5 wt% and plastic deformation from 0 to 15%. With a single experiment all the composition kinetics for intermediate Zn compositions and plastic deformation are obtained, and one can observe that increasing the Zn content results in a lower rate of precipitate growth. The extensive datasets of precipitation microstructure as a function of composition and processing parameters will be used for developing a predictive model, based on a machine learning approach.

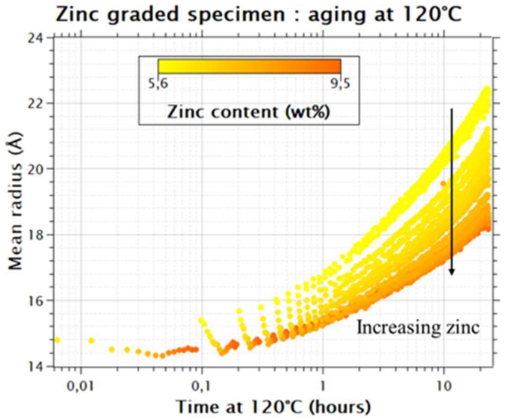

Figure 1.a: effect zinc content on precipitation kinetics at 120°C

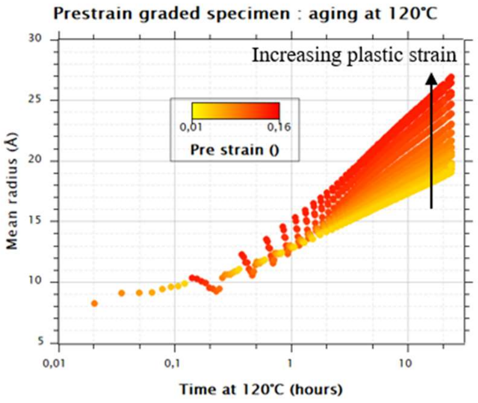

Figure 1.b: effect plastic strain on precipitation kinetics at 120°C

Solid solutions decomposition, nucleation and early stages of precipitation in aluminium alloys unravelled by small-angle X-ray scattering. Frederic De Geuser[1], Crowin[1], Thomas Pejot[1], Hugo Jean[1], Alexis Deschamps[1], Isabelle Mouton[1], Williams Lefebvre[2].

[1]Univ. Grenoble Alpes, CNRS, Grenoble INP, SIMAP Grenoble France.

[2]Univ Rouen Normandie, INSA Rouen Normandie, CNRS, Normandie Univ, GPM Rouen, France.

Precipitation strengthening is one of the metallurgist tools to tailor mechanical properties of alloys. The theoretical framework is well established, but while it enables a general understanding of the mechanisms, the predictive power of the theory is not always good enough and simulations very often only give trends. This is particularly true for the classical nucleation theory which predictions do not always compare satisfactorily with experiments mostly because precipitation strengthened alloys often reach both fundamental and experimental limits; fundamentally, the low mobility of the solutes and the small critical size of the nuclei in e.g. aluminium alloys questions the limit of validity of a continuous description of the matrix and of the notion of interfaces, leading to the rise of non-classical amendments to the nucleation theory. Experimentally, we are also at the limit of what we can confidently characterise. Here we use small-angle X-ray scattering, which enables to probe the complete composition fluctuations in reciprocal space. Classical precipitates-matrix 2-phase interpretation models for the SAXS signal, while very successful for later stages of precipitation, often lead to contradictory results at very early stages. By using model free Monte-Carlo SAXS interpretation models, it is possible to recover the size distribution of nuclei, unravelling the reorganisation of the solid solution as well as measuring *in situ* the critical size for growth of precipitates. Even without the need for an interpretation model, direct observation the SAXS intensity gives insights into the amplification or attenuation of fluctuations wavelength as predicted by the Cahn-Hilliard theory.

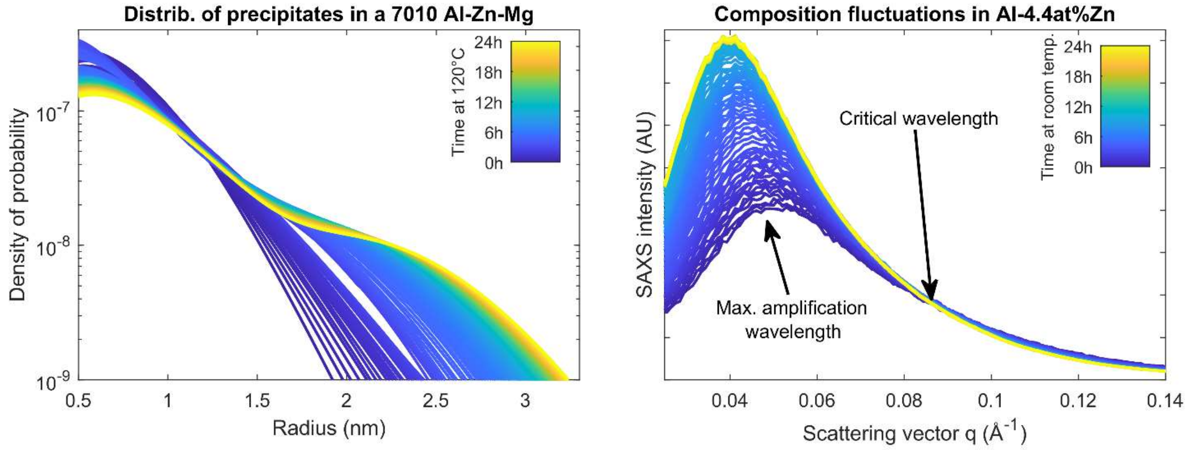

a) Precipitate size distribution in an Al-Zn-Mg alloys. b) SAXS intensity in an Al-Zn alloys during RT ageing

Tu3c.1-4: Materials for energy (II)

Thermal stability of non-equiatomic CrFeNiMn high-entropy alloys alloyed with Al and Al/Ti: microstructural and mechanical characterization. Roger Castellote-Alvarez[1, 2], Isaac Toda-Caraballo[1], Christopher Petersson[3], César Fernández Jiménez[1,2], Peter Szakalos[3], Rebeca Hernández-Pascual[4], Antonio Fernández-Viña[4], Marta Serrano[4], David San-Martin[1].

[1]National Center for Metallurgical Research (CENIM-CSIC), Madrid, Spain.

[2]Complutense University of Madrid, Madrid, Spain.

[3]Royal Institute of Technology (KTH), Stockholm, Sweden.

[4]Centro de Investigaciones Energéticas, Medioambientales y Tecnológicas (CIEMAT), Madrid, Spain.

Face-centered cubic (FCC) high-entropy alloys (HEAs) with alumina-forming capabilities present significant potential for use in Generation IV nuclear reactors, such as lead-cooled fast reactors (LFR) and molten salt reactors (MSR). Alloys intended for these applications must demonstrate exceptional microstructural stability and mechanical properties at elevated temperatures while forming a uniform and stable alumina scale to protect against the harsh conditions of reactor environments. In this study, two novel cobalt-free alumina-forming CrFeNiMn HEAs, alloyed with aluminum (Al) or aluminum and titanium (Al/Ti), were designed using thermodynamic calculations via ThermoCalc, based on the following design criteria: (i) ensuring an FCC microstructure free of sigma or B2-cubic phases above 700 °C; (ii) incorporating aluminum at low concentrations (6–8 atomic %) to promote the formation of a stable and protective alumina scale at high temperatures; and (iii) introducing titanium (1–2 atomic %) to enable precipitation hardening through the formation of the intermetallic phase γ'-$Ni_3(Ti,Al)$ at 700–900 °C. The initial microstructures, optimized through mold casting, cold rolling, and annealing, were subjected to various heat treatments at temperatures between 700 and 900 °C for up to one month to evaluate their thermal stability. Comprehensive microstructural characterization was performed using complementary experimental techniques. Additionally, the mechanical performance of the alloys was assessed through microhardness, small punch and tensile testing. Finally, the ability of these alloys to form a protective alumina scale was evaluated by exposing them to oxygen-containing molten lead for up to 1100 hours at 550 and 650 °C in a controlled environment.

Computational study of zirconium phase change using phase-field modeling. Jiho Kim, Kunok Chang.

Kyung Hee University, Yongin, South Korea.

Zirconium is used as a cladding material for the modern nuclear reactor due to its low thermal neutron absorb cross-section, which is crucial for the neutron economics of nuclear power plants. Zirconium alloy is stable at low temperatures with one single phase, HCP structure(α) zirconium. However, at a high temperature above 1100K, the BCC structure(β) zirconium starts to form. When zirconium faces a high oxygen concentration above 1100K, the β phase precipitation and oxidation process can occur. Consequently, a monoclinic zirconium oxide forms, harming the integrity of nuclear fuel cladding. The oxide film formed on the zirconium cladding surface can adversely affect the mechanical integrity. Specifically, it requires limiting the amount of maximum oxidation, or the 'equivalent cladding reacted'(ECR), which should not exceed 17% at 'loss of coolant accident'(LOCA). This criterion is proposed for maintaining mechanical integrity even during rapid cooling, assuming reflooding in the event of a LOCA. We conducted the simulation to describe the microstructural change of zirconium at the Zr-O binary system. We used three different phases: α, β, and monoclinic oxide. We also did the simulation with both one-dimensional and two-dimensional geometry. We simulated how the α, β, and oxide phases spatially and temporally evolve in zirconium cladding during oxidation. We compared the result with Wagner's metal oxidation theory. In addition, we've confirmed that the oxygen chemical potential at the boundary changes the oxidation rate. Using the phase-field modeling, we can evaluate the zirconium phase distribution under the high-temperature oxidation process.

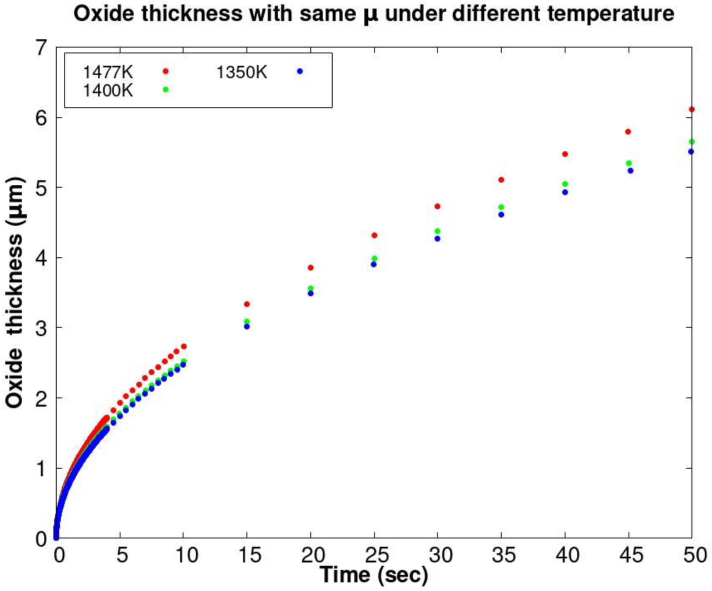

Oxide growth rate plot under the same oxygen chemical potential condition. Oxide growth rate increased along with the temperature.

Phase field modeling of elastochemical effects at the Sn anode of Lithium-ion batteries. Anil Kunwar[1], Nele Moelans[2].

[1]Silesian University of Technology, Gliwice, Poland.

[2]KU Leuven, Leuven, Belgium.

As Sn metal has a very high specific capacity (~ 994 mAh/g), it is considered a potential candidate for anode material of Lithium-ion battery (LiB). However, during the discharge process, the reaction between Sn with Li leads to the formation of Li_xM_y (e.g. Li_2Sn_5, LiSn, Li_7Sn_3 ,$Li_{22}Sn_5$ etc.) phases. These compound phases have inherently higher molar volume per mole of Sn (Ω) as compared to pure Sn metal. For example, the lithiation of Sn (Ω=16.29 cm^3/mol) to Li_2Sn_5 (Ω=20.135 cm^3/mol) is characterized with a net volume gain of 3.845 cm^3 per mole of Sn, and the volumetric expansion is even larger for further transformation to LiSn. The structural phase transformation process is associated with the evolution of mechanical stress. This work utilizes phase field method to study the elastochemical effects at the anode region of the LiB during the discharge process. For the phases of binary Li-Sn system, the total bulk free energy is considered as the sum of chemical, elastic and electric free energies. The total free energy is approximated to have a composition dependence on the mole fraction of lithium. Diagonal strain tensor is used to describe net volume gain from the constant molar volume of initial structure. The lithium deposition at the anode is described using the Butler-Volmer kinetics. The presentation discusses the new insights obtained from the phase field simulations of Li-Sn system and how they can be utilized to attain a better understanding in the role of compressive stress on dendrite growths.

Phase-field modeling of morphology evolution of intergranular and intragranular hydrides in polycrystalline zirconium. Wooseob Shin, Kunok Chang.

Kyung Hee University, Yongin-si, South Korea.

Zirconium is mainly used as fuel cladding in nuclear reactors due to its advantages such as low absorption cross-section, high corrosion resistance, and good strength. However, zirconium hydrides formed inside the cladding degrade the integrity of the cladding making it brittle and prone to cracking. Therefore, understanding the hydride formation is necessary. The hydrides can be classified into two types: intergranular and intragranular. We developed a model that comprehensively considers the texture of the Zr and the crystallographic orientation of the hydride in polycrystalline Zr to show the formation of hydrides and the interaction between grain boundaries and intergranular hydrides. We considered the morphology evolution of the hydrides and grain growth simultaneously and analyzed the effects induced by the Zr texture and grain boundary segregation on the hydride morphology. In addition, we analyzed the correlation between the type of intergranular hydrides and the interacting angle which is the angle between the basal plane and grain boundary using phase-field modeling. We adopted Multiphysics Object Oriented Simulation Environment (MOOSE) framework in this study.

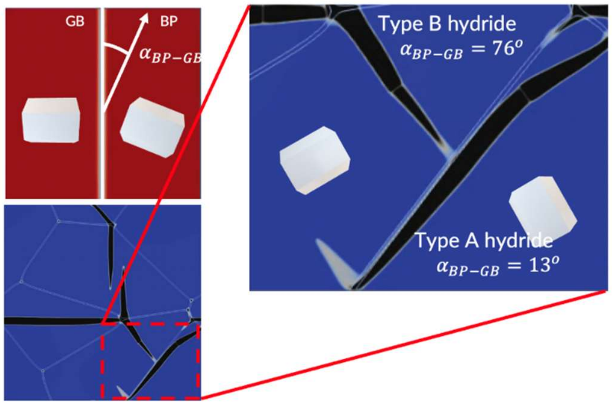

Tu4a.1-3: Martensite (IV)

Austenite stability in medium manganese steels. Dilan Munoz, Diego Zúniga, Felipe Castro.

Universidad de Santiago de Chile, Santiago, Chile.

Medium manganese steels (MMnS) are promising materials in advanced high-strength steels. These steels offer high strength, exceptional ductility, and energy absorption capacity, making them ideal for reducing vehicle weight and improving fuel efficiency. This can be achieved without compromising safety standards while contributing to sustainability goals. Despite these steels' promising mechanical properties, there is a significant need to understand the mechanisms governing their mechanical behavior. Microstructural features such as austenite stability play a crucial role in determining the strength and ductility of these steels. This research seeks to study the effect of the stability of austenite on strength and ductility. It includes the study of MMnS with a chemically patterned microstructure consisting of martensite and carbon-enriched austenite (Figure 1). This microstructure emerges because of a previous step of Mn partitioning during the pearlitic transformation, followed by a short annealing above A3 which only allows for the homogenization of carbon. A final tempering stage partitions carbon from martensite to austenite stabilizing it. Heat treatments are followed by microstructure characterization using metallographic analysis and X-ray diffraction, and a mechanical analysis using standard tensile tests. In-situ high-resolution neutron diffraction concomitant with tensile tests was also carried out for an in-depth assessment of the microstructure evolution under quasi-static standard tests. Atom Probe Tomography analysis was performed to study the alloying element partitioning from martensite to austenite during the tempering stage. Initial results indicate a late-activated TRIP effect linked to stabilized austenite, while more in-depth results are yet to be analyzed.

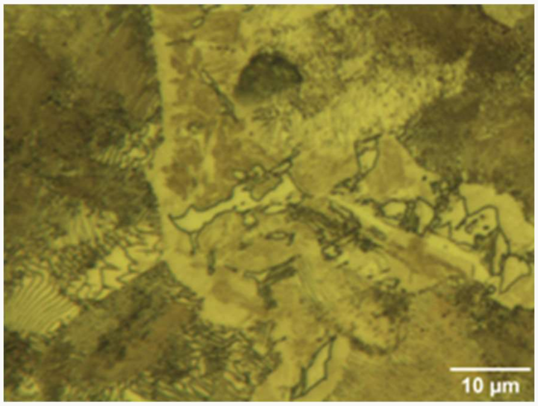

Figure 1. Chemically patterned microstructure consisting of martensite and carbon-enriched austenite.

Martensitic Transformation in Metastable Austenitic Stainless Steel during Electrochemical Process. Heung Nam Han[1], Guihyung Lee[1], Ho Jun Gwon[2], Dameul Jeong[3], Young-Kyun Kwon[3], In-Ho Jung[1], Sung-joon Kim[2].

[1]Seoul National University, Seoul, South Korea.

[2]Pohang University of of Science and Technology, Pohang, South Korea.

[3]Kyung Hee University, Seoul, South Korea.

We found that remarkable martensitic transformation occurs during both anodic electrochemical polishing (AEP) and cathodic hydrogen charging (CHC) in metastable austenitic stainless steels. In case of anodic electrochemical polishing, interestingly, a comparison of EBSD, XRD, and ferritescope measurements confirmed that the martensitic transformation is confined to the surface. To investigate how the AEP process induces martensitic transformation, COMSOL Multiphysics was used to calculate the electric charge distribution on the specimen surface at various voltages. To accurately consider the surface shape of the specimen, we used AFM to measure the three-dimensional distribution of asperities, which was utilized as the initial condition for COMSOL Multiphysics simulation. Finally, first-principles calculations reflecting the obtained charge distribution in the surface region concluded that significant stress from surface charge build-up could induce stress-induced martensitic transformation on the surface of the metastable austenitic stainless steel during AEP. In case of cathodic hydrogen charging, EBSD analysis confirmed that significant martensitic transformation occurred when hydrogen was charged under the conditions exceeding the critical current density and time. To confirm the hydrogen polarity (charge effect) within the specimen, an external magnetic field was applied to generate a Lorentz force along various directions. From hardness tests and microstructural analysis, we observed a gradient in martensitic fraction along the Lorentz force. Additionally, comparisons of martensitic fraction using EBSD, XRD, and ferritescope measurements confirmed that the transformation was limited to the surface region. Consequently, it was found that charged hydrogen near the surface induces martensitic transformation during CHC.

Deformation induced martensite transformation in chemically heterogeneous austenite: a 3D molecular dynamics study. Jun Chai1, Tsinghua University, China (online). Hao Chen[1], Shichun Liu[2], Haokai Dong[3], Junsheng Wang[4], Zhigang Yang[3], Sybrand van der Zwaag[5].

[1]Tsinghua university, Beijing, China.

[2]Key Laboratory of Advanced Materials of Ministry of Education, Beijing, China.

[3] State Key Laboratory of Advanced Marine Materials, Ningbo , China.

[4]State Key Laboratory of Metallic Materials for Marine Equipment and Applications, China.

[5]Faculty of Aerospace Engineering, Delft University of Technology, Delft, Netherlands

This study investigates the deformation-induced martensitic transformation in compositionally core-shell austenite particles using molecular dynamics (MD) simulations, focusing on the role of chemical boundary engineering (CBE) in regulating this process. The 3D MD model concerns uniaxial loading of a spherical initially austenitic particle embedded in a ferritic matrix. In the model the core and the shell have different Ni concentrations and the core to shell ratio has been varied. The results show that Ni-rich shell structures delay the formation of the martensite, while Ni-rich core structures promote martensite formation in the shell region. There is little to no effect of the particle architecture and the core and shell behave primarily transform as determined by their own chemical composition. The composition of the shell affects the transformations at the particle-matrix interface. The internal chemical boundary does not trigger martensite nucleation, but is very effective in constraining the martensite formation to the particle fraction with the lowest mechanical stability. This work highlights the potential of CBE in designing advanced high-strength steels with tailored martensite transformation at the level of individual retained austenite grains.

Tu4b.1-3: Al alloys (IV).

High throughput study of long-term thermal ageing of precipitation hardened Aluminium alloys. Deschamps[1], Thomas Perrin[1,2], Arthur Després[1], Pierre Heugue[2], Frédéric De Geuser[3]

[1]Grenoble Institute of Technology – UGA, Grenoble, France.

[2]Safran Transmission Systems, Colombes, France.

[3]CNRS SIMAP, Grenoble, France.

Precipitation hardening Aluminium alloys subjected to long service times at intermediate temperatures are subject to microstructure evolutions that result in loss of mechanical properties. Predicting the service lifetime requires predictions for both microstructures and strength along ageing times extending to 10^5h. Microstructure evolutions can involve phase coarsening, transformation from metastable phases to more stable variants, and morphology evolutions. In the present work, a high throughput methodology has been setup to study extensively the long-term ageing behaviour of two Aluminium alloys, AA2219 and AA2618A, both initially in the T8 state. Samples were subjected to ageing up to 10000h in a furnace designed to present a stable temperature gradient between 170 and 240°C, allowing to continuously determine the effect of ageing temperature on precipitation and strength. The microstructure of these samples has been quantitatively characterized using spatially-resolved synchrotron small-angle and wide-angle X-ray scattering (SAXS & WAXS), providing the size, volume fraction and structure type. These measurements were complemented by local transmission electron microscopy and atom probe tomography. The systematic database obtained enables to determine the coarsening kinetics in both alloys, which is controlled by Cu diffusion and thus can be modelled by an equivalent time approach. At long ageing times and high temperature, a bifurcation is observed in AA2618A alloy where Si-rich L phase evolved towards Si- and Cu-rich Q phase, accelerating the loss of properties. In the AA2219 alloy, a high stability of strength is obtained, which is correlated with a Mn segregation of the θ' precipitates.

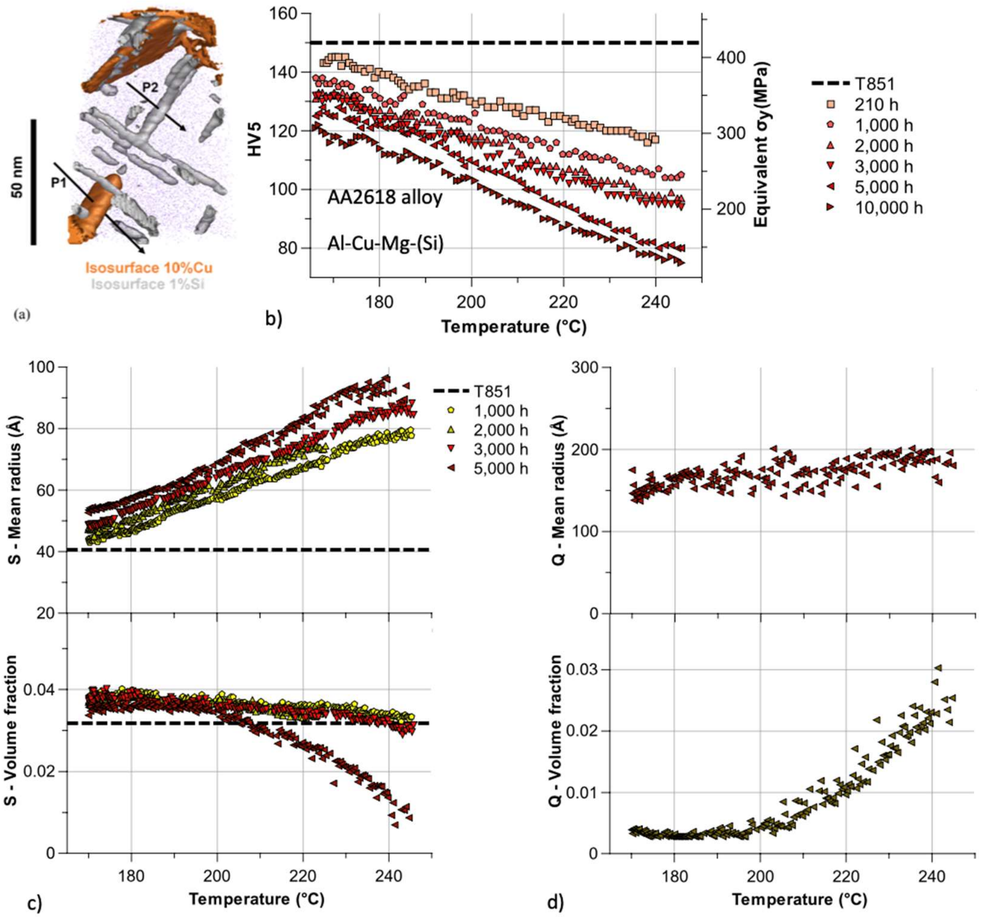

Figure 1 : Strength and microstructure evolution during long term ageing of the AA2618 alloy, studied continuously as a function of ageing temperature. (a) microstructure in the T8 state showing L and S phases ; (b) Evolution of hardness and corresponding yield strength ; (c) Evolution of diameter and volume fraction of S precipitates, showing the strong destabilization at 5000h above 200°C ; (d) Evolution of the Q phase after 5000h showing the complementary evolution to the partial destabilization of the S phase.

Dynamic room-temperature precipitation of 7XXX aluminum. Adam Bouayoune, Michel Perez, Jean-Yves Buffière.

MateIS, INSA Lyon, France.

Aluminum is a lightweight metal that is easy to shape, making it a major asset for lightening vehicles. The high resistance of certain aluminium alloys, such as the 2XXX and 7XXX series, is obtained by precipitation hardening. After solution treatment, the alloy is quenched to obtain a saturated solid solution. Usually, the alloy is then artificially aged at a relatively high temperature to improve the diffusion of the alloying elements in the aluminum matrix (thermal energy, vacancy formation...) to form precipitates. Plastic deformation can enhance precipitate formation during ageing by inducing excess vacancies and dislocations. The purpose of this work is to understand and describe the influence of plastic deformation on precipitation at room temperature. The samples are deformed by strain-controlled low-cycle fatigue tests at room temperature either after quenching or after a short heat treatment to annihilate quenched-in vacancies. Small-angle X-ray scattering (SAXS) is employed to measure the volume fraction and radii of the precipitates. This indirect method is complemented by transmission electron microscopy (TEM) observations to understand the distribution homogeneity of the precipitates. It is considered that the influence of deformation is primarily due to the excess vacancies induced in the matrix, which increase the mobility of the solute atoms. The evolution of precipitate growth is modelled using a KWN-type model, which adds the concentration of these vacancies as a multiplication factor for the diffusion coefficient.

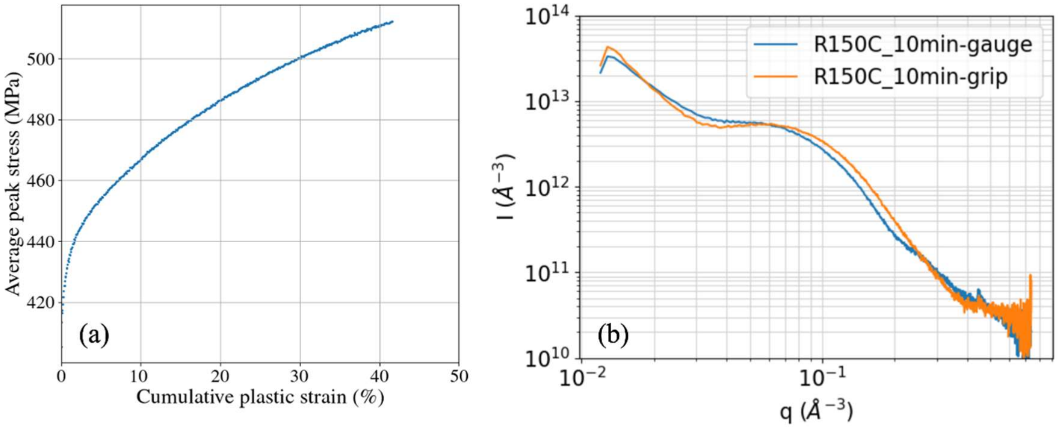

(a) Evolution of the tensile stress during cyclic deformation on a sample after an oil bath of 10 minutes at 150°C at a frequency of 0.2 Hz and a plastic strain amplitude of $\Delta\epsilon_p = 10^{-4}$, (b) the corresponding SAXS curves of the grip (non-deformed) and gauge (deformed) part of the sample.

Impact of recycled contents in 6xxx series aluminum alloys: studying and modeling precipitation.

Seyyed Ezzatollah Moosavi[1], Cyril Cayron[1], Jonathan Friedli[2], Loïc Aron[2], Zeqin Liang[2], Elisa Cantergiani[2,3], Roland Logé[1].

[1]Epfl, Laussane, Switzerland.

[2]Novelis Sierre, Switzerland.

[3]Monash, Monash, Australia.

The automotive industry extensively utilizes 6xxx series aluminum alloys, particularly for car body components due to their excellent corrosion resistance and processability. However, the high CO_2 footprint of primary aluminum production necessitates increased use of recycled aluminum. Recycling introduces impurities such as Fe and Mn, which affect precipitation, recrystallization, texture, and final sheet properties, including formability, surface quality, and bending capabilities. Managing these impurities while optimizing recycled content is critical to broadening alloy composition. In this research, a precipitation model was developed for prime-based and recycled AA6014 using classical nucleation and growth theories, incorporating thermodynamic and kinetic computations. The model simulates the nucleation, growth, and coarsening of β-Mg_2Si precipitates at sites such as grain boundaries, sub-grain boundaries, dislocations, intermetallics, and dispersoids, with varying diffusion rates. It was refined to better account for impurities and intermetallics introduced by recycling. The model allows tracking of precipitate number density, volume fraction, and size distribution of each precipitate family. In parallel, an advanced image analysis technique was developed to statistically differentiate precipitates and their distribution in the matrix. This method couples Backscatter Electron (BSE) imaging and Electron Backscatter Diffraction (EBSD) to distinguish different types of precipitates. Results indicate that β-Mg_2Si precipitates evolve differently depending on nucleation sites. Increased recycled content altered the chemical composition of intermetallics and increased their number density, providing more nucleation sites for β-Mg_2Si precipitation. Model adjustments based on these observations improved its predictive capabilities, and future work will evaluate the model's applicability to other alloys and thermomechanical treatments.

Tu4c.1-3: Magnetic effects

Concise magnetic model for thermodynamic calculations of iron from 0 to 1800 K. Stefan van Bohemen.

Tata Steel R&D, the Netherlands.

The proposed magnetic model represents magnetic entropy using two exponential functions: one for long-range order below the transition temperature and another for short-range order above it. This approach ensures that both the magnetic entropy and its temperature derivative approach zero smoothly as temperature nears absolute zero. Differentiating this expression yields a magnetic heat capacity curve with a lambda peak, defined by two adjustable parameters that control its temperature dependence on either side of the transition. This magnetic contribution is integrated with established components of heat capacity, including electronic, harmonic, and anharmonic lattice terms. The overall thermodynamic model was optimized using experimental data for bcc and fcc iron, encompassing transition temperatures, heat capacity measurements from 10 to 1800 K, enthalpy differences, Bohr magneton values, and the magnetic enthalpy fraction attributed to short-range order.

Effect of pre-straining on magnetic ageing of Fe-Si steels. Ajay Kumar Jagannath Rao[1], Myriam Dumont[1], Lea Saleh[2], Oualid Messal[2], Abdelkader Benabou[2], Stéphane Clenet[2], Laurent Barrallier[3].

[1] Arts et Métiers Institute of Technology, EA7350 - MSMP Lille, France.

[2] Univ. Lille, Arts et Metiers, Centrale Lille, HEI, ULR 2697 - L2EP Lille France.

[3] Arts et Métiers Institute of Technology, EA7350 - MSMP Aix-en-Provence, France.

The study examines the impact of plastic strain on the magnetic ageing of Fe-Si alloys in the context of electrical motor efficiency, where iron losses are critical. Fe-Si steels, containing 1.6%-2.6% silicon and 50-80 ppm carbon, experience magnetic property degradation during operation of the machine due to carbide precipitation at moderate temperatures. Silicon content mitigates magnetic ageing, while carbon segregation influences magnetic losses significantly. Three specimens with 0%, 2%, and 5% plastic strain were analyzed. Strain uniformity was ensured via Digital Image Correlation (DIC), and ageing was conducted at 160-200°C. Scanning Electron Microscopy (SEM) characterized the evolution of carbide precipitates mean radius and volume fraction, while magnetic losses were measured using a Single Sheet Tester (SST). Results show that pre-straining facilitates carbon segregations due to increased dislocation

density. This leads to two magnetic loss mechanisms: domain wall pinning by dislocations and precipitation during ageing. Pre-strained samples exhibited higher initial and ageing-induced magnetic losses compared to non-strained specimens depending on quantity of dislocation densities. SEM revealed that increased plastic strain reduces remaining carbon to form precipitates due to carbon segregation towards dislocations, limiting long-term magnetic ageing. This investigation highlights the role of dislocations, carbon segregation and precipitation in regulating the microstructural and magnetic behavior of Fe-Si alloys, providing insights into improving production and operational conditions to reduce iron losses.

Nanoscale investigation of the impact of High Magnetic Field on the 15-5 PH stainless steel. Sonia Guehairia, Zhou Tao.

KTH Royal Institute of Technology, Stockholm, Sweden.

The development of high-performance Fe-based alloys with superior mechanical properties, such as strength and toughness, is essential for advanced engineering applications. Fresh martensite, formed through fast cooling of the high temperature phase austenite, is normally brittle, and a tempering treatment is usually needed to induce sufficient ductility and toughness. However, the strength is decreased by tempering unless the steel is alloyed with precipitation-forming elements, to stimulate clusters and nano-particles during the tempering process. In our study, a 15-5 PH stainless steel is subjected to different tempering time at 500°C under a high magnetic field, leading to a microstructure that promotes the nucleation and growth of copper (Cu) precipitates. Using atomic-scale experimental characterization, especially Atom Probe Tomography (APT), we quantitatively mapped the evolution of Cu precipitates (fig.1), analysed their composition, size, density etc. Notably, results show that applying a magnetic field during tempering dissolves the Ni-rich shell surrounding the Cu precipitates, altering the diffusion kinetics of Cu during precipitation. This modification in kinetics offers promising control over precipitate size, and composition enhancing the alloy's strength and toughness without compromising ductility. These data are crucial for developing precipitation kinetics models, supporting predictions of stress-strain behaviour for high-performance steel. This comprehensive approach - combining magnetic field effects, rapid quenching, and advanced characterization - provides a robust framework for designing Fe-based alloys with tailored properties, advancing the alloy development process.

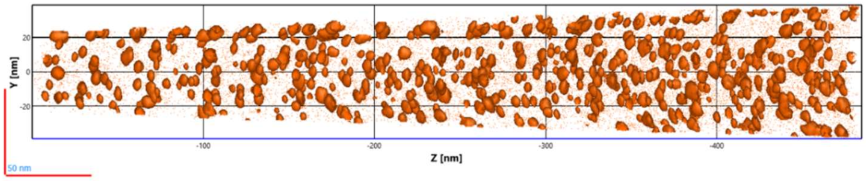

Figure 1: 3D mapping of Cu atoms obtained by APT analysis of the sample tempered for 150 minutes at 12T.

Plenary 4. ALEMI: 25 Years of Collaborative Research on Alloying Element Effects on Migrating Interfaces. Hatem Zurob.

McMaster University, Hamilton, Canada.

The first Alemi meeting was held in October 2000. This informal gathering aimed to stimulate research on the modeling of the phase transformations in steels with emphasis on the fundamentals of alloying element interactions with moving interfaces. Most importantly, the organizers of the first meeting (all senior researchers in the field) viewed the workshop as an opportunity to attract young researchers to work on this topic. Over the last 25 years, a total of 22 meetings were held to share results and ideas and to discuss some of the scientific and technical challenges in the field. This contribution will review the progress that has been made on the topic of austenite decomposition within the Alemi community. Special emphasis will be placed on problems that were identified as part of the Alemi gatherings/workshops. These include (i) developing novel experimental methods to identify the contact conditions at the migrating ferrite/austenite interface, (ii) modelling ferrite growth taking into account the role of kinetic transitions and the solute drag effect, (iii) experimental and theoretical examination of the chemistry and structure of ferrite/austenite interfaces, (iv) developing a comprehensive model for the formation of bainite and (v) application of high throughput techniques to the study of phase transformations.

ALEMI 13th workshop
Kyoto
May 26 & 27, 2014

Opening Remarks at the 13th ALEMI Workshop in Kyoto, 2014

Wednesday, July 9

Plenary 5. Strategies for designing sustainable steels: leveraging chemical heterogeneity, atomic clustering, nanoscale precipitation, and phase Stability. Elena Pereloma[1], Ilana Timokhina[2].

[1]University of Wollongong, Wollongong, Australia.

[2]Luleå University of Technology, Luleå, Sweden.

A global priority in steel industry is the development of cost-effective, sustainable steels using readily available natural resources. Over the last couple of decades, the advances in nano- and atomic-scale material characterization techniques have unlocked new possibilities for understanding complex phenomena at unprecedented depth, driving innovation in alloy design and processing. This, consequently, underpins the design of innovative steel compositions and optimizing processing routes for a wide range of applications with enhanced mechanical properties and performance. This talk will highlight approaches in using atomic clusters and chemical heterogeneities in steels microstructure to improve the balance of strength and ductility. It will also explore multi-component nanosized precipitation in steel design and how to control retained austenite stability in transformation-induced plasticity-assisted steels.

W1a.1-5: Bainite formation (I)

Invited. **Effect of deformation on bainitic transformation.** Benrabah[1], Deboer[2], Geandier[1], Van Landeghem[3], Hutchinson[4], Brechet[4], Zurob[2].

[1]Université de Lorraine, CNRS, IJL Nancy F-54000, France.

[2]McMaster University 1280 Main Street West, Hamilton, ON Canada.

[3]SIMaP, Université Grenoble Alpes, CNRS, Grenoble France.

[4]Monash University Clayton, VIC 3800 Australia.

Bainitic transformation is important in developing steels with superior mechanical properties. Plastic deformation, particularly ausforming—where austenite is deformed before transformation—significantly affects transformation kinetics and microstructure. Similarly, dynamic transformation, where bainite forms concurrently with deformation, plays a critical role in thermo-mechanical processing. Despite this, a comprehensive understanding of these effects remains incomplete, and quantitative models addressing these phenomena are scarce. This study investigates deformation effects on bainitic ferrite growth kinetics under two conditions: (1) deformation preceding transformation (ausforming) and (2) concurrent deformation and transformation. High-energy X-ray diffraction experiments were performed to analyze deformation effects at various temperatures. Electron backscatter diffraction (EBSD) was used to characterize the resulting microstructure and texture. Results show ausforming accelerates nucleation and refines the microstructure, but stored dislocations impede ferrite plate growth, slowing transformation in later stages. Conversely, concurrent deformation accelerates the whole transformation kinetics and results in higher bainite fraction compared to non deformed case. A modified Zener-Hillert model was developed to rationalize these findings, highlighting the interplay between deformation, dislocations, and transformation mechanisms. In case of ausforming, the interaction between the moving disconnection and the generated defects results in a higher barrier to the transformation. Conversely, concurrent deformation accelerates growth kinetics, as applied deformation acts as a driving force for disconnection motion.

Microstructural evolution and crystallographic metrics in bainitic and martensitic steels. Adam Ståhlkrantz, Tuomo Nyyssönen.

Swerim AB, Stockholm, Sweden.

Martensite and bainite are technologically highly important microstructures in steels with carbon contents between 0.6 – 1.0 wt-% C. In this work, the crystallographic and structural aspects of four low-alloy compositions in this carbon range have been characterized following quenching or austempering at temperatures in the 275 – 450 °C range. The parent-child orientation relationship, variant pairing characteristics, as well as the habit plane and the aspect ratios of the three-dimensional variant structures were investigated by parent grain reconstruction of two-dimensional orientation maps. The samples were analyzed by scanning electron microscopy (SEM) together with electron backscatter diffraction (EBSD) to obtain the crystallographic information. This data was then processed and analyzed using the MTEX crystallography toolbox on Matlab. The post-processing of the crystallographic information showed distinct changes in microstructure, orientation relationships and variant pairing tendencies due to differences in austempering conditions. In addition, significant variation was observed in the habit planes and aspect ratios of the three-dimensional structures depending on the austempering temperature. The combinations of the determined orientation relationships and habit planes were then compared to the predictions of the phenomenological transformation model proposed by Wechsler, Lieberman and Read. Understanding the relationships between alloying, austempering, and changes in microstructure is important for material development and to increase the effectiveness and development of new steel grades. This is important for the continued development of different grades that can be designed to have more of the desired properties for specific applications.

Bainitic and reverse transformation in Fe-Ni-Al-Cu-C steel: in-situ TEM/STEM observation of structure evolution. Aleksandra Królicka[1], Andrzej Żak[1], Francisca G. Caballero [3]

[1] Wrocław University of Science and Technology, Wrocław, Poland.

[2] National Centre for Metallurgical Research (CENIM-CSIC), Madrid, Spain.

Dynamics in matter and processes observed using in-situ microscopy methods provide an immense capability for better understanding the crucial mechanisms in the nanoscale. Although steel is classified as a well-known engineering material, there are still pivotal research challenges related to developing new steel grades with higher in-use and mechanical properties, which are controlled by the evolution of the microstructure. The Fe-8.0Ni-2.8Al-0.8Cu-0.4C (wt.%) steel was designed considering the synergistic effect of intermetallic strengthening by (Ni, Al)-rich B2-ordered phase in the ultra-fine bainitic matrix. This study aims to reveal the precipitation sequence during tempering up to the reaching reverse transformation using dynamic STEM/TEM observations using a heating holder (NanoEx i/v MEMS). It was noticed that the formation and growth processes of the NiAl phase are strongly dependent on the tempering temperature. Due to the metastable nature of the bainitic matrix, its decomposition was also evaluated and correlated with the precipitation phenomena. The growth of austenite after reaching A_{c1} temperature confirmed the "austenite memory" effect. To observe the bainitic nucleation and growth the in-situ transformation inside the microscope column was performed preserving a similar thermal cycle to conventional heat treatment routes. To indicate the differences between the nature of bainite and martensite transformation, the martensite transformation was also conducted in the heating holder. The results of in-situ STEM/TEM observation were compared to ex-situ investigations of dilatometry samples after complete bainitic transformation. The findings of this study confirm the outstanding capabilities of advanced microscopy methods in revealing the phenomena occurring in engineering materials.

In situ study of carbide-free bainite transformation kinetics. Philipp Retzl, Ernst Kozeschnik, Roman Schuster.

TU Wien, Vienna, Austria.

To optimize the properties of TRIP-assisted steels, a comprehensive understanding of the kinetics of carbide-free bainite transformation is essential. This study primarily focuses on two critical aspects: the evolution of phase fractions, specifically bainitic ferrite and austenite, over time, and the partitioning of carbon into different austenite regions. These austenite regions include untransformed "blocky" austenite and film-like austenite located between ferritic subunits formed during bainite transformation. Due to the potential transformation of some austenite into martensite during quenching to room temperature, it is challenging to accurately determine the carbon content and phase fraction of austenite at specific points during the transformation using ex-situ investigations. To address this challenge, in situ X-ray diffraction (XRD) measurements are employed to study these aspects during isothermal bainite transformation of a steel containing 0.4 wt% C, 1.5 wt% Mn, and 1.5 wt% Si at various temperatures. These measurements enable the observation and analysis of phase fractions and carbon distribution with high temporal resolution. This provides precise data on the microstructural development. The samples are heat-treated with a dilatometer during the in-situ investigation to ensure precise control of the thermal conditions.

HE-XRD study of the effect of substitutional alloying on bainitic transformation kinetics in continuous cooling. Marion Bregeault, Hugo Van Landeghem.

Grenoble INP, SIMAP Grenoble, France.

Substitutional alloying elements (Mn, Ni, Mo, Si, Cr) in low-alloy steel forgings play a major role in the nature and kinetics of austenite decomposition. Their local distribution strongly affects the final microstructure established during cooling. This is particularly relevant for nuclear pressure vessels steels that present persistent chemical heterogeneities inherited from ingot solidification. This work studies the effect of local alloying content on bainitic phase transformation during continuous cooling. A high-throughput combinatorial method is used to map the transformation kinetics in composition space of substitutional solutes. The method relies on in-situ time- and space-resolved synchrotron high-energy X-ray diffraction (HEXRD) and compositionally graded samples. Varying conditions of carbon content and cooling rate are applied. The large amount of collected data is used to train a machine learning model predicting transformation kinetics for a given composition and cooling rate, using a decoder architecture with transposed 1D convolutions. A physical kinetic model is also developed. Both the nucleation and growth of bainite plates are considered. The evolution of transformation conditions in the austenite along time is incorporated, as the carbon content in the different phases (austenite, bainitic ferrite and carbides) is extracted from the in-situ HEXRD data.

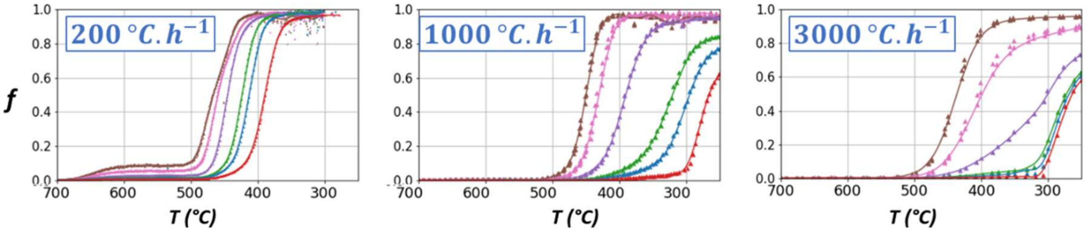

Figure 1. Transformation kinetics measured during continuous cooling in different regions of a compositionally-graded sample for 3 constant cooling rates.

W1b.1-3: Recrystallisation and grain growth (I)

Variant selection and crystallographic texture evolution during phase transformation in low carbon steels. Nguyen-Minh[1], Petrov[1,2], Kestens[1,2].

[1] Ghent University, Ghent, Belgium.

[2] Delft University of Technology, Delft, Netherlands.

Transformation of solid-state materials commonly occurs with a specific crystallographic orientation relationship between parent and product phases. Thanks to this relationship, the orientation preference of the parent phase will transfer to the product ones. Structure and statistical symmetries, on the other hand, result in multi-variant transformations and texture weakening effects in the product microstructures. Only when these symmetries change to the lower order ones will specific variants be selected and thus a strong texture will develop. Structure transformation and symmetry breaking have been since long an interesting topic for materials research. These studies do not just bring insight in physical phenomena but also provide a powerful tool to control microstructure and texture of metallic materials via thermomechanical processes. In this study, variant selection, and texture development during phase transformation of low carbon steel grades are investigated. Microstructure and texture of the materials after cold rolling and annealing are characterized by EBSD technique. Evolutions of phase transformation textures are predicted by statistical model calculations. Depending on heat treatment parameters, particularly on the heating and cooling rates, different textures develop in the annealed samples. The absence of recrystallization before the α→γ transformation retains the deformation texture with the highest texture intensity at the {112}<110> component to the annealed sample. Additionally, the cyclic heat treatment results in texture weaking associated with a fine grain size in the steel microstructure.

Dynamic recrystallization of Zn-Mn-Ca biodegradable alloy during cold rolling. Mahmood Fatemi, Solenn Benedic, Jose Maria Cabrera.

Universitat Politècnica de Catalunya (UPC), Barcelona, Spain.

Thermomechanical processing is regarded as an effective secondary technique to enhance the mechanical properties of zinc alloys for biodegradable implant applications. In this study, a novel Zn alloy containing 0.5 wt.% Mn and 0.5 wt.% Ca was successfully processed through rolling at room temperature with varying area reductions of 30%, 60%, and 85%. The evolution of second-phase particles and the recrystallization behavior of the Zn matrix were systematically investigated. Mn-rich particles were fragmented and uniformly distributed throughout the microstructure. Additionally, fine and ultrafine grains were formed during rolling, with an almost fully recrystallized matrix achieved at an 85% area reduction. The recrystallization mechanism and the development of crystallographic texture were analyzed using EBSD (electron backscatter diffraction) and discussed in the context of the role of slip systems during deformation and recrystallization. The mechanical properties of the rolled materials were evaluated through micro-tension tests, and the results were correlated with changes in grain structure, texture, and the distribution of second-phase particles.

Texture control through phase transformation in low-carbon steel sheet. Leo Kestens[1], Tuan Nguyen Minh[1], Roumen Petrov[1], Felipe Castro Cerda[2]

[1] Ghent University, Ghent, Belgium.

[2] University of Santiago de Chile, Santiago, Chile.

By virtue of a specific crystallographic orientation correspondence, an existing crystallographic texture in the parent phase will induce a crystallographic texture in the product phase. This offers a degree of freedom to control the texture of low-carbon steel sheet through Thermo-Mechanical Process Controlled rolling (TMPC). By accurately controlling the temperature of subsequent rolling passes during hot rolling, the finish rolling temperature and the coiling cycle, it is possible to either obtain a fully recrystallized FCC texture (cube component) or an FCC rolling texture (β-fiber texture), whether rolling was carried out above or below the recrystallisation-stop temperature Tnr. These FCC textures may transform to different types of BCC product textures of the hot band depending on chemical composition of the alloy and precise TMPC conditions. The orientation correspondence also plays a role during recrystallization annealing after cold rolling, if carried out in the two-phase or the single-phase austenite domain. The occurrence or absence of variant selection may trigger or block the texture memory effect and will either reinforce or weaken the initial texture prior to transformation, associated with grain coarsening or grain refinement, respectively.

W1c.1-4: Advanced experimentation (I).

Invited. **Linking defects and 3D chemical fields of composition by in situ combination of atom probe tomography and transmission electron microscopy.** Williams Lefebvre, Mohammed Ilhami, Gérald Da Costa, Juan Macchi, Celia Castro, Aidar Zakirov, Antoine Normand, Charly Vaudolon, François Vurpillot.

Univ Rouen Normandie, INSA Rouen Normandie, CNRS, Normandie Univ, GPM UM R6634 Saint Etienne du Rouvray, France.

The interaction between defects lies at the core of the relationship between microstructure and properties in metals and alloys. Consequently, much research in metallurgy focuses on accurately describing the structure and chemistry of defects across various scales, from microns to nanometers. The relatively recent application of correlative APT and STEM techniques has proven highly effective in understanding defect interactions across various systems, such as grain boundary segregation, stacking faults, and dislocations. Moreover, by leveraging in situ STEM, it is also possible to observe the kinetics driving microstructural evolution in real time. Building on the success of these correlative APT and STEM approaches, the concept of combining both techniques into a single instrument [1] has gained attraction. In 2024, the authors of the present work have demonstrated the feasibility of joining an atom probe to a standard commercial TEM [2]. This achievement opens the door to a closer integration of these techniques for precise three-dimensional characterization of matter at the atomic scale, particularly for analyzing defect interactions at the nanometric level. This study will showcase some results obtained with this new tool wherein the link between defects and 3D chemical fields of is made to investigate decomposition pathways in alloys.

[1] Kelly, T. F., Miller, M. K., Rajan, K. & Ringer, S. P. Atomic-Scale Tomography: A 2020 Vision. *Microsc. Microanal.* **19**, 652–664 (2013).

[2] G. Da Costa et al., Nature Commun 15, 2024, 9870. https://doi.org/10.1038/s41467-024-54169-2

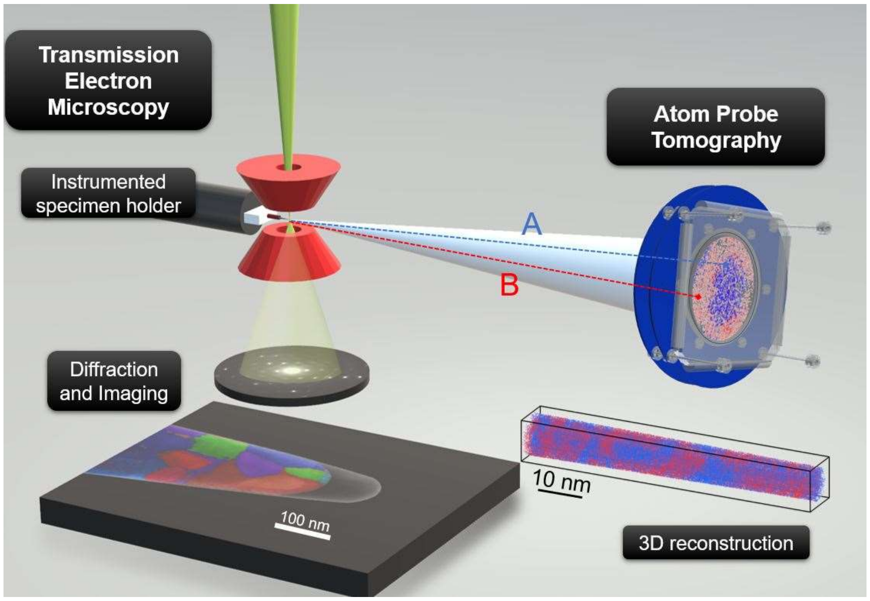

Sketch illustrating the combination of APT and TEM in a singe tool.

Phase stability of CoCrFeMnNi alloy through crystallization of free-standing amorphous thin film.

Abira Rashid, Abhay Gautam.

Indian Institute of Technology, Gandhinagar. Gandhinagar, Gujarat. India

Multicomponent Alloys have gained prominence due to their versatile and significantly improved properties. CoCrFeMnNi is one of the most studied stable HEA with a single phase fcc structure at elevated temperature range (beyond 900°C). However, recent investigations have revealed phase decomposition in this alloy, occurring not only at elevated temperatures over extended durations but also at intermediate temperatures within a few minutes. Despite these findings, the exact temperature range and phase stability of CoCrFeMnNi remain uncertain. Limited studies have explored phase stability in thermo-mechanically processed alloys or in film forms coated on substrates. Both of these route imposes constraints from processing route including film-substrate interaction, high energy nucleation sites, etc. To address these limitations, the current study examines phase stability in Cantor alloy (CoCrFeMnNi) using vapor-deposited, free-standing thin films. This work includes the deposition of equi-atomic alloy films on salt crystal using thermal evaporation route at cryogenic temperature to fabricate amorphous films. These films were released from salt substrate and free-standing films were annealed under vacuum at various temperatures and for different time durations. The annealed films were investigated for the phases that formed during crystallization and possible clustering/segregation. The onset of crystallization in amorphous films resulted in the formation of the fcc phase. However, additional phase was observed along with fcc, even before the complete crystallization was achieved, at a temperature range different from reported in literature till now. These results along with the critical survey of the existing literature will be presented as part of this study.

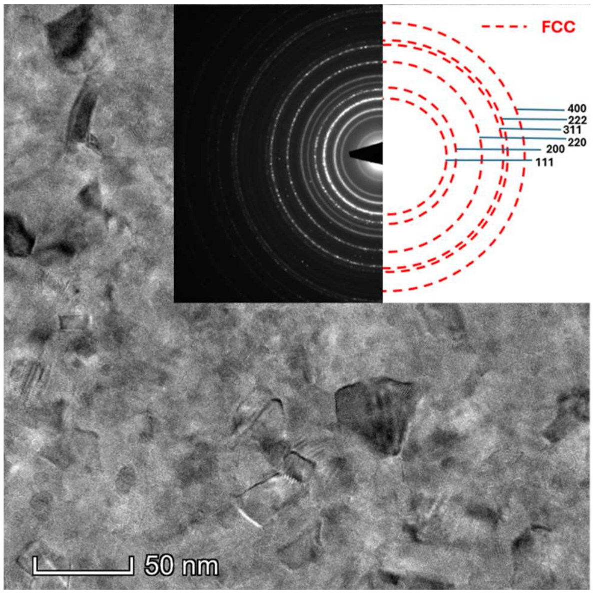

CoCrFeMnNi amorphous film annealed at 400°C for 4hr in vacuum. Inset shows SAED pattern with FCC + additional phases.

Optimization of duplex medium manganese steel microstructures by high-throughput characterization methods. Olha Nakonechna[1], Guillaume Geandier[1], Benoit Denan[1], Imed-Eddine Benrabah[1], Lionel Germain[2], Hugo Van Landeghem[3], Alexis Deschamps[3], Sebastien Allain[1].

[1]IJL, CNRS, Université de Lorraine, Nancy, France.

[2]LEM3, CNRS, Université de Lorraine, Metz, France.

[3]SIMaP, CNRS, Grenoble INP, University of Grenoble Alpes, Grenoble, France.

Medium-Mn steels exhibit a unique microstructure characterized by a refined ferritic matrix and a substantial fraction of retained austenite, offering an exceptional combination of high strength and ductility. The link between their microstructure and mechanical behavior has been extensively studied and is now well understood. However, the accurate prediction and optimization of these properties remain challenging due to the high sensitivity of phase transformation kinetics to both processing parameters and alloy composition. These factors strongly influence the development of the final microstructure during thermal treatment, making it difficult to establish a robust and quantitative relationship between processing, microstructure, and properties. As a result, significant research efforts are still required to address these challenges. Therefore, this study aims to propose a comprehensive combinatorial high-throughput methodology for accelerating the investigation of the formation mechanisms of these complex microstructures. To achieve this, materials with macroscopic composition gradients of substitutional elements were fabricated and subjected to time- and space-resolved *in situ* high-energy X-ray diffraction experiments. These experiments reveal an original way to explore wide manufacturing spaces (composition and processing conditions) in a single experiment. Beyond capturing austenitization kinetics during intercritical annealing, the methodology also provides insights into the precipitation and dissolution of carbides during thermal treatment. Consequently, a large experimental dataset linking processing parameters, microstructure evolution, and material properties has been obtained.

In-situ measurement of austenite conditioning and decomposition. Minghui Lin, Matthias Militzer.

The University of British Columbia, Vancouver, Canada.

The properties of metals and alloys are determined by their microstructure evolution during thermo-mechanical processing. For hot-rolled steels austenite conditioning in the rough and finishing rolling mills and subsequent decomposition on the runout table are the critical microstructure features. Although these two phenomena have been extensively studied with conventional methods such as optical and electron microscopy for prior austenite grain size and dilatometry for austenite decomposition kinetics, these measurements are typically performed separately and therefore do not capture the continuous microstructure changes along the entire processing path. In this context, laser ultrasonics offers a promising alternative for rapid, in-situ and non-interrupted measurements based on ultrasonic responses of changes in microstructure parameters such as grain size and phase fraction. In the present study, laser ultrasonics is employed with a novel experimental design for in-situ monitoring of austenite grain growth, recrystallization, and decomposition in a single test for selected low-carbon steels and thermo-mechanical treatments. Austenite grain size measurements from laser ultrasonics are compared to EBSD reconstruction on as-quenched samples whereas the decomposition kinetics are validated with dilatometric measurements. The refinement of austenite grain size after hot deformation is correlated with the fraction recrystallized. The strengths and limitations of the proposed measurement approach will be critically analyzed. Overall, these results highlight laser ultrasonics as a promising tool to expedite microstructure studies for a wide range of steels and thermo-mechanical conditions with high throughput in-situ measurements.

W2a.1-4: Bainite formation (II).

Phase-field simulation framework for modeling martensite and bainite formation in steel. Hesham Salama, Muhammad Adil Ali, Oleg Shchyglo, Ingo Steinbach.

Ruhr-Universität Bochum, Bochum, Germany.

In this study, we present a combination of phase evolution, chemical diffusion, temperature evolution, and finite strain elasto-plasticity to simulate the martensitic and bainitic transformation using the phase-field software library OpenPhase [1]. It is demonstrated how the carbon concentration significantly influences the martensite start temperature and the resulting microstructure. Furthermore, the kinetics of the transformation is strongly influenced by plasticity. For bainitic transformation, it is demonstrated how the holding temperature significantly influences carbon partitioning and the resulting microstructure: higher holding temperatures allow increased carbon diffusion and partitioning, stabilizing retained austenite, which is in good agreement with experimental observations. The present study offers new insights into the microstructure formation mechanisms during martensitic and bainitic transformations in low-carbon steel and offers a consistent modeling approach to model complex phase transformation scenarios in steel and other construction materials.

[1] https://openphase.rub.de/

Phase field simulations of bainite transformation in steels. Ali Khajezade, Ashish Dhole, Matthias Militzer.

The University of British Columbia, Vancouver, Canada.

Steels with fully or partially bainitic microstructures are increasingly of interest for a range of applications in transportation, energy and construction including carbide-free bainite (CFB) and line pipe steels. In this study, the multi-phase field method (MPFM) is employed to investigate the mechanisms governing isothermal and continuous cooling bainite transformation. Here, bainite is considered as a diffusional transformation product. The simulations incorporate anisotropic energy and mobility of bainite-austenite interfaces. Further, the role of elasticity is explored through simulations incorporating different eigenstrain tensors. Selected simulation results are benchmarked and validated with dilatometry measurements of bainite formation in CFB steels. The extension of the proposed modelling approach to austenite decomposition into complex ferrite-bainite microstructures will be discussed with reference to line pipe steels. The findings of the MPFM simulations provide insights into phase transformation kinetics and contribute to advancing knowledge on the formation of bainitic microstructures in steels. Strengths and limitations of the current status of phase field based bainite modelling will be critically analyzed.

Phase-field approach to simulate bainitic transformation in steel. Muhammad Adil Ali, Hesham Salama, Oleg Shchyglo, Ingo Steinbach.

Ruhr-Universität Bochum, Bochum, Germany.

Bainitic steels are widely utilized in automotive and railway industries due to their exceptional mechanical properties, including high strength, hardness, and fatigue resistance. Achieving optimal properties poses significant challenges owing to the intricate bainitic microstructures formed through solid-state phase. transformations. This study employs the phase-field software library OpenPhase to model microstructure transformation, incorporating phase evolution, chemical diffusion, temperature evolution, and finite strain elasto-plasticity (see figure). The findings highlight the critical role of thermomechanical treatment, particularly holding temperature, in influencing carbon partitioning and the resulting microstructure. Higher holding temperatures promote enhanced carbon diffusion and partitioning, stabilizing retained austenite, in agreement with experimental observations. These insights contribute to resolving the debate on diffusion-controlled mechanisms versus massive transformation dominance in bainitic transformations, offering a framework for designing ferrous alloys with tailored properties through advanced microstructure transformation modeling [1, 2, 3].

[1] I. Steinbach, M. Uddagiri, H. Salama, M. Ali, O. Shchyglo, MRS Bulletin, 49, 583–593, (2024).

[2] H. Salama, M. Ali, O. Shchyglo, I. Steinbach, Computational Materials Science, 241, 113033, (2024).

[3] D. Nerella, M. Ali, H. Salama, O. Gulbay, M. Ackermann, O. Shchyglo, U. Krupp, I. Steinbach, Advanced Engineering Materials, 2400905, (2024).

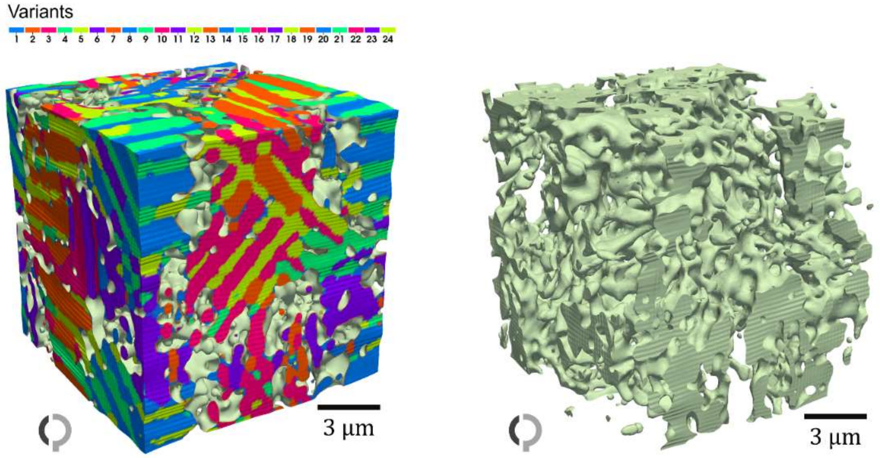

(a) Bainitic microstructure and (b) retained austenite at heat extraction rate of 0.2 1/s.

Modelling of the diffusional-displacive bainitic transformation. Zongbiao Dai[1], Yang Su[2], Junjie Sun[3], Hao Chen[2], Sybrand Zwaag[4], Jun Sun[1].

[1]Xi'an Jiaotong University, Xi'an, China.

[2]Tsinghua University, Beijing, China.

[3]Xi’an Jiaotong University Xi'an, China.

[4]Delft University of Technology, Delft, Netherlands.

The bainitic transformation has been generally recognized as a displacive-diffusional transformation. In order to understand the formation mechanism of bainitic ferrite, we consider its similarities to martensite in terms of displacive behavior and to Widmanstätten ferrite regarding diffusional characteristics. The bainite/martensite start (BMs) temperatures can be predicted using a unified thermodynamic model that incorporates the phenomenological theory of martensite crystallography. This BMs model accounts for the energy dissipation resulting from the transformation strain associated with the displacive process, and indicates that bainitic ferrite forms below 858K(585°C) approximately. Based on the phenomenon of carbon supersaturation in bainitic ferrite, the lengthening behavior of a single bainitic/Widmanstätten ferrite plate was analyzed using a modified Zener-Hillert model that relaxes the local equilibrium assumption of carbon partitioning across the migrating interface. This model suggests that the lengthening behavior of bainitic ferrite is controlled by carbon diffusion within the interface, which exerts a solute drag force on the plate tip, resulting in a slower lengthening rate than that predicted by the classical Zener-Hillert model. Finally, the thickening behavior was investigated by considering the Gibbs energy balance between the chemical driving force and the energy dissipation resulting from the transformation strain and the carbon solute drag effect. The dependence of carbon content in bainitic ferrite and austenite on temperature and alloying compositions at the transformation stasis was also successfully predicted.

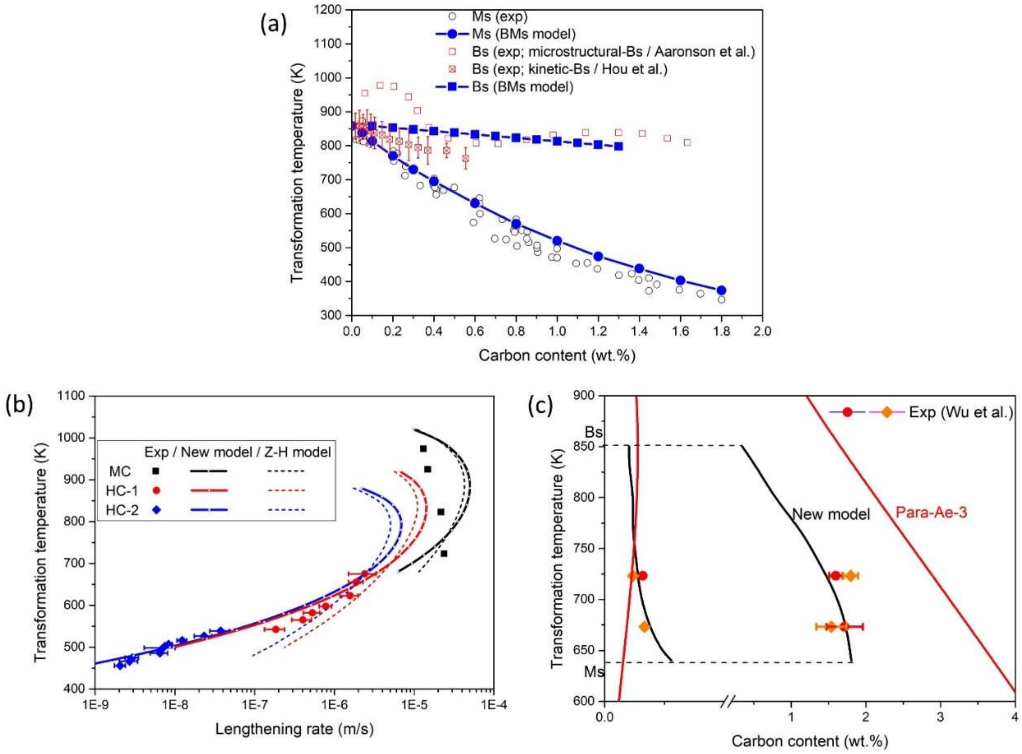

Comparion between model predictions and experiments: (a) Bs/Ms temperatures; (b) lengthening rate; (c) C content in bainitic ferrite and austenite.

W2b.1-4: Recrystallisation and grain growth (II).

New insights in understanding the interaction between recrystallization and phase transformation during intercritical annealing in DP steels. Clélia Couchet[1], Guillaume Geandier[2], Julien Teixeira[2], Frédéric Bonnet[3], Sébastien Allain[1].

[1]Université de Lorraine, Nancy, France.

[2]CNRS Nancy, France.

[3]ArcelorMittal Maizières Research, Maizières-lès-Metz, France.

The formation of microstructures is essential for steelmakers, particularly in Dual-Phase (DP) steels used in the automotive industry. It occurs during intercritical annealing after cold rolling. After heating, the microstructure consists of recrystallized ferrite and austenite. Upon cooling, austenite partially transforms into ferrite, followed by martensite, creating the desired ferrite/martensite structure. The austenitization step is critical for controlling the final phase proportions and sizes, which influence the mechanical properties. While several studies suggest that the heating rate affects the transformation kinetics and austenite morphology, the exact mechanisms remain debated, with the overlap of ferrite recrystallization and austenite formation often implicated. Using recent in situ synchrotron experiments, we offer new insights into ferrite recrystallization and austenite formation interactions, developing a predictive model for austenite kinetics. Our primary advancement is a new time-resolved analysis method based on High-Energy X-ray Diffraction. These analyses were supplemented by microstructural observations after interrupted treatments in microscopy (optical, SEM and TEM), and from local chemistry measurements (EDXS and WDS). We examined the heating rate's influence on DP steel during intercritical annealing and designed experiments to decouple heating rate effects from recrystallization overlap. Our findings reveal that austenite kinetics are driven by thermodynamic conditions at interfaces, not recrystallization. Through thermo-kinetic simulations and experiments, we also investigated the impact of minor alloying elements on austenite growth. Overall, this work establishes that austenite formation during intercritical annealing is diffusion-controlled, with variations in kinetics explained by microstructural factors affecting diffusion distances.

Ferrite recrystallization characterization by isolated diffraction spot tracking during high-energy X-ray diffraction experiments. Clélia Couchet[1], Guillaume Geandier[2], Julien Teixeira[2], Frédéric Bonnet[3], Sébastien Allain[1].

[1]Université de Lorraine, Nancy, France.

[2]CNRS, Nancy, France.

[3]ArcelorMittal Maizières Research, Maizières-lès-Metz, France.

Steel offers various metallurgical approaches, such as grain refinement, phase transformations leading to multiphase structures, and precipitation hardening, to design microstructures and enhance mechanical properties. Among these, recrystallization holds a crucial role, as it softens the alloy, improves formability, and controls microstructure size. Since recrystallization significantly impacts the material's microstructure and mechanical properties, its control and characterization are essential. Recrystallization in bulk alloys is typically studied through microscopy techniques. While optical microscopy reveals recrystallized grains after etching, its resolution limits its use in early-stage analysis, favoring SEM and Electron BackScattering Diffraction (EBSD) for detailed orientation mapping. Mechanical tests, such as hardness measurements, are also used to track recrystallization progress via strength reductions linked to dislocation density decreases. Most existing methods are ex situ and post-mortem. In situ techniques, such as electrical resistivity and 3DXRD tomography, provide insights but face limitations, especially for materials with small grains. Building on previous 3DXRD studies, we developed the Isolated Diffraction Spot Tracking (IDST) method using High Energy X-Ray Diffraction (HEXRD) to monitor recrystallization kinetics in situ. This method was validated through comparisons with EBSD and Vickers micro-hardness, offering enhanced time resolution and broader applicability. Our IDST method offers excellent time resolution compared to ex situ techniques and is easily coupled with in situ methods for phase transformation (Rietveld analysis) or recovery (modified Williamson-Hall or modified Warren-Averbach methods) analysis. By leveraging high statistics of detected recrystallization spots, due to newly recrystallized grains, it accurately quantifies the recrystallized fraction, effectively capturing early-stage recrystallization.

Mesoscopic transformation in aluminum alloys during deformation and recrystallization. Jurij Sidor, János Bátorfi.

ELTE Eötvös Loránd University (ELTE), Szombathely, Hungary.

Mesoscopic transformations are examined in technically pure Al and Al-Mg alloys. The evolution of substructure and dislocation density during deformation is analyzed in this contribution. The relationship between the deformed state and substructure development is performed by means of both indentation techniques and the implementation of numerical approaches. A generic relationship for the estimation of representative substructure size change in materials is presented. The derived relation accurately describes the experimentally observed counterparts. The experimental findings and numerical analysis of substructure evolution allowed the determination of Stored Energy. Assessment of stored energy enabled determination of both nucleation rate and subsequent growth rate of nuclei during recrystallization. It is shown that the driving force for recrystallization in metals can be determined by physically sound numerical approaches and from the indentation measurements under the condition that the material and process-dependent parameters are properly determined.

Recrystallisation and recovery during relaxation trials with in-situ microstructure measurement.

Hans Magnusson[1], Pablo Garcia Chao[2], Adam Ståhlkrantz[1], Tuomo Nyyssönen[1], Mikael Malmström[1], Johan Lönnqvist[1], Linda Bäcke[3].

[1]Swerim, Stockholm, Sweden.

[2]TU Delft, Delft, Netherlands.

[3]SSAB Europe, Borlänge, Sweden.

Recrystallisation kinetics at hot-working conditions is studied for both low-alloyed and stainless steels in the austenite regime. The processes are simulated at high-temperature using Gleeble thermomechanical simulator coupled with laser-ultrasonic measurements (LUS). The LUS-measurements provide in-situ data of grain size evolution during thermomechanical processing, which is especially valuable for low-alloyed steels which phase transform forming ferrite phases when cooling to room temperature. With a better understanding of the structure evolution at hot-working it is possible to further optimise heating strategies, allowing for a sustainable processing of steels. Different deformation strategies are tested with Gleeble, followed by isothermal relaxation studies. Force data is monitored by the Gleeble system together with grain size evolution obtained via the LUS system. The information is then complemented by EBSD characterisation on quenched samples, at which the low-alloyed steels are reconstructed to obtain prior austenite grain sizes. The experimental data on force recovery and grain recrystallisation are fitted to semi-empirical models for the different steel grades. This include both fraction and grain size of the recrystallised grains. A good correlation is seen when comparing the different experimental methods, demonstrating the advantages with online measurements. With the combination of methods, it is possible to separate the relaxation effects of dislocation-based recovery to recrystallisation of deformation-free grains.

W2c.1-4: Advanced experimentation (II).

Mapping of transformation-induced elastic strains by TEM.

Arthur Després[1], Bregeault[1], Le Gloannec[2], Marceaux-Dit-Clément[2], Roch[2], Scott[3], Zurob[4], Veron[1], van Landeghem[1]

[1]SIMaP - Grenoble INP, Grenoble, France.

[2]Framatome, Courbevoie, France.

[3]Canmet Materials, Hamilton, Canada.

[4]McMaster University, Hamilton, Canada.

Many phase transformations induce elastic strains. For example, in aluminium alloys, nanoscale precipitation induces strain fields whose intensity depend on the precipitates morphology and structure. In steels, the elastic strains induced by the martensitic transformation may induce plasticity in the austenite and affect variant selection. Despite their strong influence on the progress of the transformation, these elastic strains are rarely measured. Here, a method of elastic strain mapping in the TEM is presented. Elastic strains and micro-rotation are calculated from the shifts of the diffraction spots position between the nano-diffraction patterns acquired in the field of view and a reference pattern taken from an unconstrained region of the crystal. The spatial resolution is 1nm and the fields of view can reach several microns. The method is applied to two cases. In the first case, the elastic strains are mapped around a coherent Al_3Sc precipitate in an aluminium alloy. The measurements agree very well with the theoretical predictions of the Mott-Nabarro model (Figure 1a,b). In the second case, the elastic strains and micro-rotation are mapped around martensite laths growing in the austenite parent phase (Figure 1c,d). An asymmetry of the strain field and micro-rotations is found, which is consistent with previous EBSD and conventional TEM observations. Strains and micro-rotations induced by interface defects and dislocations in austenite are also detected. Finally, perspectives for the study of phase transformations are discussed.

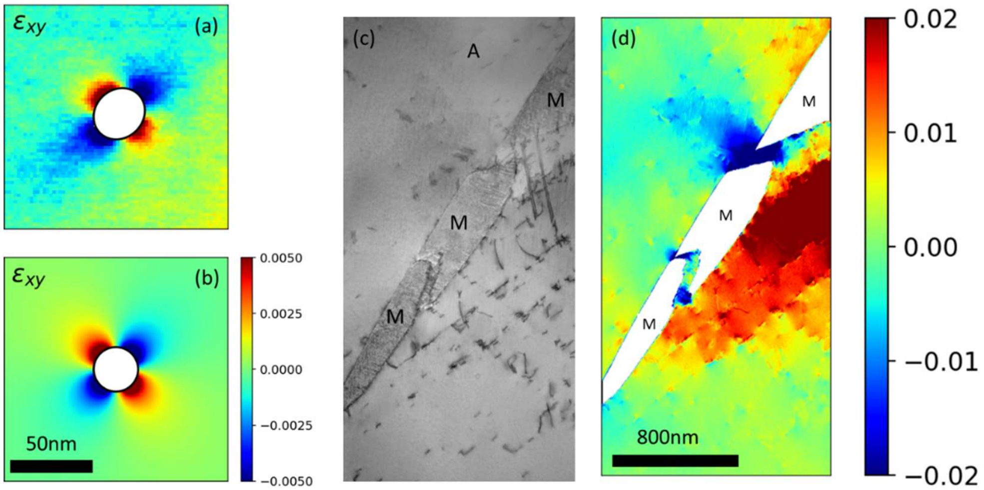

Figure 1 : (a,b) shear strain field measured and predicted around an Al3Sc particle in an aluminium alloy. (c,d) Bright-field image and in plane micro.

EBSD and TKD Study of Microstructure Evolution in NiTi Alloys. Junfeng Xiao, Cyril Cayron, Roland Loge.

Ecole Polytechnique Fédérale de Lausanne (EPFL), Neuchatel, Switzerland.

NiTi alloys are of great interest due to their exceptional mechanical properties, such as superelasticity and the shape memory effect, driven by reversible phase transformation between the parent B2 phase and monoclinic B19' martensite. Understanding the microstructural evolution during martensitic transformation is vital for enhancing the functional performance of NiTi alloys. Compared to transmission electron microscopy (TEM) and X-ray diffraction (XRD), electron backscatter diffraction (EBSD) and transmission Kikuchi diffraction (TKD) offer direct orientation mapping and global analysis of martensitic variants. This study utilizes EBSD and TKD, integrated with the theoretical framework of Interaction Work (IW), to explore the microstructural evolution of martensite in NiTi alloys. IW quantifies the mechanical work during transformation, favouring variants with high positive IW. EBSD analysis reveals variant selection, texture evolution, and deformation twinning in superelastic NiTi. All of these changes are explained by the IW criterion. In shape memory NiTi, martensite morphology evolves from needle-like to block-like structures, with orientations of remaining martensite aligning along the loading direction, consistent with IW predictions. The IW framework is particularly effective in explaining complex microstructure changes under multi-dimensional stresses, such as those introduced by laser shock peening, including reorientation and texture formation. Fine-scale TKD observations demonstrate that reorientation initiates with detwinning, followed by transformation twinning under applied strain. These findings suggest that the martensitic microstructure evolves with strains following a trajectory with increasing maximum IW of different deformation modes. These insights into microstructural evolution are crucial for guiding the design and optimization of next-generation shape memory alloys.

Evolution of phase transformations and lattice defects in steels: an X-ray diffraction and modelling perspective. Ernst Gamsjäger[1], Manfred Wiessner[2].

[1] Montanuniversität Leoben / Chair of Mechanics, Leoben, Austria.

[2] Anton-Paar GmbH, Graz, Austria.

The influence of tempering temperature and its associated holding time on the microstructure of carbon-free Cr stainless steels is investigated using in-situ high temperature X-ray diffraction (HT-XRD). The evolution of individual phases, particularly reverted austenite and martensite, is monitored. The formation of reverted austenite during tempering and the retransformation to martensite during cooling after the annealing process strongly depends on the local mole fraction of Ni in austenite. These coupled diffusion interface migration phenomena are investigated by thermodynamically based simulations. Thereby, it is shown that equilibrium is usually not attained during processing at elevated temperatures. During retransformation to martensite the dislocation density in this newly formed martensite increases and thereby the impact strength of the steel is reduced. By investigating these effects of tempering temperature and time on the microstructure via in-situ experiments and simulations, heat treatments can be suggested that may result in tailored mechanical properties for this class of steels.

Room-temperature recrystallization of Mo induced by nanoindentation. Feitao Li[1], Afnan Mostafa[2], Niaz Abdolrahim[2], Eugen Rabkin[1].

[1]Technion – Israel Institute of Technology, Haifa, Israel.

[2]University of Rochester, Rochester, United States.

We performed nanoindentation on molybdenum (Mo) single-crystal (SC) and polycrystalline (PC) samples utilizing a spheroconical indenter. Load-displacement curves of SC samples exhibited characteristic pop-in (displacement burst) indicating an abrupt transition from elastic to plastic deformation at the maximum elastic shear stress of 12-16 GPa. On the contrary, much weaker pop-ins were observed in the PC sample (the corresponding maximum shear strength was below 0.5 GPa). The cross-sectional transmission electron microscopy of the indented area in SC samples revealed the formation of new near-surface grains when the loading was terminated manually immediately after the pop-in event. By contrast, no new grains could be observed in the PC sample, indicating that the pop-in and recrystallization are correlated. We propose that the dislocations nucleated during a singular pop-in event are driven by high elastic stress and self-organize into a low-angle grain boundary (LAGB). We estimated the density of geometrically necessary dislocations generated by the nanoindentation using the Nix-Gao model and demonstrated that misorientation of 3-4° could be achieved when all the dislocations assemble in a grain boundary, resulting in the formation of new grains. When the SC Mo sample was continuously indented to the loads significantly exceeding the first pop-in, no visible new grains were formed. Molecular dynamics simulations were performed to track the evolution of a LAGB upon indentation. Our results shed new light on the deformation mechanisms during the nanoindentation of defect-free Mo. Room-temperature recrystallization is unprecedented for Mo which usually recrystallizes at temperatures above 1000 °C.

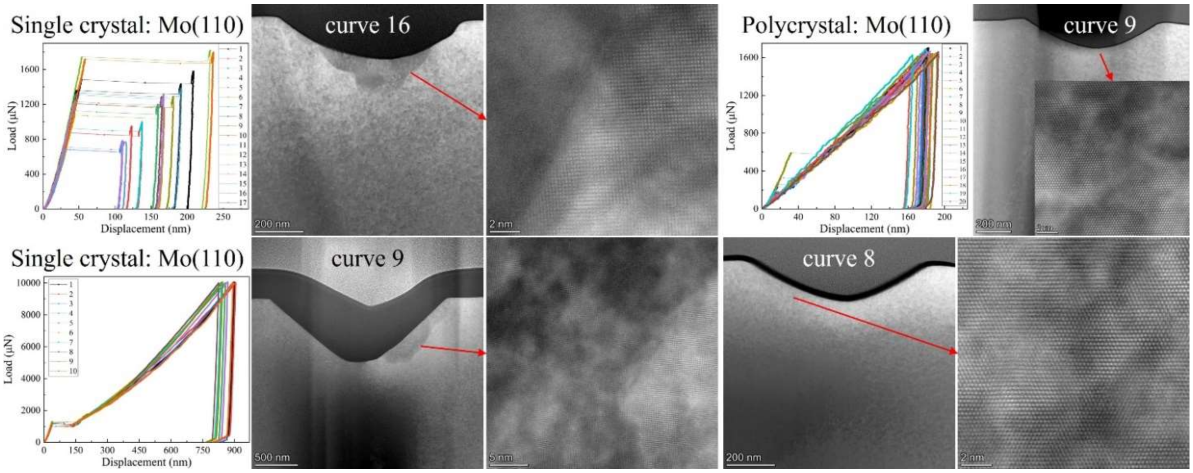

Load-displacement curves and HAADF-STEM graphs showing microstructures below imprints.

Thursday, July 10

Plenary 6. Hillert-Cahn Lecture. Precipitate growth and spinodal decomposition in AlCrFeNi alloys studied through phase-field simulations. Nele Moelans.

KU Leuven, Leuven, Belgium.

Since the emergence of High-Entropy Alloys (HEAs), there has been significant interest in studying phase transformations and microstructure evolution in AlCrFeNi alloys. These alloys are renowned for their exceptional mechanical strength, corrosion resistance, and thermal stability. The vast array of possible compositions and processing routes present numerous opportunities to optimize microstructure and properties towards a specific application context. However, this flexibility also complicates the optimization process, necessitating a profound understanding of the phase transformations that occur within these alloys. In recent years, we have put extensive efforts in developing an advanced phase-field modeling approach that captures the simultaneous evolution of multiple phases and grains within this quaternary alloy. The model accounts for the full composition dependence of Gibbs energies and diffusion mobilities of the different phases, as well as local strain effects. The presentation will discuss how this model enabled us to simulate and study a number of complex and intriguing multicomponent microstructural processes, involving diffusion, precipitation and spinodal decomposition, occurring in these alloys. Important insights are obtained from the simulations on the role of the diffusion behavior of the different elements, the interfacial properties, and, both local and overall, phase equilibria. These findings are very useful for the further optimization of AlCrFeNi based alloys and can inspire new research paths for multi-component alloy design in general.

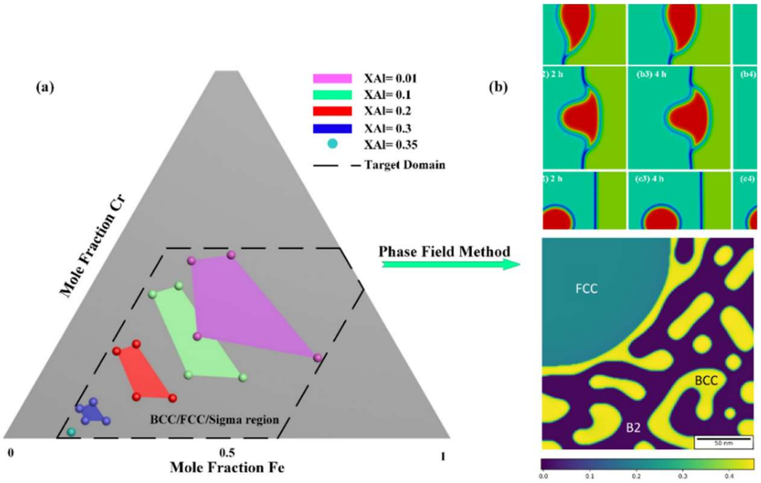

Th1a.1-4: Precipitation (I)

Invited. **In-situ study of discontinuous precipitation in Mg-Al.** Joseph Robson.

University of Manchester, Manchester, United Kingdom.

Competitive continuous and discontinuous precipitation (CP and DP) have been studied in-situ in the Mg-Al system. This has revealed new insights into DP and its competition with CP that demonstrate complex behaviours not captured in current DP growth theory. Firstly, it has been shown that the DP reaction front (RF) does not move with a constant velocity, but rather in an irregular stop-start fashion. The arrest times may be very long, several hours, before the RF resumes its motion. Secondly, the interaction of the RF with CP has been shown to depend strongly on the orientation of the CP plates. Sympathetic and unsympathetic relationships between the RF movement and the precipitate orientation have been identified, which determines the behaviour of the CP when engulfed by DP. Finally, it has been demonstrated that there is a factor 4 difference in the maximum and minimum mean growth velocities for DP regions in different grains. The results are explained by a simple model that considers the RF moving through a non-uniform solute field caused by CP, with the stop-start boundary motion explained by the need to transport solute along the RF from enriched to depleted regions to maintain forward motion.

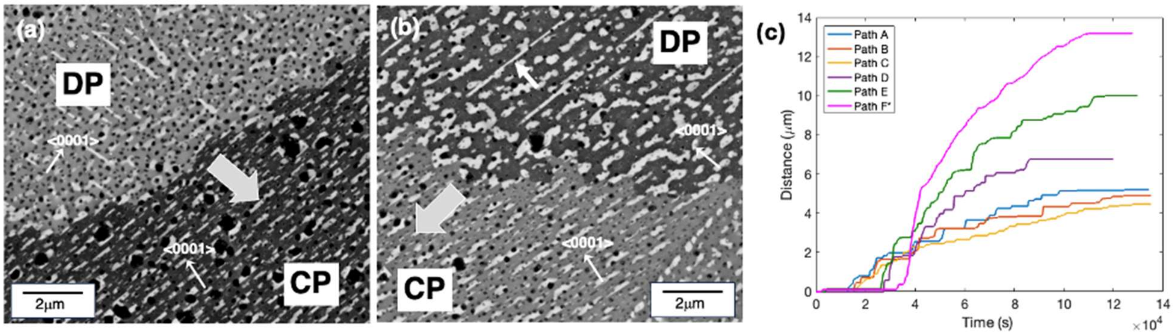

Growth of DP into matrix containing CP in (a) unsympathetic and (b) sympathetic orientation. (c) In-situ tracking of DP along 6 paths (A-F)

Electropulsing induced ultrafast phase transformation in non-equilibrium conditions. Yuanshen Qi.

Guangdong Technion - Israel Institute of Technology, Shantou, China.

Using periodic electric current pulses, i.e. electropulsing (EP) treatment, to stimulate microstructure evolution such as recovery, recrystallization and grain boundary migration, and precipitate formation and dissolution after solution and aging treatment, has been drawing increasing attention. Moreover, the pulsed electric current scattering on the crystal lattice defects also triggers unique phenomena that cannot be achieved by thermal treatments. Therefore, EP treatment as a novel post-thermomechanical processing technique possesses the potential to surpass the conventional heat treatments with respect to energy saving and property enhancement and provides unique microstructure design strategy. In this talk, I will present our recent studies on EP induced ultrafast precipitation and dissolution. Peak hardness can be achieved in Al-Cu binary alloys at room temperature after 2 min of EP treatment, compared to ~50 h of artificial aging at 160 °C. Moreover, for Al 7075 alloys, full dissolution from peak hardness of 183 HV to 85 HV that requires solution treatment at 482 °C for 20 min, can be shortened to 1 ms by EP treatment. These unique phase transformation phenomena can be attributed to non-equilibrium conditions triggered by high energy electropulse(s). We conducted in-depth in-situ biasing electron microscopy to elucidate the mechanisms.

Size focusing of core-shell precipitates leading to near-uniform size dstribution. Soumya Mishra, T A Abinandanan.

Indian Institute of Science (IISc), Bengaluru, India.

Size focusing is a phenomenon where a broader size distribution of precipitates transitions to a narrower one. While chemical synthesis of nanoparticles from solutions routinely employs the principles of size focusing to obtain a monodisperse size distribution, this is not common in alloy systems. In an interesting study, Radmilovic et al. [1] showed that size focusing is possible in an Al-Sc-Li alloy with an α matrix containing two precipitates in a core-shell morphology, with a β core surrounded by a γ shell. While they used arguments using the LSW theory of coarsening to explain their observation, this is not quite correct because it implies that monodispersity is related to coarsening. We show, using theory and phase field simulations, that size focusing is essentially a growth phenomenon when it is achieved through the formation of γ shells around pre-existing β cores; moreover, size focusing actually stops when the growth of the shell phase is nearly complete. The simulations are based on a phase field model of a ternary alloy in which the wetting criterion holds: $\sigma_{\alpha\beta} > \sigma_{\beta\gamma} + \sigma_{\alpha\gamma}$ where σ_{XY} is the interfacial energy between phases X and Y. With these simulations, we have studied the effects of factors such as initial size distribution, mobilities and volume fractions of core and shell phases during size focusing. Our results provide simple guidelines for designing alloys with near-monodisperse precipitates.

[1] V. Radmilovic et al., Highly monodisperse core–shell particles created by solid-state reactions, *Nature Materials*, **10**, 710-15 (2011).

Direct evidence and kinetics of Cu precipitation in the austenite phase of a maraging stainless steel. Tao Zhou, Gabriel Spartacus, Peter Hedström.

KTH Royal Institute of Technology, Stockholm, Sweden.

In this work, we present the precipitation kinetics of Cu in a 15-5 PH maraging stainless steel during high-temperature thermal treatments in the fully austenitic state. Thus direct evidence that Cu precipitation can occur in the austenite phase of martensitic or ferritic steels is provided. The Cu precipitation kinetics in austenite is detailed at 700 and 800 ˚C using *in situ* synchrotron small-angle and wide-angle X-ray scattering (SAXS/WAXS), complemented by atom probe tomography (APT) investigations on the precipitates, particularly the chemistry, post heat treatment. The resulting experimental data on Cu precipitation kinetics, including the evolution of size, volume fraction, number density and chemical composition, are further used to feed precipitation kinetics modelling using the Langer-Schwartz-Kampmann-Wagner (LSKW) approach coupled with CALPHAD thermodynamic and kinetic databases. The simulations are able to capture the experimental data by modifying the interfacial energy in an inverse modelling approach. The insight that Cu precipitation occurs in austenite and subsequently in martensite paves the way for design of hierarchical structures with a bi-modal particle size distribution of Cu precipitates with different crystal structures and compositions. Furthermore, the validated LSKW-modelling approach provides a foundation for designing such Cu-alloyed high-performance steels considering various manufacturing routes.

Th1b.1-3: Q&P (martensite/austenite)

Invited. **Microstructure evolution during quench & partitioning and intercritical annealing combined with press-hardening of sedium-manganese steels.** Ulrich Krupp[1], Alexander Gramlich[1], Vinola Jeyaraj[1], Charline Blankart[2].

[1]IEHK Steel Institute, RWTH Aachen University, Aachen, Germany.

[2]C.D. Wälzholz GmbH & Co. KG Hagen, Germany.

Press hardening of manganese-boron steels has become a very popular process to produce ultra-high-strength steels for autobody components. However, the residual formability of these sheet components is greatly limited by the formation of fully martensitic microstructure during in-die quenching, which makes them only to a limited extent suitable for crash-relevant anti-intrusion parts. In order to extend the application range of press-hardened components, the use of third-generation advanced high strength steels (AHSS), i.e., medium-manganese steels, attracts increasing attention. Aim of the presented research is to analyze the potential of press hardening of lean medium manganese steel in combination with a quenching & partitioning (Q&P) treatment in comparison to intercritical annealing and double soaking. For this reason, dilatometer investigations on Fe-0.3%C-5%Mn-1.5%Si with varying Q&P parameter were performed. By adjusting the heat treatment parameters, the microstructure and hence the mechanical properties were modified to fit the application´s load requirements. The results demonstrated that the performed Q&P treatments lead to multi-phase microstructures, as analyed by EBSD (band-slope contrast) in combination with EPMA. The microstructures consist of martensite (tempered and fresh) and retained austenite resulting in high tensile strength, comparable to martensitic 22MnB5, and significantly improved total elongation up to 18 %. It was shown that a reasonable ductility requires not only the adjustment of the retained austenite content bit also a reduction of fresh martensite to prevent brittle failure. Finally, selected heat treatments were successfully transferred to a laboratory-scale press hardening system equipped with a heatable hat-shaped pressing tool.

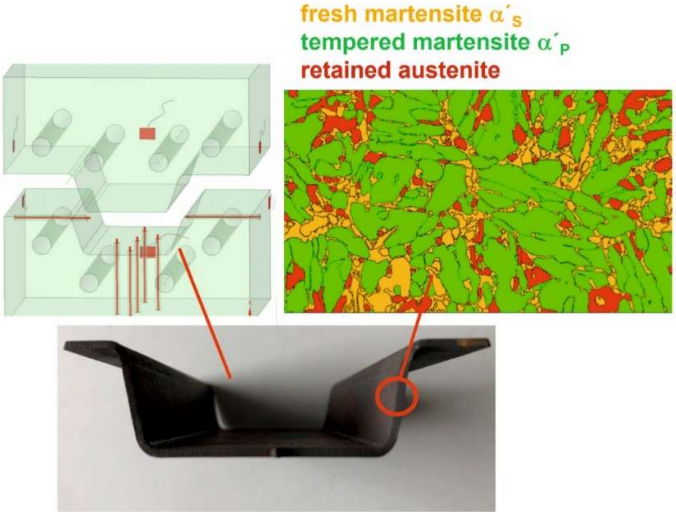

Fig. 1: Lab-scale press-hardening of hat-shaped profile and resulting microstructure evolution (Q&P), identified by band slope contrast

Critical insights into the contributions to carbon enrichment of austenite and related competitive reactions during Quenching and Partitioning treatments with various Mn contents. Eve-Line Cadotte[1], Mohamed Gouné[2], Stéphane Godet[1].

[1]4MAT, Materials Engineering, Characterization, Processing and Recycling, Univer Bruxelles, Belgium.

[2]ICMCB, Bordeaux INP, CNRS, Université de Bordeaux, Bordeaux, France.

The contributions to carbon enrichment in austenite during the partitioning step of Quenching and Partitioning (Q&P) treatments was studied. The phase transformations in two steels with different Mn contents (2.3, 3.9, and 5.6 wt.%) were characterized. Particular attention was paid to the carbon partitioning from martensite to austenite, carbide precipitation in martensite, and bainite transformation in austenite. A model was developed to account for the thermodynamics and kinetics of those phenomena. The theoretical calculations revealed the important role of bainite transformation in the carbon enrichment of austenite. When carbon partitioning completes before bainite stops forming, the carbon enrichment is constant and limited by the carbon content at the bainite transformation stasis. In steels with higher Mn, where bainite does not form, the carbon enrichment is instead controlled by chemical potential equilibration across the martensite/austenite interface. Under these conditions, the final carbon content in austenite depends on the martensite fraction and is highly sensitive to carbide precipitation.

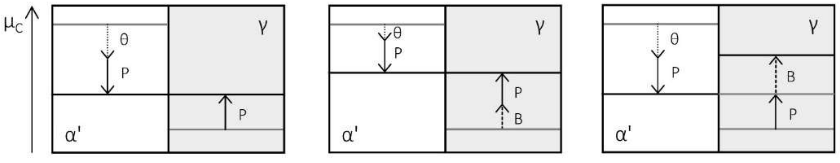

$X^{\gamma}_{C,fin} = X^{\gamma}_{C}(\mu^{\alpha'}_{C} = \mu^{\gamma}_{C})$

$X^{\gamma}_{C,fin} < X^{\gamma}_{C,CCE}$

(a)

$X^{\gamma}_{C,fin} = X^{\gamma}_{C,stasis}$

(b)

$X^{\gamma}_{C,fin} = X^{\gamma}_{C}(\mu^{\alpha'}_{C} = \mu^{\gamma}_{C})$

$X^{\gamma}_{C,stasis} < X^{\gamma}_{C,fin} < X^{\gamma}_{C,CCE}$

(c)

Evolution and final state of the chemical potentials in martensite and austenite, summarising the 3 conditions for the end of austenite C enrichment

Martensite/austenite interface migration and elemental partitioning in a high-temperature Q&P processed medium Mn steel. Sudhindra Ayenampudi[2], Carola Celada Casero[1], Shanoob Balachandran[3], Michael Herbig[4], Jilt Sietsma[5], María J. Santofimia[5].

[1]Spanish National Research Council (CSIC), Madrid, Spain.

[2]NLMK Group La Louvière, Belgium.

[3]Alloyed Yarnton, United Kingdom.

[4]Max-Planck-Institut für Eisenforschung, Düsseldorf, Germany.

[5]Delft University of Technology, Delft, Netherlands.

Austenite stabilisation by carbon and manganese enables the design of martensite-austenite (α'/γ) microstructures with enhanced strength-ductility combinations in steels by high temperature Quenching and Partitioning (Q&P) treatments. Controlling this austenite stabilisation requires insight into the concurrent redistribution of C and Mn and its impact on the microstructure. By combining multi-phase field modelling and 3D atom probe tomography (3D-APT), we investigate the partitioning kinetics of C and Mn at 600 °C in an Fe-0.19C-6Mn (wt.%) steel. Mn enrichment near the equilibrium concentration and over a range of 5 nm is experimentally observed in the retained austenite after partitioning for 300 s. One- and two-dimensional phase-field simulations indicate that, firstly, rapid local chemical potential equilibration for carbon at the diffuse α'/γ interface might lead to a carbon concentration in austenite that is higher than the overall equilibrium. This creates a driving force for austenite growth accompanied by a carbon-concentration decrease in austenite. Mn equilibration at the α'/γ interface is too slow to reach equilibrium. Further austenite growth reduces the carbon concentration and increases the Mn concentration in austenite until local equilibrium is reached. Although the Mn concentration in martensite from 3D-APT slightly exceeds the local equilibrium value, this mechanism explains the experimental observations. We conclude that the austenite growth due to carbon partitioning at 600 °C assists the Mn enrichment in the newly grown part of the austenite grains. As a consequence, high austenite fractions can be stabilized in high-temperature Q&P processed microstructures.

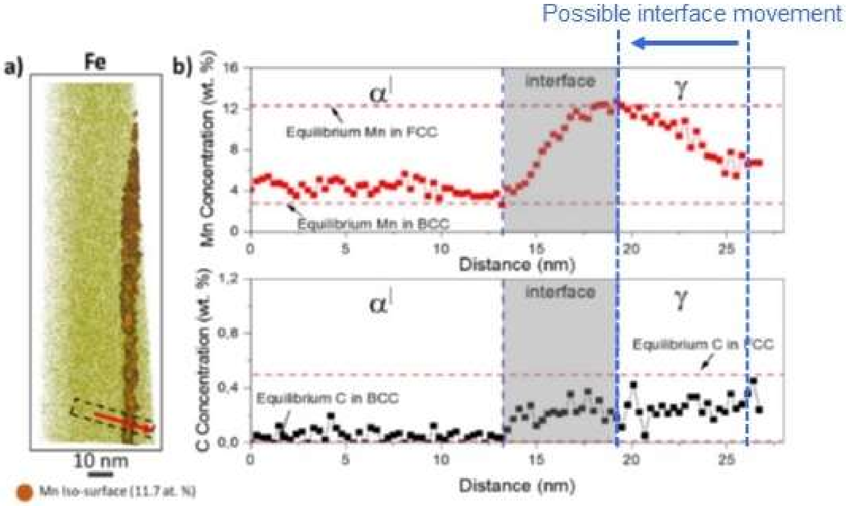

3D-APT results for the Q&P processed steel, partitioned at 600 °C for 300 s. a) Iron atom map, b) Mn and C concentration profiles along the red arrow

Th1c.1-4: Ordering

Invited. **Statistical fluctuations, clustering and short-range ordering: a CALPHAD based Thermodynamics perspective.** Alisson Kwiatkowski da Silva[1,2], Qing Chen[1,3], Dierk Raabe[2].

[1]Thermo-Calc Software AB, Solna, Sweden.

[2]Max Planck Institute for Sustainable Materials, Dusseldorf, Germany.

[3]KTH Royal Institute of Technology Stockholm, Sweden.

The physical quantities which describe a phase in equilibrium are, almost always, very nearly equal to their mean values. Nevertheless, deviations from the mean values, though small, do occur (quantities are said to fluctuate at a very small scale). Clustering and short-range ordering are examples of local deviations or fluctuations from the average disordered solid solution state of the alloy. We will discuss how the statistical distribution of clusters can be inferred from the Gibbs energy description and used to predict the existence of clustering and short-range ordering. These fluctuations must also be distinguished from fluctuations that arise in the early stage of phase decomposition, leading to phase separation and/or the formation of long-range ordered phases. In this context, the theories of nucleation and growth and spinodal decomposition will be briefly reexamined. We will explore some experimental cases of equilibrium and non-equilibrium fluctuations and how a thermodynamic description based on CALPHAD can help us understand them.

On ordering on BCC and O-phase. Suzana G. Fries[1,2], Silvana Tumminello[2], Joachim Gussone[2]and Guillermo Requena[2,3].

[1]Ruhr University Bochum, Bochum, Germany.

[1]Materials Research Department, Ruhr Universität Bochum, D-44780 Bochum, Germany.

[2]German Aerospace Center DLR, Institute of Materials Research, Linder Höhe, D-51147 Cologne, Germany.

[3]RWTH Aachen University, Metallic Structures and Materials Systems for Aerospace Engineering, D-52062 Aachen, Germany.

Phase transformations involving order-disorder in BCC alloys, which were discussed with a view point of application in the late 1990s by Naka and Kahn, [97Nak] are raising again interest. Amidst the reasons, are the potential of the use of these alloys in high temperature applications, and the fact that new pathways are being found during additive manufacturing processes, like laser powder bed fusion, LPBD, which show phase transformations that instigates understanding. Alloys in the system Ti-Al-Nb have high temperature and oxidation resistance and are light what implies in a large number of applications. In this system, A2-B2 and B2 to the orthogonal O-phase transformations were pioneering studied by [94Ben] and [02Sad] in its crystallographic and thermodynamic modelling, respectively. We discuss these phases formation during LPBD additive manufacturing [23Gus] where the equilibrium condition is not present.

Ref:

[97Nak] S. Naka and T. Khan: J. Phase Equil., 1997, vol. 18, pp. 635–49.

[94Ben] L. A. Benderskyi, A. Roytburd, and W. J. Boettinger, Acta metall. mater. Vol. 42, No. 7, pp. 2323-2335, 1994.

[02Sad] F.A Sadi and C. Servant, Materials Science and Engineering, vol 346 (1-2) 15 pp. 19-28, 2003

[23Gus] J. Gussone et al., Materials and Design, vol. 232, 112154, 2023

Order-disorder phase transformation makes Ni-Pt nanoparticles spin and dance. Rabkin, Levi, Bisht.

Technion - Israel Institute of Technology, Haifa, Israel.

We fabricated single crystalline faceted nanoparticles of near-stoichiometric NiPt alloy employing the solid state dewetting of Ni-Pt bilayers deposited on a sapphire substrate. The particles were annealed within the stability range of the ordered L1_0 phase. We uncovered the oscillatory cyclic-type changes of the fraction of disordered (100)-oriented particles, which were correlated with particle rotation and re-orientation. The nucleation and expansion of ordered domains within the disordered (111)-oriented particles resulted in an increase of internal stresses and concomitant nucleation of twinning dislocations. Subsequent out-of-plane rotation *via* twinning has resulted in intermittent nanoparticles disordering due to the slip geometry in the ordered L1_0 phase. Notably, the re-orienting particles exhibited a macroscopic linear transformation strain reaching a value of 23% (see Figure). The discovery of ordering-induced particle rotation and reorientation in our study introduces a novel approach for engineering the functional properties of supported metal nanoparticles.

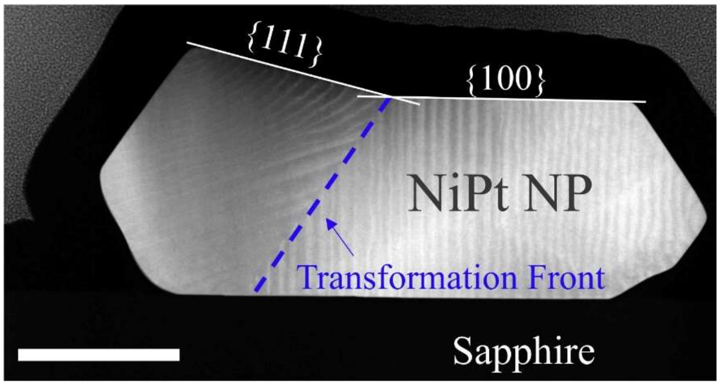

The cross-sectional STEM-HAADF micrograph of the Ni-Pt nanoparticle obtained by solid state dewetting of Ni-Pt bilayer at 1000 °C for 72 h, followed by ordering anneal at 550 °C for 24 h. Scale bar is 200 nm.

Atomistic simulations of diffusion properties and ordering kinetics in Fe-Ni alloys. Zexin Fang[1], Frédéric Soisson[1], Maylise Nastar[1], Charlotte S. Becquart[2].

[1]Université Paris-Saclay, Gif-sur-Yvette, France.

[2]Université de Lille, Lille, France.

Atomistic simulations are crucial for studying diffusion and ordering kinetics in metallic alloys but face challenges at high temperatures due to the computational cost and limitations of ab initio methods, particularly in accounting for vibrational and magnetic effects. To address this issue in the Fe-Ni system, we introduce an on-lattice model of vacancy-atom jump frequencies based on a kinetic pair interaction model (k-PIM), integrated with kinetic Monte Carlo simulations. The pair interaction model is parameterized using the CALPHAD model and *ab initio* calculations of formation enthalpies for both ordered and disordered structures, including special quasi-random structures (SQS). Additionally, this model builds upon vacancy formation and migration properties derived from experimental data and *ab initio* calculations for the FeNi-$L1_0$ and $FeNi_3$-$L1_2$ phases. The model predictions are in good agreement with the experimental phase diagram. We analyze the tracer diffusion coefficient (D^*) and the interdiffusion coefficient (D^{int}) in Fe-Ni alloys with varying compositions. In particular, we investigate the ordering process within the $L1_2$ phase, including the evolution of the vacancy concentration and comparing the evolution of domain size, the long-range order parameter (LRO), and the short-range order parameter (SRO), which shows good agreement with the experiments.

Th2a.1-5: Precipitation (II)

Invited. **Role of the Burgers vectors of interfacial dislocations in precipitation crystallography.** Wenzheng Zhang.

Tsinghua University, Beijing, China.

The interfaces formed during phase transformations in materials often adopt low-energy structures to minimize nucleation barriers. These structures typically exhibit specific lattice matching, at least in localized regions. When a one-to-one lattice match exists, the interface geometry required by the matching usually defines a unique zone for possible orientation relationships (ORs) between two phases. However, in systems where one-to-one matching is impractical, as seen in alloys containing intermetallic compounds, each non-one-to-one matching geometry corresponds to its own OR zone, resulting in a multiple OR zones. Traditional interpretations of the observed OR zones are based on conventional criteria like dense matching sites and minimal lattice mismatch in major interfaces. However, these criteria may not fully explain all observed phenomena. In most systems, interfacial misfit is accommodated by dislocations. The Burgers vectors of these interfacial dislocations can significantly influence the final precipitation crystallography, including the OR zones. In systems with non-one-to-one matching, the selection of small Burgers vectors is particularly crucial. In an interface with good none-one-to-one matching, a small Burgers vector may not always be available. This presentation will illustrate the influence of Burgers vectors on precipitation crystallography with examples from various systems. It is suggested that the criterion of small Burgers vectors should be considered along with the conventional criteria for understanding ORs and preferred interfaces in systems with none-one-to-one matching and with a need for dislocations to accommodate interfacial misfit.

Unravelling precipitation kinetics in nanosteels using Small Angle Neutron Scattering. Zamran Zahoor Khan[1], Sven Erik Offerman[1], Steven R. Parnell[2], Niels Dijk[1].

[1] TU Delft, Delft, Netherlands.

[2] ISIS Neutron and Muon Source, Didcot, United Kingdom.

The formation of nanoscale vanadium carbide (VC) precipitates is studied in steels subjected to two different thermal cycles. The thermal cycling leads to either interphase precipitation (IP) or random precipitation (RP) mechanisms. Small-Angle Neutron Scattering (SANS) measurements coupled with

Transmission Electron Microscopy (TEM) analysis are employed to determine the differences between these two precipitation processes. Specimens exhibiting interphase precipitation show a higher volume fraction and number density of VC precipitates compared to those undergoing random precipitation. Moreover, a broader size distribution of the precipitate radii is observed in specimens with random precipitation, where lens-shaped nanoscale precipitates are found predominantly at grain boundaries and sub-grain boundaries, with smaller precipitates dispersed within the matrix. The effect of varying carbon and vanadium concentrations on the VC precipitation strengthening is found to be more pronounced in RP in comparison with IP for samples annealed for 20 min at 650 °C. These findings shed light on the distinct characteristics of VC precipitation under different thermal cycles, offering valuable insights for the design and optimization of steel microstructures.

Carbide is ferritic steels: defects and atomic diffusion from ab-initio based studies. Adrien Lemercier, Chu-Chun Fu, Frédéric Soisson, Jean-Luc Béchade.

CEA S2CM/SRMP, Saclay, France.

Carbides are generally present in steels like ferritic steels. Many of their properties are still unclear, especially the atomic-scale driving forces and mechanisms. Among the elementary properties, atomic diffusion is crucial in controlling various kinetic processes including the growth, dissolution, and amorphization of carbides. We start by focusing on cementite, appearing in Fe-C and dilute Fe-Cr-C alloys, in which carbon and metal elements migrate via points defects, such as vacancy, self-interstitial atom and Frenkel pair. We perform density functional theory (DFT) calculations to determine energetic properties for the point-defects formation and migration. Then, we determine the diffusion coefficients through DFT-parameterized kinetic Monte Carlo simulations. We consider not only the stoichiometric but also off-stoichiometric cementite. Concerning the diffusion of carbon, various mechanisms are identified, some of them being highly anisotropic. The computed energetic barriers range from 2.0 to 2.4 eV, which is much larger than the carbon migration energy in bcc iron. The dominant mechanism depends strongly on the concentration of carbon in cementite as well as the direction of diffusion. On the other hand, the metallic elements mainly migrate via the vacancy mechanism. The orthorhombic structure and the arrangement of the intrinsic C atoms induces very different energy barriers, from 0.5 to 1.7 eV for iron. Finally, as shown experimentally, the $M_7C_3$and $M_{23}C_6$carbides tend to form, instead of cementite, with increasing concentration of Cr in Fe-Cr-C alloys, we investigate the relative energetic and mechanical stability of these carbides with respect to cementite, as a function of Cr content.

On the precipitation and transformation kinetics of precipitation-hardening steel X5CrNiCuNb16 4 in a wide range of heating and cooling rates. Benjamin Milkereit , Christian Rowolt[1], Dipanwita Chatterjee[2], Randi Holmestad[2], Ruben Bjorge[3], Matteo Villa[4], Frank Niessen[5], Frederic De Geuser[6], Andreas Stark[7], Olaf Kessler[1].

[1] University of Rostock, Rostock, Germany.

[2] NTNU, Trondheim, Norway.

[3] SINTEF, Trondheim, Norway.

[4] Politecnico di Bari, Bari, Italy.

[5] DTU Copenhagen, Denmark.

[6] Univ. Grenoble Alpes, Grenoble, France.

[7] Helmholtz-Zentrum Hereon, Geesthacht, Germany.

In this work, the transformation and dissolution/precipitation behaviour of the soft martensitic, precipitation-hardening steel X5CrNiCuNb16-4 (often referred to as 17-4 PH or AISI 630) has been investigated by various analytical in situ techniques. First, austenite formation during the heating stage of a solution treatment (or austenitization) is examined. Subsequently, a major part of this work evaluates precipitation during cooling from the solution treatment (i.e., the quench-induced precipitation of Cu-rich particles). The following analytical in situ techniques were utilised: synchrotron high-energy X-ray diffraction, synchrotron small-angle X-ray scattering, differential scanning calorimetry, and dilatometry. These were complemented by ex situ high-angle annular dark-field scanning transmission electron microscopy coupled with energy-dispersive X-ray spectroscopy on as-quenched samples after various cooling rates. The continuous heating transformation and continuous cooling transformation diagrams have been updated. Contrary to previous reports, X5CrNiCuNb16-4 is rather quench sensitive and the final properties after ageing degrade if cooling is done slower than a certain critical cooling rate. Quench-induced Cu-rich precipitation happens in two reactions: a larger, nearly pure Cu face-centred cubic phase forms at higher temperatures, while at medium temperatures, spherical Cu-rich nanoparticles form, which are found to be body-centred cubic at room temperature. The dimensions of the quench-induced particles range from several µm after cooling at 0.0001 K/s down to just a few nm after cooling at 1 K/s. The maximum age hardening potential of X5CrNiCuNb16-4 can be exploited if a fully supersaturated solid solution is reached at cooling rates above the critical cooling rate of about 10 K/s.

SHarp Interface FUll field precipitation Model. Michel Perez[1], Mathilde Eymann[1], Thomas Elguedj[2], Thibaut Chaise[2], Pierre-Antoine Geslin[1].

[1]INSA Lyon, CNRS, UCBL, MATEIS, UMR5510 69621 Villeurbanne Cedex, France.

[2]INSA Lyon, CNRS, LaMCoS, UMR5259 69621 Villeurbanne Cedex, France.

Modeling precipitation in metallic alloys is a topic of great importance in physical metallurgy as the resulting strengthening strongly depends on the precipitate microstructure. We propose here a numerical full-field model for precipitation that describes precipitates with shape functions, thereby allowing to bridge scales between phase-field approaches - that accurately describe the precipitate evolution but require a fine discretization grid - and mean-field approaches - that are computationally very efficient but rely on strong assumptions. Our results demonstrate the capability of the full-field approach to model the different stages of precipitation during isothermal treatments. The comparison with mean-field results allow to discuss the influence of solutal impingement and precipitate coagulations on the evolution of the precipitate microstructure.

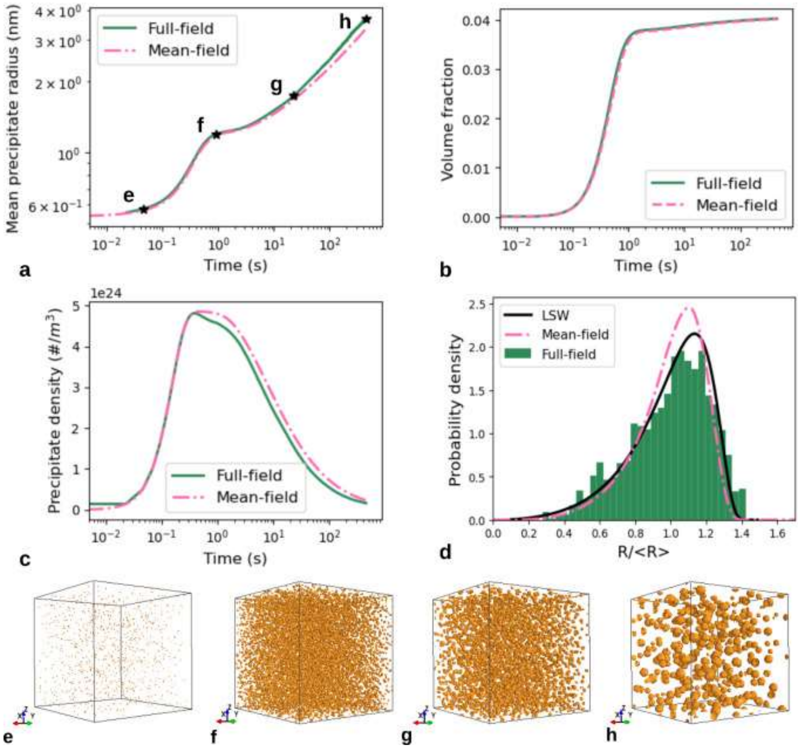

Comparison of the mean-field and full-field model: (a) average radius; (b) volume fraction; (c) precipitate density; (d) distribution.

Th2b.1-5: Tempering.

Invited. **Spontaneous transition from para-equilibrium to ortho-equilibrium: a study of cementite precipitation kinetics.** Qing Chen[1], Kaisheng Wu[2].

[1] Thermo-Calc Software AB, Solna, Sweden.

[2] Thermo-Calc Software Inc, McMurray, United States.

The spontaneous transition from para-equilibrium (PE) to ortho-equilibrium (OE) during the carbide formation in tempered steels, first discovered over 70 years ago by Axel Hultgren, remains a complex yet pivotal phenomenon. Despite its significance and several modeling attempts, a convincing and satisfactory solution has been elusive. This study presents a streamlined kinetic model to simulate the PE-OE transition during cementite precipitation in martensitic steels. By capturing the intricate interplay between the vastly different diffusivities of interstitial and substitutional elements, the model accurately describes the gradual evolution of interface conditions, enabling a smooth transition from carbon-dominated kinetics to solute-partitioned growth. Implemented within the TC-PRISMA module of Thermo-Calc, this model is seamlessly coupled with TCFE and MOBFE, the widely used thermodynamic and kinetic databases for steels, providing a practical tool for steel design and simulation. The model's predictions are validated against experimental data, with a discussion on the necessity of enhanced diffusion in the martensite matrix at the tempering temperatures. Additionally, the influence of alloying elements on the PE-OE transition is critically examined. By offering a quantitative and operational framework for simulating this complex phenomenon, the present study lays a foundation for optimizing alloy composition and microstructure to improve the performance of martensitic steels. The approach proposed here is expected to find broad relevance in the field of phase transformations, particularly in systems where transitions between PE, OE, non-partitioning local equilibrium (NPLE) occur.

Impact of carbon content on carbide precipitation sequences in low alloy steel. Victor Labussiere[1], Caroline Toffolon-Masclet[2], Estelle Meslin[3], Michel Perez[4], Bernard Marini[1].

[1] Université Paris-Saclay, CEA, SRMA Gif-sur-Yvettes, France.

[2] Université Paris-Saclay, CEA, S2CM Gif-sur-Yvettes, France.

[3] Université Paris-Saclay, CEA, SRMP Gif-sur-Yvettes, France.

[4] Université de Lyon, INSA Lyon, Laboratoire MATEIS, Lyon, France.

Low-alloy bainitic steel, used in nuclear reactor primary circuits, is subjected to irradiation and thermal aging at 300°C. These conditions can affect mechanical properties by altering the carbide population, size, and distribution, with carbon content variations influencing microstructure and mechanical properties. Within this framework, it is necessary to understand the impact of alloying elements and carbon variation on the precipitation sequences of carbides (such as cementite, M2C, and ξ carbides) and their evolution under irradiation. Thus, three model quaternary ferritic alloys containing the main alloying elements of 16MND5 (Mn, Ni, and Mo) and different carbon contents (0.23%, 0.30%, and 0.42%C) were fabricated and tempered at 650°C. The evolution of the carbide precipitation sequences was studied by in-situ and ex-situ XRD synchrotron radiation, allowing the determination of the influence of carbon content on the nature and fraction of carbides through a thorough analysis by Rietveld refinement. The crystallography of the studied carbides was determined through TEM characterization using conventional diffraction. Observation of the phase transformations during thermal tempering reveals a reorganization of Mo2C carbides into Ksi carbides, in agreement with the literature, regardless of the carbon content. However, the latter appears to influence the volume fraction observed. Finally, first insights into the radiation response of the model alloys, studied under representative conditions (300°C, a few tenths of dpa), will be presented, focusing on microstructural evolution and carbide precipitation sequences with TEM characterization. According to the literature, radiation-induced segregation can be expected.

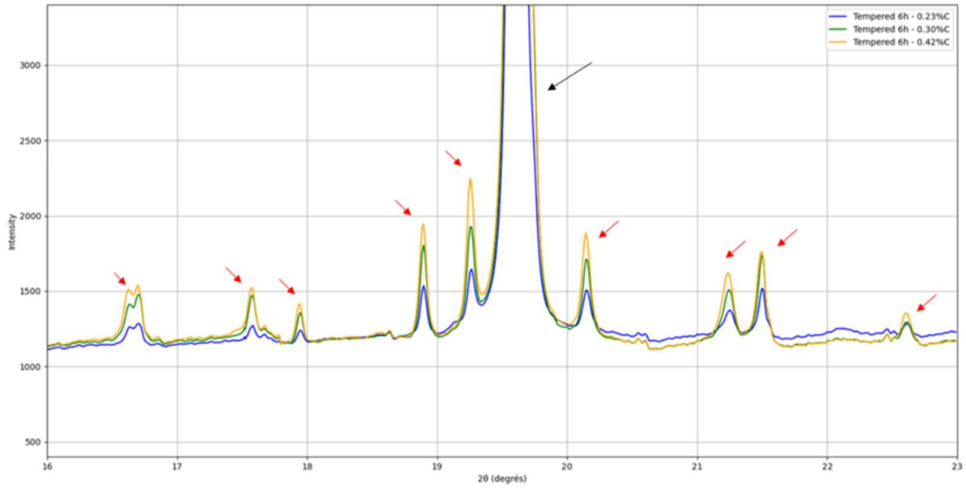

Diffraction pattern of Fe-X%C-1.3%Mn-0.7Ni-0.5Mo after 6-hour tempering at 650°C for carbon contents of 0.23%C (blue), 0.30%C (green), and 0.42%C (orange). The main peak (black arrow) belongs to the ferritic matrix, while small peaks (red arrows) represent those of carbides.

Nanocrystalline grain refinement induced by hard turning in a tempered martensitic dual-hardening Hybrid 60 steel. Sahith Kokkirala[1], Seyed Hosseini[2], Hirotsugu Iwasaki[3], Jonas Holmberg[4], Thomas Björk[5], Uta Klement[1].

[1] Chalmers University of Technology, Gothenburg, Sweden.

[2] AB SKF, Gothenburg, Sweden.

[3] SUMITOMO ELECTRIC Hartmetall, GmbH Willich, Germany.

[4] RISE AB, Mölndal, Sweden.

[5] Ovako AB, Stockholm, Sweden.

In the present work, the novel bearing alloy Hybrid 60 steel with the combined properties of maraging steel, tool steel and structural steel is subjected to a hard turning process. This low-carbon tempered martensitic dual-hardening steel, obtains its strength both by the precipitation of β-NiAl intermetallics and secondary carbides. During the hard turning process, the initial lath tempered martensite, β-NiAl intermetallics and secondary carbides undergo thermo-mechanical deformation, leading to the formation of a white layer with refined nanocrystalline grains on the machined surface. The formation mechanism of these nanocrystalline grains is influenced by specific cutting conditions such as feed rate and cutting speed. In the current study, hard turning at a cutting speed of 100 m/min and a feed rate of 0.05 mm/rev formed nanocrystalline grains through severe plastic deformation, whereas at 200 m/min and 0.2 mm/rev, refinement was driven by potential phase transformation. For both conditions, the refinement thickness observed is around 200-350 nm. Further, the nanograins are examined using scanning electron microscopy (SEM), scanning transmission electron microscopy (STEM), transmission electron microscopy (TEM), and transmission Kikuchi diffraction (TKD) techniques. These techniques are employed to characterize the microstructural evolution, as well as the behaviour of β-NiAl intermetallics and secondary carbides on the machined surface. The results offer valuable insights into the machinability of dual-hardening Hybrid 60 steel and its microstructural evolution on the machined surface, particularly for potential bearing applications.

The abnormal carbon redistribution in lath martensite during tempering in Mn-patterned steels. Zhiping Xiong.

Beijing Institute of Technology, Beijing, China.

Martensite tempering is a critical step to achieve high strength with decent ductility. It is well-known that, during tempering, the carbon is sequentially arranged as segregation, transition carbide and cementite. Abnormally, this study shows the absence of carbide precipitation in Mn-depleted martensite during tempering when Mn distribution is heterogeneous between austenite and martensite. After fast heating and short austenitization from Mn-depleted ferrite and Mn-enriched cementite, the high-temperature austenite with Mn heterogeneous distribution has formed, resulting in the formation of alternating Mn-depleted lath martensite and Mn-enriched film retained austenite (RA) after quenching. In comparison with the carbide precipitation in conventional lath martensite with Mn homogeneous distribution during tempering at 150–500◦C, carbide formation is completely inhibited in Mn-depleted lath martensite. Instead, carbon atoms diffuse from Mn-depleted martensite to its neighboring Mnenriched film RA, leading to an increased carbon content in RA. This is mainly attributed to the strong interaction between

Mn and carbon, further assisted by high dislocation density and small width of lath martensite. Additionally, this RA can promote carbon diffusion in the interior due to its gradient Mn distribution.

Decomposition of retained austenite during tempering of high-strength tool steels. Myriam Dumont[1], Jules Audard[1,2], Marine Lachal[2], David Quidort[2], Mohamad-Farès Slim[3], Denis Delagnes[4], Moukrane Dehmas[5].

[1]Arts et Métiers Institute of Technology, EA7350 - MSMP Lille, France.

[2]Industeel, ArcelorMittal Group, Le Creusot, France.

[3]Arts et Métiers Institute of Technology, EA7350 - MSMP Aix-en-Provence, France.

[4]Institut Clément Ader ICA ; Université de Toulouse, CNRS, IMT Mines Albi, Albi, France.

[5]CIRIMAT, Université de Toulouse, CNRS, Toulouse, France.

Decomposition of retained austenite (RA) during tempering in tool steels is of prime importance in the good balance between strength and toughness for plastic injection moulding applications. Grades with different compositions and with a mixed bainitic/martensitic initial microstructure were investigated using in-situ synchrotron high-energy X-ray diffraction (HEXRD) during tempering at temperatures between 550 °C and 600 °C for a dwell time up of one hour. Results indicated first carbide formation during heating or holding time of the tempering stage; however, austenite remains untransformed up to the end of the tempering holding time in all investigated conditions for both grades. In-situ HEXRD brings direct evidence of the transformation of austenite into fresh martensite on cooling from the tempering stage. This behaviour was correlated to the evolution of the carbon enrichment of retained austenite and the effect of composition is discussed.

Th2c.1-5: Nucleation and spinodal (I).

Invited. **A new approach to solid-state nucleation in kinetically constrained systems.** Christopher Hutchinson, Yves Brechet.

Monash University, Melbourne, Australia.

Nucleation is the first step of the phase transformations that we use to control the microstructures of engineering materials. The starting point for questions of nucleation is usually Classical Nucleation Theory (CNT) but for solid-state nucleation at low temperatures where atomic mobility is limited, such as in engineering alloys, CNT has not been very successful in quantitatively predicting nucleation. A strong assumption of CNT is that all thermally-induced stochastic fluctuations, no matter how far their compositions lie from the bulk alloy composition, are possible and that they become nuclei when a critical size determined from thermodynamics is reached. Here we present a new and complementary model for solid-state nucleation. We consider the other extreme where atomic mobility is limited and thermally-induced stochastic clusters cannot form in the time scale relevant for a nucleation event. Instead, we consider the geometric clusters that are a statistical feature of any solution as the origin of the nuclei and present a simple model for the number of nuclei and their rate of 'activation'. This new 'geometric cluster' model is shown to be able to successfully predict the competition in phase nucleation during the crystallization of a series of Al-Ni-Y metallic glass, predict the solvent trapping that is increasingly seen in solid-state nucleation and predict the peak number density of precipitates observed in Cu-Co and Fe-Cu alloys. The relationship between the new model and CNT is discussed as well as conditions where we will see a transition from the geometric cluster model to CNT.

Using impurity atoms to inoculate the solid-state homogeneous precipitation through a nonclassical nucleation pathway. Yanjun Li, Shiwei Pan, Chunan Li, Hanne Sofie Søreide, Xuezhou Wang, Dongdong Zhao, Constantinos Athanas Hatzoglou, Feng Qian.

Norwegian University of Science and Technology, Trondheim, Norway.

Solid-state homogeneous precipitation of nanosized precipitates is an effective method to strengthen materials. Here, we report a new strategy to inoculate the homogeneous precipitation in metal alloys by using impurity atoms. It is shown that the precipitation of nanosized $L1_2$ structure Al_3Zr precipitates in technologically important dilute Al-Zr alloys can be dramatically inoculated by addition of a trace level of non-$L1_2$ phase forming impurity atoms X or both X and Si, achieving substantially faster precipitation kinetics and 8 times higher number density of precipitates at peak ageing conditions. We demonstrate that inoculation could change the precipitation behavior from the classical nucleation and growth to a non-classical nucleation pathway, where Al_3Zr precipitates through the instantaneous formation of local concentration fluctuation of Zr atoms on low energy Zr-X-Vacancy and Zr-X-Si-Vacancy atom complexes followed by a continuous increase of the concentration and chemical short-range ordering (CSRO) of Zr atoms during aging. This precipitation pathway is analogous to the spinodal decomposition but in a heterogeneous manner. With the generalized selection principles of potential inoculation impurity elements proposed in this work, we could identify several impurity elements having similar inoculation effect to X. It is expected such an inoculation strategy can be widely applied to enhance the solid-state precipitation strengthening in different alloy systems.

Fundamental study of nonclassical nucleation mechanisms in iron: heterogeneous nucleation at grain-boundary dislocations. Xiaoqin Ou[1,2], Jilt Sietsma[2], María J. Santofimia[2].

[1]Central South University, Changsha, China.

[2]Delft University of Technology, Delft, the Netherlands.

Nucleation during phase transformations plays an important role in the crystal structure, the grain size and the texture of the forming product phase, and thus determines the properties of the obtained material. In the present study, molecular dynamics simulation is employed to study the heterogeneous nucleation of bcc phase in fcc iron. Two systems are studied: one has a coherent twin grain boundary and a semicoherent twin boundary, the other has two low-angle grain boundaries. It is found that the bcc phase nucleates at the dislocations in the low-angle boundaries and semicoherent twin boundary in a pseudo-cylindrical morphology. The energy change as a function of the bcc nucleus size conforms to the Cahn's classical model with no energy barrier, and provides interface energies and elastic constants comparable to theoretical calculations and experimental data. Nevertheless, there are aspects that cannot be explained by the classical Cahn nucleation theory: (a) the bcc nucleation at dislocations follows a stepwise "fcc→intermediate→bcc" process rather than a single-step "fcc→bcc" phase transformation; (b) the individual bcc nucleus is an aggregate of discrete subnuclei bound by the intermediate state; (c) the local temperature of regions containing bcc nuclei is higher than the surroundings regardless of the isothermal conditions for the entire system.

Microstructural design by combining nanograins and spinodal decomposition in a Fe-Cr alloy.
Macchi[1], Nakonechna[1], Henry[1], Castro[1], Edalati[2], De Geuser[3], Sauvage[1], Lefebvre[1].

[1]Univ Rouen Normandie, INSA Rouen Normandie, CNRS, Normandie Univ, GPM UMR 6634 F-76000 Rouen, France.

[2]WPI, International Institute for Carbon-Neutral Energy Research (WPI-I2CNER), Fukuoka, Japan.

[3]University Grenoble Alpes, CNRS, Grenoble INP, SIMaP, Grenoble F-38000, France.

In order to achieve new high-performance alloys their microstructure design requires the combination of multiple hardening mechanisms. In this study the combination of high Hall-Petch effect with spinodal decomposition hardening has been chosen and an Fe-51.4Cr (at.%) alloy was selected[1]. High-pressure torsion (HPT) was applied for producing nanograins which presented a 51 nm grain size (determined by TKD). The obtained material was then aged at 525 °C for varying holding times up to 200h. The grain size only increased by a factor of 3 after a 100h ageing. The spinodal decomposition was characterized by atom probe tomography (APT). The amplitude and the wavelength were then determined by the analysis of the radial distribution function (RDF). In the highly-deformed condition, the spinodal decomposition was revealed after one hour of annealing while 100h were required at the undeformed state. The thermodynamic-predicted amplitude was reached after only 100h in the HPT state while without deformation 1000h-2000h were needed to reach such state. HPT accelerated decomposition kinetics is due to the high vacancy concentration. The hardness increased by 500 HV after the HPT process and its decrease due to the grain growth was highly compensated by the spinodal decomposition strengthening. The fracture toughness evolution was determined by in-situ micro-flexion tests. A decreased of the toughness was observed. The authors acknowledge ANR for its support through the project SpinodalDesign (ANR-22-CE08-0016-01).

[1] J. Macchi, O. Nakonechna, R. Henry, C. Castro, K. Edalati, F. De Geuser, X. Sauvage, W. Lefebvre, Scr Mater 252 (2024) 116247. https://doi.org/10.1016/J.SCRIPTAMAT.2024.116247.

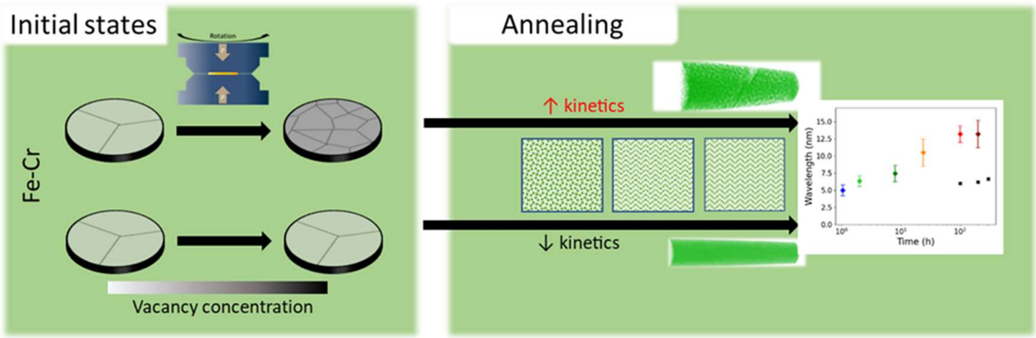

Spinodal decomposition induced nano-sized clustering during low-temperature nitriding of Fe-35Ni-X (X=Cr, V, Mo, Al, Mn) alloys. Yulin Xie, Goro Miyamoto, Tadashi Furuhara.

Institute for Materials Research, Tohoku University ,Sendai, Japan.

The expanded austenite (γ_N) produced by low-temperature nitriding of austenitic stainless steels with a high Cr content is conventionally regarded as a nitrogen-supersaturated fcc solid solution with Cr-N short-range ordering. However, there is a significant possibility for γ_N to be decomposed by nanoscale phase separation or spinodal decomposition due to the strong Cr-N attractive interaction. In the present study, the alloying effect of X elements (X = Al, V, Cr, Mo) with different X-N interactions on the nanostructure evolution of Fe-35Ni-10X (at%) alloys plasma nitrided at 673 K is revealed using transmission electron microscopy (TEM) and three-dimensional atom probe (3DAP). The formation of expanded austenite (γ_N) with nitride precipitation near the surface is observed in all the specimens. The N concentration and hardness of γ_N increased in the order of Al, Mn, Mo, Cr, V, consistent with the magnitude of the X-N attractive interaction in fcc. The nano-sized X-N (X=Mo, Cr, V) clusters were directly revealed in γN as strong <001>γ streaks in selected area diffraction, obvious modulated structure along <010>γ in TEM and simultaneous enrichment of X and N inside the clusters observed by 3DAP. Thermodynamic computations of coherent spinodal were conducted with the help of Thermo-Calc. The results showed that X-N clusters were formed by spinodal decomposition for the Mo, Cr and V added alloys due to strong X-N attractive interaction while the spinodal decomposition is thermodynamically impossible for Al and Mn added alloys.

Th3a.1-4: Precipitation (III) – Microalloying.

Precipitation evolution in microalloyed steels during welding.

Hugo Lannay[1], Michel Perez[1], Sophie Cazottes[1], Thibaut Chaise[2], Antoine Facco[3], Miguel Yescas[4].

[1] MatéIS, Lyon, France.

[2] LaMCoS, Lyon, France.

[3] EDF Moret-Loing-et-Orvanne, France.

[4] Framatome, Paris, France.

This study explores the precipitation of (Nb,V)C carbides in microalloyed steels during welding and stress relief heat treatment (SRHT) of nuclear power plant secondary circuit pipes. A focus is made on how the heat history influences the mechanical properties of the material through particle size distribution evolution. This research investigates the effect of thermal cycles and alloying elements (Nb and V) on the nucleation and growth of precipitates within the Heat-Affected Zone (HAZ). Four model steel alloys (without Nb and V, with Nb, with V, with both) are studied and a thermomechanical simulator is used to reproduce welding cycles and SRHT. The chemistry and the distribution of precipitates are characterised using electron microscopy. Hardness and Charpy impact tests are performed to assess the link between precipitation and mechanical properties. Simultaneously, a KWN model [1] is developed to simulate the evolution of the precipitation distribution at each point of the HAZ, during welding and SRHT, incorporating classic nucleation and growth theories (CNGTs). This study provides valuable insights that emphasise the link between thermal cycles, precipitation and mechanical properties. In particular, far from the weld, precipitates do not evolve; in the opposite, near the weld, they are completely dissolved. However, in the sub-critical HAZ (just below Ac1), precipitates can grow up and be one of the causes of the ductility drop observed at these distances (*cf.* Figure).

[1] Wagner R, Kampmann R, Voorhees PW. Homogeneous Second-Phase Precipitation. In: Kostorz G, editor. Phase Transform. Mater., John Wiley & Sons, Ltd; 2001, p. 309–407.

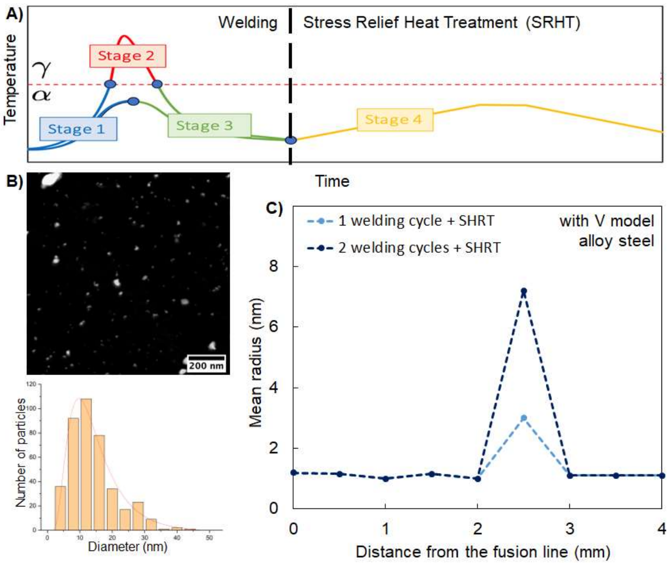

A) Welding + SRHT; B) Distribution of VC carbides after 2 welding cycles + SRHT; C) Mean radius as function of the distance from the fusion line.

Mean Field modeling of microstructure evolution of micro-alloyed steels in thermomechanical processing. Shabnam Fadaei Chatroudi, Robert Cicoria, Hatem Zurob.

McMaster University, Hamilton, Canada.

A comprehensive through-process model is crucial for understanding how thermomechanical treatments affect microstructure evolution during hot rolling process [1]. A new Mean Field numerical approach has been developed to efficiently model complex microalloyed systems across various conditions, linking process parameters to final material properties. This approach simplifies grain interactions by embedding each grain in an average medium. In this contribution existing models of recovery, recrystallization, grain growth and precipitation [2] are coupled in order capture grain size evolution during hot rolling. The effects of the deformed grain shapes as well as annealing twin formation were considered for a more realistic microstructure description. In order to ensure efficiency and maintain accurate grain number throughout the entire simulation, Upsampling and Downsampling algorithms were introduced to dynamically adjust the grain ensemble [3]. This adaptation prevents under- and over-sampling artifacts encountered in case of extended growth as well as nucleation of new grains during recrystallization, facilitating the modeling of multi-pass operations compatible with industrial applications. The accuracy of the model is verified against analytical solutions and experimental data over a range of processing parameters, demonstrating high agreement. The effect of different initial microstructures is successfully investigated, demonstrating the versatility of this model.

[1] Sellars, C.M., Materials Science and Technology, 1990. **6**(11): p. 1072-1081.

[2] Zurob, H.S., et al., *effect of coupling recovery, precipitation and recrystallization*. Acta Materialia, 2002. **50**(12): p. 3077-3094.

[3] Chatroudi, S.F., R. Cicoria, and H.S. Zurob, Materials, 2024. **17**(10): p. 2341.

Detecting iron in vanadium carbide nanoprecipitates by atomic-resolution scanning transmission electron microscopy techniques. Amir Sabet Ghorabae, Bart J. Kooi.

University of Groningen, Groningen, the Netherlands.

Microalloyed low-carbon steels strengthened by vanadium carbide (VC) nanoprecipitates are receiving increasing attention for use in automotive industry. Recent analyses of small-angle neutron scattering (SANS) and atom probe tomography (APT) data suggest that interphase-precipitated VC nanoprecipitates are enriched in iron in the initial stages of their nucleation and growth during the austenite-to-ferrite phase transformation. Iron may reduce the coherency strain resulting from the lattice mismatch between the precipitate and the matrix, thereby lowering the nucleation barrier during the interphase precipitation. However, it is not yet clear whether the iron is present as a shell or in the core of the nanoprecipitates and whether the iron also plays a role in random precipitation of VC nanoprecipitates during aging of bainitic/martensitic microstructures. Here a model vanadium-microalloyed low-carbon steel with interphase and random nanoprecipitates was studied through detailed (scanning) transmission electron microscopy (S/TEM) of carbon extraction replicas. Energy-dispersive X-ray spectroscopy (EDS) spectrum imaging combined with experimental and simulated high-angle annular dark-field (HAADF) and integrated differential phase contrast (iDPC) microscopy by STEM was employed for detection of iron in the VC crystal structure. The VC nanoprecipitates formed by the interphase precipitation mechanism indicated the presence of iron in their crystal structure whereas the VC nanoprecipitates formed by the random precipitation mechanism were almost iron-free. These results are supported by thermodynamic and kinetic evaluations of the precipitation mechanisms, improving our understanding of the evolution of VC nanoprecipitates in microalloyed low-carbon steels.

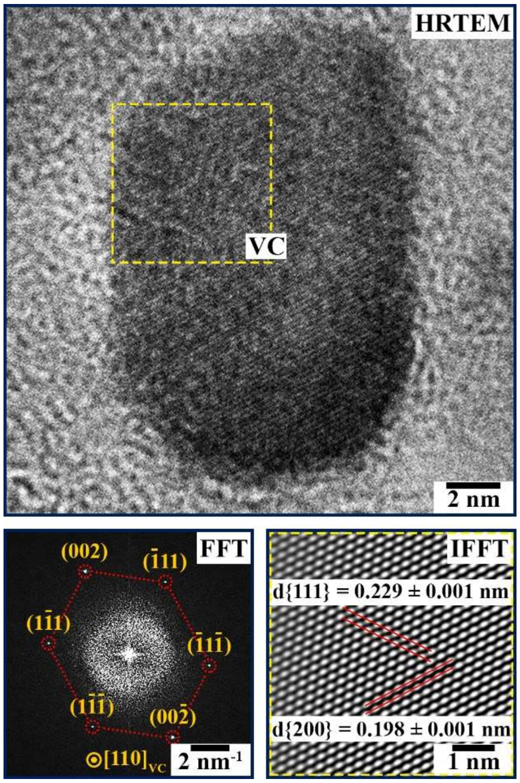

High-resolution transmission electron microscopy (HRTEM) image of a vanadium carbide nanoprecipitate in a low-carbon low-vanadium steel.

Influence of the precipitation state on the work hardening in 6016 and 6061 alloys. Anna Lena Krejci[1], Ernst Kozeschnik[1], Thomas Schöngruber[1], Raquel Nalda Berganza[2].

[1] TU Vienna, Vienna, Austria.

[2] Universidad de Deusto, Bilbao, Spain.

Understanding the influence of microstructure on dislocation evolution is crucial for accurately simulating material behavior under plastic deformation. This study investigates how the transition from clusters to shearable and then to non-shearable precipitates affects work-hardening behavior and dynamic recovery in the aluminum alloys 6061 and 6016. Compression tests are conducted following various artificial and natural aging treatments to analyze the influence of precipitation states on the material's response. The thermo-kinetic software package MatCalc is employed to model flow curves using an extended Kocks-Mecking approach. This provides insights into how the precipitation state impacts dislocation generation and annihilation rates. Preliminary results emphasize the significant role of precipitates in modifying dislocation dynamics, enhancing our understanding of constitutive modeling in aluminum alloys.

Th3b.1-4: Segregation.

Modeling the interaction of carbon segregation to defects and carbon partitioning in multiphase steels. Konstantina Traka, Jilt Sietsma, María J. Santofimia.

Delft University of Technology, Delft, the Netherlands.

Carbon segregation to defects in martensite is a phenomenon known for its occurrence and interference with mechanisms such as carbon partitioning in multiphase steels. Especially in martensite – austenite partitioning, carbon trapping at / de-trapping from martensite defects interacts with the austenite enrichment. We develop a physics-based model in which we incorporate the concurrent evolution of carbon partitioning and trapping at / de-trapping from martensite defects. The model describes the global and local, time-dependent distribution of carbon between three lattice types, namely martensite defects, martensite solid solution, and austenite. No trapping is assumed to take place in the latter two. A simulation example is shown in Fig. 1 for annealing at 400 ◦ C a microstructure of austenite fraction $f^{\gamma} = 0.10$, starting from the quenched state, i.e. 0 s. Fig. 1, (a),(b) show the total carbon concentration $x_{C,i}^{tot}$ at 0 s and 300 s, respectively, (c),(d) show the trapped-carbon concentration $x_{C,i}^{trap}$ at 0 s and 300 s, respectively, and (e),(f) show the free-carbon concentration $x_{C,i}^{free}$ at 0 s and 300 s, respectively. It is evident that during annealing, carbon partitions to austenite, de-traps from martensite defects, but at the same time enriches some martensite boundaries much more compared to the quenched state. Regarding the overall austenite enrichment, this model explains the limited austenite enrichment reported in many experimental studies. Additionally, we apply the model in several martensite - austenite microstructures and discuss the dependence of carbon evolution on specific microstructural features, i. e. phase fractions and microstructural banding.

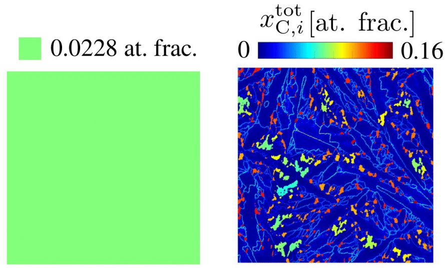

(a) 0 s : $x_{\mathrm{C},i}^{\mathrm{tot}}$ (b) 300 s : $x_{\mathrm{C},i}^{\mathrm{tot}}$

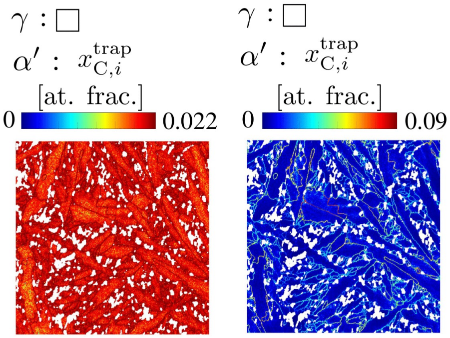

(c) 0 s : $x_{\mathrm{C},i}^{\mathrm{trap}}$ (d) 300 s : $x_{\mathrm{C},i}^{\mathrm{trap}}$

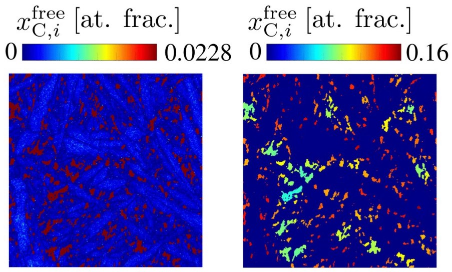

(e) 0 s : $x_{\mathrm{C},i}^{\mathrm{free}}$ (f) 300 s : $x_{\mathrm{C},i}^{\mathrm{free}}$

Simulation of annealing at 400 ∘ C a martensite-austenite microstructure (fγ = 0.10) starting from the quenched state (0 s); (a),(b) show the total carbon concentration at 0 s and 300 s, respectively, (c),(d) show the trapped-carbon concentration at 0 s and 300 s, respectively, (e),(f) show the free-carbon concentration at 0 s and 300 s, respectively.

Phase transformation upon cooling in steels alloyed with Mn and Si. Monika Krugla[1,2], S.Erik Offerman[2], Jilt Sietsma[2], Dave Hanlon[1].

[1]Delft University of Technology, Delft, the Netherlands.

[2]Research and Development, Tata Steel Europe, the Netherlands.

The phase transformation from austenite to ferrite and a second, carbon-rich phase in steel is a critical process that significantly influences the microstructure and mechanical properties of the material. One of the consequences of steel production as a strip is presence of micro-segregation. Additionally, most steels contain a certain concentration of silicon (Si) and manganese (Mn). The present study systematically investigates the influence of micro-segregation of those two elements on the phase transformation upon cooling. The impact of cooling rates, austenite grain size at the beginning of cooling, and the presence of micro-segregation on the transformation behaviour from austenite to ferrite and second phase in steel is investigated. This effect is studied experimentally by studying two material variants per alloy, one in the segregated state and one that underwent a homogenization treatment. Heat treatments are continuous cooling experiments with three different cooling rates applied to all materials. The results reveal that the phase transformation process from austenite to ferrite and second phase is significantly influenced by both parameters. We observed differences not only in nucleation behaviour but also in the transformation rates.

Boron subsurface depletion in cold rolled hot dip galvanized AHSS strip steel. Joost van Krevel.

Tata Steel R&D, IJmuiden, the Netherlands.

Cold rolled Advanced High Strength Steel (AHSS) strip grades are applied in automotive crash safety parts after being processed through continuous annealing and hot-dip galvanising for corrosion protection. The addition of boron enhances hardenability by segregating to dislocation rich areas such as primary austenite grain boundaries, which in turn inhibits the transformation of austenite to ferrite upon cooling. While the impact of boron in the bulk is well established, there is still a need to comprehensively understand surface phenomena related to boron. The objective is to develop a better understanding of phase formation at the surface. Two boron containing AHSS chemical compositions, MnCr and 14C, were selected from the Tata Steel plants in IJmuiden. Both alloys contain an excess of either Al, Ti, or Nb to capture N and prevent the formation of BN. Steel grade MnCr undergoes austenitic annealing at approximately 830°C while grade 14C is intercritical annealed at around 800°C. Samples from hot rolled and pickled, cold rolled and continuous annealed strips were subjected to surface and bulk analysis using SEM, EBSD and GDOES techniques. Depletion of boron up to 70 µm into the surface is detected in the intermediary hot rolled and pickled strip products, surpassing the depth of decarburization, which ranges from 20-30 µm. During continuous annealing, further deboronisation occurs, leading to the accumulation of boron-containing oxides at the interface between zinc and steel. Depletion of boron during continuous annealing is observed at depths ranging from 40-60 µm for 14C and MnCr grades accompanied by decarburization to depths of 10-20 µm. Microstructure images of two boron-containing AHSS grades reveal higher contents of ferrite in the steel strip surface after continuous annealing compared to the bulk. The increased ferrite content is attributed to a reduction in hardenability caused by the absence of boron in the outer surface profiles, as well as a shift in ferrite austenite transformation temperatures during annealing due to additional decarburization in the outer surface.

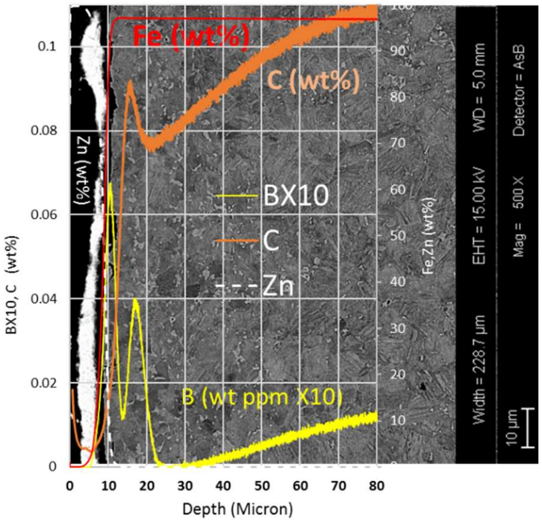

SEM and GDOES overlay surface microstructure image of MnCr alloy . The magnification is 500X.

Role of interfacial coherency and carbon in niobium segregation at ferrite/austenite interface: an atomistic study. Haokai Dong[1], Hao Chen[2].

[1]Ningbo Institute of Materials Technology and Engineering, CAS, Ningbo, China.

[2]Tsinghua University, Beijing, China

Segregation of substitutional alloying elements at the moving interface can remarkably influence the kinetics of phase transformation in steels. It has been experimentally verified that the elemental segregation behavior strongly depends on the interface character and foreign atoms presence, e.g. carbon (C), while the underlying mechanism particularly in atomic scale remains unclear. Here, we employ Molecular Statics and hybrid Molecular Dynamics/Monte Carlo simulation approaches to comparatively investigate the niobium (Nb) segregation behaviors at both the incoherent and semi-coherent ferrite/austenite interfaces in Fe-C-Nb systems. The calculations reveal that the atomic Virial stress perpendicular to the interface is crucial for the binding energy of Nb to the interface, and the C presence at the interface has both physical and chemical interactions with Nb. It is conventionally believed that C addition can promote Nb segregation due to their attractive interaction, while the current study demonstrates that C and Nb atoms tend to form clusters in ferrite, thereby weakening the Nb segregation. The present study provides a promising computational approach for investigating the elemental co-segregation in steels.

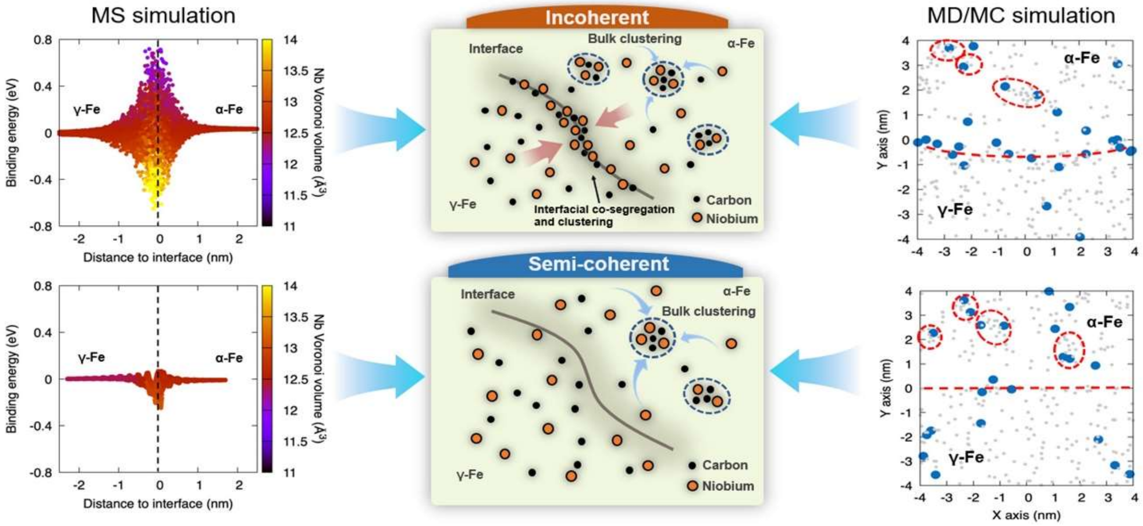

Th3c.1-5: Nucleation and spinodal (II).

Invited. **Hydrogen-assisted spinodal decomposition in a TiNbZrHfTa complex concentrated alloy.** Wu[1], Aota[1], Rao[1], Zhang[1], Perrière[2], Duarte[1], Raabe[1], Ma[1,3].

[1]Max Planck Institute of Sustainable Materials, Dusseldorf, Germany.

[2]Université Paris-Est Créteil, Paris, France.

[3]Delft University of Technology, Delft, the Netherlands.

Understanding hydrogen-metal interactions is crucial for developing refractory complex concentrated alloys (CCAs), applicable to the hydrogen economy. In this study, we revealed a hydrogen-assisted spinodal decomposition phenomenon at the nanoscale in an equiatomic TiNbZrHfTa CCA upon its exposure to H_2 at 500 °C. Such a decomposition pathway was characterized by a periodic compositional modulation with an up-hill diffusion behavior of the principal metallic elements, probed by 3D atom probe tomography. Consequently, the decomposed alloy consisted of a needle-shaped phase enriched in Zr and Ti and a phase enriched in Nb and Ta. To better understand the role of hydrogen in spinodal decomposition, a statistical thermodynamic model was further developed by incorporating hydrogen to predict the phase stability of the TiNbZrHfTa-H system. This analysis suggested that hydrogen destabilizes the single solid-solution phase by expanding the spinodal region to higher temperatures. This study not only provides fundamental insights into the effect of hydrogen on phase stability but also demonstrates a novel alloy design strategy by introducing hydrogen as an interstitial alloying element to tailor microstructure.

Phase separation in pre-patterned metastable Ag-Cu thin films. Vivek C Peddiraju, Subhradeep Chatterjee, Shourya Dutta-Gupta.

Indian Institute of Technology Hyderabad, Sangareddy, India.

Dimensional and material constraints present in a film-substrate system are known to influence phase separation in metastable thin films. We show that pre-patterning of the film and chemical reaction between film and substrate too can significantly alter the phase separation. We sputter-deposit nominally equimolar Ag-Cu thin films on Si substrates and make circular apertures (wells) of varying diameter on them using FIB-milling. On annealing, a random mixture of Ag-rich and Cu-rich domains form away from the apertures by phase separation of the metastable film. However, near the apertures, the Si-substrate reacts with Cu in the film to form Cu_3Si, altering the phase separation locally and creating a distinct *halo* structure made up of two concentric rings around the apertures. The chemical reaction and halo formation are not observed below a certain critical annealing temperature. The characteristic length scale of the halo follows a power-law relationship with annealing time with an exponent of about 0.3. This marks a clear departure from the $\sqrt{t}$-type bulk diffusion controlled kinetics. A similar behavior is observed for films deposited on a SiN_x/Si substrate as well. We also extracted kinetic parameters of spinodal deposition and domain coarsening in the bulk film by image analysis and additional X-ray diffraction experiments, which are compared with those for the reaction-diffusion controlled halos around milled apertures. Results of the study suggest a novel route to locally tune the microstructure of Ag-Cu thin films with potential applications in, *e.g.*, plasmonics.

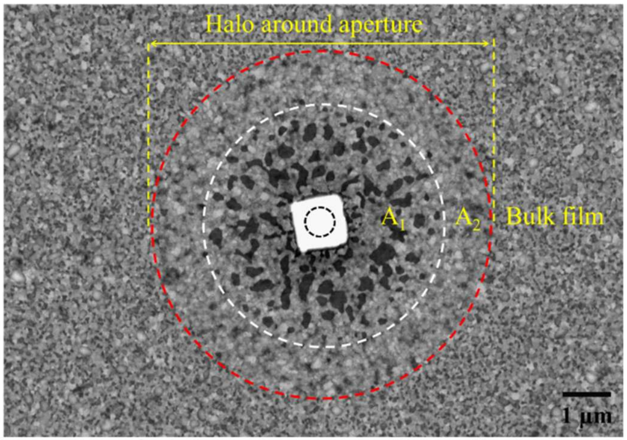

Formation of a halo structure around FIB milled apertures on a metastable Ag-Cu film

The formation of κ-carbides through spinodal decomposition and their effect on the mechanical properties of a low-density steel. Alexandros Banis[1,2], Efthymios Polatidis [3], Nikos Boukos[1], Ilchat Sabirov[4], Roumen Petrov[2].

[1]National Centre for Scientific Research 'Demokritos', Athens, Greece.

[2]Ghent University, Ghent, Belgium.

[3]University of Patras, Patras, Greece.

[4]IMDEA Materials, Getafe, Spain.

The current work studies the precipitation of κ-carbides in austenitic low-density steel and their effect on the mechanical properties. Such steels are heavily alloyed with Mn and Al, elements that tend to reduce the density of the material, resulting in lightweight materials with high specific strength. The austenitic matrix in such alloys ensures outstanding ductility, while the precipitation hardening effect of the κ-carbides increases the strength of the material significantly. The studied alloy has a composition of Fe-28Mn-9Al-1C in wt.%. The steel was aged at 550℃ for 8 h, and the size, morphology, and volume fraction of the κ-carbides and their interactions with the dislocations upon deformation were quantitatively studied via High-Resolution Transmission Electron Microscopy (HRTEM) and Synchrotron X-ray diffraction. From the microstructural analysis, it is found that at the initial stages of aging at 550°C, fluctuations of Al and C in the chemical composition led to the precipitation of intragranular κ-carbides with a diameter less than 4 nm. These carbides are homogeneously distributed and coherent with the austenite matrix, leading to their shearing from the gliding dislocations. The increasing size and fraction of these carbides lead to higher hardness (up to 390HV) and tensile strength (up to 1100MPa) but reduced dislocation mobility and, thus, reduced elongation at fracture (48%). It is concluded that the size, fraction, and interparticle spacing of the κ-carbides are crucial in the dislocation-particle interaction during plastic deformation.

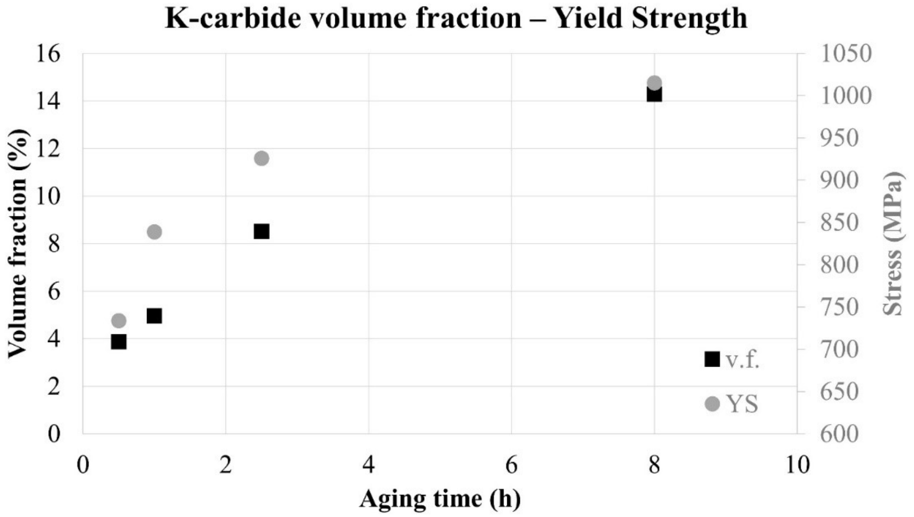

The effect of the κ-carbide volume fraction on the yield strength of the low-density steel.

Spinodal decomposition in the Li-Mg system. Leonardo Shoji Aota[1], Aubin Leray[2], Alisson Kwiatkowski da Silva[3], Júlio César Pereira dos Santos[3], Dominique Larcher[2], Dierk Raabe[1], Baptiste Gault[1,4].

[1] Max Planck Institute for Sustainable Materials, Düsseldorf, Germany.

[2] Université de Picardie, Jules Verne, Amiens, France.

[3] Thermocalc, Stockholm, Sweden.

[4] Imperial College, London, United Kingdom.

Li-rich Li-Mg alloys are promising anode candidates for lithium metal batteries, since the large Li solubility in the BCC phase (30-100 at.% Li) allows homogeneous lithium plating due to the decreased nucleation overpotential. This effect is believed to decrease the propensity for the uncontrolled Li deposition, i.e. dendrite growth, which would otherwise decrease the cycle stability of the anode. Despite the Li solubility, the local Li distribution in the nanoscale can directly affect the microstructure evolution, and hence the properties of such anodes in terms of electrochemical performance. Here, we galvanostatically lithiate Mg-25.7 at.% Li anodes to sweep the whole BCC phase range in the Li-Mg system. By using atom probe tomography, we reveal chemical fluctuations typically ranging from 50-80 at.% Li, characteristic of a spinodal decomposition, thus indicating the presence of a previously unknown miscibility gap in the BCC phase from the Li-Mg system. The obtained chemical composition in Li-rich and Li-poor regions are used in thermodynamic assessment based on the CALPHAD methodology to draw a new phase diagram. We suggest that a conditional spinodal decomposition exists, where the formation of a B2 phase around 50 at.% Li drives the phase separation. We discuss the likely positive effect of a spinodal decomposition in enhancing the overall Li diffusivity in Li-Mg alloys, further favoring the homogeneous lithium plating.

Revisiting decomposition kinetics in the Al-Zn binary alloys. Hugo Jean[1], Isabelle Mouton[1], Hugo Van Landeghem[1], Williams Lefbvre[2], Frédéric De Geuser[1].

[1] Université Grenoble Alpes, UGA, CNRS, SIMaP Grenoble France.

[2] Normandie Université, UNIROUEN, INSA Rouen, CNRS, GPM Rouen, France.

When saturated with solute elements, alloys containing a miscibility gap can decompose via a mechanism called spinodal decomposition. Current commercial alloys are too dilute in alloying elements to present this behaviour and the formation of a new phase is usually described by nucleation and growth. However, in certain conditions, some precipitation strengthened alloys exhibit a behavior which is neither nucleation/growth nor spinodal decomposition. This is particularly true at early stages, low temperature and high composition. This work aims to assess the behaviour of aluminium alloys falling in this indeterminate region by revisiting the Al-Zn binary system, known for its spinodal decomposition. The kinetics of decomposition in different Al-Zn binary alloys are assessed using in-situ Small Angle X-ray Scattering (SAXS). The evolution of the size and the quantity of solute-rich features are extracted from the SAXS curves with time and temperature variations. These observations are complemented by atom probe tomography (APT) analysis of selected states. We show the effect of composition by studying the decomposition kinetics of several Al-Zn alloys close to the spinodal line (4.4at%, 6.8at%, 9.4at% and 12.1at%) at different temperatures after quench. To elucidate the effect of quenched-in vacancies, we also compare these results with the kinetics of the same alloys after a slow cooling, as well as with binary alloys with a small addition of Sn which is known to trap vacancies in aluminium alloys.

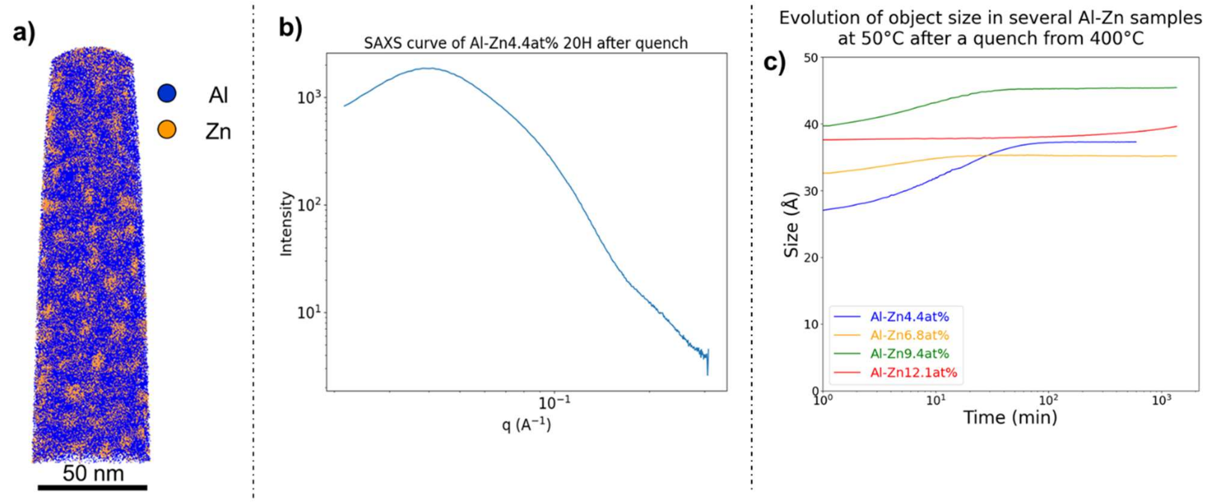

a) APT tip of Al-Zn4.4at% one week after quench from 400°C, b) SAXS curve of Al-Zn4.4at% 20H after a quench from 400°C, c) Evolution of object size at 50°C in several Al-Zn samples with time (extracted from SAXS curves)

Friday, July 11

Plenary 7. Interface character-dependent energy dissipation and interaction of alloying element during ferrite/austenite interface migration. Goro Miyamoto, Kanon Sato, Yongjie Zhang, Tadashi Furuhara.

Tohoku University, Sendai, Japan.

The kinetics of the austenite-to-ferrite transformation are significantly influenced by alloying elements through modifications in phase stability, local partitioning, and segregation at the migrating interface. Energy dissipation during interface migration is an important concept for quantitative understanding the impact of alloying on interface behavior. Our research group has developed a method to quantify this energy dissipation based on the non-equilibrium carbon content at the interface, measured using field-emission electron probe microanalysis (FE-EPMA). By integrating these measurements with analyses of interface crystallography and local element enrichment, we systematically investigated the origins of energy dissipation in Fe-X-C systems, where X includes Mn, Ni, Mo, Nb, and Si. Our findings reveal that incoherent interfaces, such as non-Kurdjumov-Sachs (non-K-S) interfaces, exhibit lower energy dissipation due to their larger intrinsic mobility compared to semi-coherent near K-S interfaces in Fe-C system. In Fe-X-C systems, non-K-S interfaces demonstrate a stronger tendency for alloying element segregation, causing large solute drag effect than near K-S interface. A comparison with the solute drag model indicates that energy dissipation is dominated by local partitioning, segregation of element, and intrinsic mobility at slow, intermediate and fast velocity, respectively. It is also found that the trans-interfacial diffusivity of alloying elements is comparable to their diffusivity in ferrite. Finally, comparative discussions will address energy dissipation during ferritic, bainitic, and martensitic transformations.

F1a.1-4: Impurities and novel production methods (I).

Invited. **Full field modelling of the impact of tramp elements on the microstructure evolution of Nb-containing high-strength low alloy steel during hot rolling.** Lekshmi Sreekala, Kees Bos.

Tata Steel Nederland B.V. (Tata Steel IJmuiden), IJmuiden, the Netherlands.

The green transition in the steel industry emphasizes sustainable practices, notably the increased use of recycled steel scrap to reduce carbon emissions. The use of scrap in steelmaking potentially changes the chemistries, process requirements and property response of various steels. Tramp elements such as Cr, Mo, Ni and Sn in steel, introduced through the use of scrap, are difficult to remove during steelmaking and can change the microstructural evolution of the base material. This study focuses on the impact of tramp elements on the microstructure evolution of a Nb-containing high strength low alloy (HSLA) steel during hot rolling. Physics based mean field model descriptions that capture the important interactions in HSLA grades between precipitation, recovery and recrystallisation are readily available from literature. In this work an existing Cellular Automata based full field recrystallisation model has been extended by applying such a mean field model at the grain scale. After optimization of the model parameters against available double hit dilatometry data for the base HSLA grade, the full field model is applied to assess the impact of tramp elements on the microstructure evolution in multi stand hot rolling.

Fine-Tuning machine learned potentials to study diffusion of tramp elements in bcc Fe. Naveen Mohandas[1], Sebastian Echeverri Restrepo[2], Marcel Sluiter[1].

[1]Delft University of Technology, Delft, the Netherlands.

[2]SKF, Utrecht, the Netherlands.

During steel recycling, impurities such as copper and tin are difficult to remove. These elements tend to segregate at grain boundaries (GBs), leading to defects like hot shortness. Introducing solute atoms, such as nickel, can mitigate these detrimental effects. However, identifying such elements requires high-throughput atomistic simulations that account for all possible combinations of elements, which is computationally expensive. Recently, machine-learned interatomic potentials (MLIPs) have emerged as a more efficient alternative to density functional theory, offering comparable accuracy at lower computational costs. Among these, some MLIPs, like the Crystal Hamiltonian Graph Neural Network (CHGNet), have been developed as universal interatomic potentials applicable to any combination of elements in the periodic table. In this work, we explore fine-tuning strategies for CHGNet to improve defect energy predictions in the Fe system. We then use the universal nature of the potential to study the diffusion behavior of C, Cu, Ni, and Sn in bcc Fe when these elements are present in combination.

The effect of residual alloying elements on the isothermal γ → α transformation in low carbon low alloy steels. Yulin Ju, Martin Strangwood, Jiaqi Duan, Carl Slater, Claire Davis.

University of Warwick, Coventry, United Kingdom.

The change in steelmaking route from carbon-intensive BF-BOF to predominantly scrap-based EAF means there will be enrichment of residual alloying elements in the produced steels. In lean low carbon low alloy steels consisting of ferrite with some second hard phases, residual alloying elements may segregate to grain boundaries, decreasing the grain boundary energy and providing solute drag on moving interfaces. It is important to establish the effect of residual alloying elements on the isothermal $\gamma \rightarrow \alpha$ transformation behaviour in lean grades, in this work Sn is considered. A series of laboratory-cast and hot-rolled model alloys (Fe-0.12C-1.9Mn-0.23Si) with varied additions of Sn (0 - 0.2 wt%) was used. Re-austenisation conditions were determined that gave the same prior austenite grain size (PAGS) for the different alloys, to eliminate the influence of PAGS on transformation behaviours. Two different PAGS were selected for testing with mode PAGS of 30 - 40 and 60 - 70 μm, both log-normal PAGS distributions with similar skew factors. A Bähr DIL 805 dilatometer was used to determine the isothermal $\gamma \rightarrow \alpha$ transformation behaviour at 700 °C after rapid cooling from the varied re-austenisation treatment. A sigmoidal time dependence of ferrite volume fraction was established, and an Avrami transformation analysis was carried out to determine the influence of Sn on the $\gamma \rightarrow \alpha$ transformation kinetics, along with metallographic examination providing quantitative information on ferrite nucleation and growth. The effect of Sn content and boundary coverage is considered to account for the composition effect on transformation rates.

Compositionally flexible alloy design towards recycling mixed stainless steel scraps. Lingyu Wang[1], Qiqi Liu[1], Chenchong Wang[1], Yuxiang Wu[2], Xiaolu Wei[1], Yong Li[1], Jiahua Yuan[1], Jun Hu[1], Dengping Ji[3], Sybrand Van der Zwaag[4], Wei Xu[1].

[1]Northeastern University, Shenyang, China.

[2]Monash University, Clayton, Australia.

[3]Zhejiang Tsingshan Iron & Steel Co., Ltd Qingtian, China.

[4]Delft University of Technology, Delft, the Netherlands.

Recycling-oriented alloy design is a crucial part of material sustainability, as it reduces the need for raw material extraction and minimises environmental impact. This requires that scraps be reused or repurposed effectively, even when the scraps are co-mingled and have higher costs for further sorting and separation. In this work, we explore an alloy design concept by creating a compositionally flexible domain that can recycle multiple alloy grades and yet maintain relatively consistent properties across chemical variations. This is demonstrated through the Fe-Cr-Ni-Mn system to identify compositionally flexible austenitic stainless steels (CF-ASS) and accommodate the recycling of mixed austenitic stainless steel scraps. Alloys within the nominal composition spaces exhibit relatively consistent mechanical properties and corrosion resistance despite significant variations in different alloy compositions. We illustrate how we can utilise the compositionally flexible austenitic stainless steels to recycle mixed 200 and 300-series stainless steel and ferronickel scraps, demonstrating its practical viability. While this demonstration focuses on the stainless steel system, the underlying principles can be extended to other systems related to mixed scrap recycling.

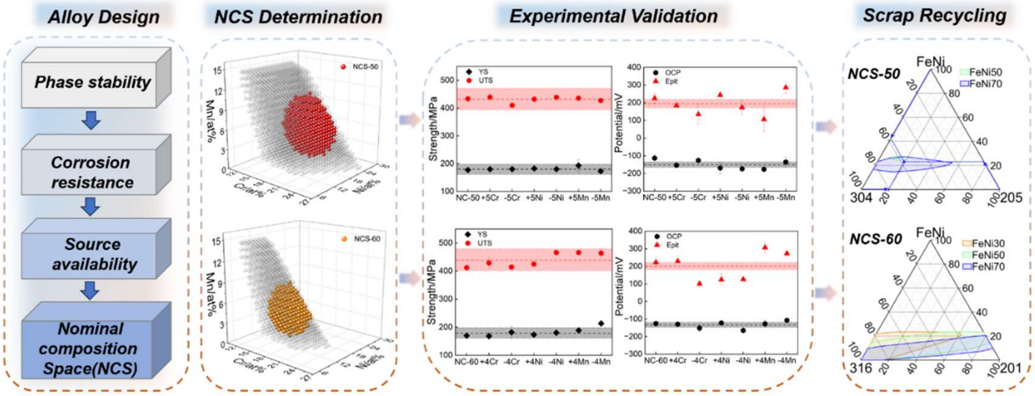

F1b.1-4: Pearlite (I).

Invited. **Modeling the growth kinetics of divergent (partitioned) pearlite.** Jiayi Yan.

Tsinghua University, Beijing, China.

Pearlite transformation in steels has been investigated over a long time not merely for its industrial significance, but also for a better scientific understanding of eutectoid transformation in general. In contrast to the probably more common case of "constant pearlite" with steady-state growth, "divergent" or "partitioned" pearlite is featured by a reducing growth velocity and an increasing lamellar spacing as growth proceeds, even under isothermal conditions. Such features relate to a net partitioning of alloying elements between pearlite and the matrix austenite, which is absent in the problem of steady-state pearlite. To enable a quantitative modeling of the non-steady-state growth kinetics of divergent pearlite, a previous model for steady-state pearlite[1] is extended to allow for net partitioning between pearlite and austenite. Transition between divergent pearlite and constant pearlite can be realized by finite trans-interface diffusivities which control the degrees of net partitioning of alloying elements. Like in the previous model, a finite interfacial mobility also influences growth rate and its relation with lamellar spacing. Quantitative modeling of pearlite transformation kinetics and its features (phase compositions and lamellar spacing) is expected to facilitate microstructural engineering practices, such as utilizing pearlite to produce other patterned microstructures for improved mechanical properties.

[1] JY Yan, J Ågren, J Jeppsson, Metall Mater Trans A, 51A (2020) 1978–2001.

Recovery annealing mechanisms in cold rolled C-Mn ferrite pearlite high strength steels by correlative electron microscopy. Jaiprakash Gautam.

University of Hyderabad, Hyderabad, India.

Present work investigates the mechanisms in low temperature recovery annealing of 80% cold rolled ferrite-pearlite high strength steel sheets. Annealing within the temperature range of 100-250 °C was examined using in-situ annealing transmission electron microscopy to observe sub structural evolution, coupled with Vickers micro hardness measurements on post-annealing samples for evolution of mechanical properties. Analysis of the isothermal fraction derived from hardness changes during aging was used to determine the activation energies of the underlying process or mechanisms. Low temperature annealing in 80% cold rolled steels appears to unfold in two distinct stages, suggesting the engagement of different atomistic mechanisms. First stages take place in the range of (100-175 °C), where small increase in the hardness, accompanied by the observed dislocation rearrangements within the ferrite phase and at its cell boundaries as observed by In situ TEM. In the second stage (175-250 °C), a pronounced increase in hardness is observed, along with gradual sharpening of cell boundaries leading to sub boundary formation in ferrite and in pearlite cementite appears to be completely diffused from In situ TEM. The probable mechanisms that governing these two stages of low temperature annealing are discussed, drawing insights from the observed activation energy.

Exploring Non-cooperative Eutectoid Transformations in Steel: A Decade of Phase field Modeling. Kumar Ankit.

Arizona State University, Tempe, United States.

Pearlitic lamellae in steel are typically softened through annealing to transform them into a more machinable and fabrication-friendly globular microstructure for engineering applications. However, predicting and controlling microstructural evolution during annealing remains difficult due to limited understanding of non-cooperative transformation pathways, particularly in bearing steels, where the complexities of multicomponent diffusion further complicate analysis. In this presentation, I will provide an overview of a calibrated, multicomponent, multiphase-field model that simulates microstructure evolution and diffusion pathways during the thermal treatment of eutectoid steels. Extensions of this model, focusing on Widmanstätten ferrite, will also be presented. Simulation results will be analyzed to identify processing conditions that promote non-cooperative pearlite evolution and to highlight the model's versatility in simulating a variety of eutectoid morphologies, including divergent and divorced pearlite.

The non-steady-state growth of pearlite in Fe-C-Mn-(Al) steels. Carlos Capdevila[1], Maria Aranda[1], Jonathan Poplawsky[2], Esteban Urones-Garrote[3].

[1]Centro Nacional Investigaciones Metalúrgicas (CENIM-CSIC), Madrid, Spain.

[2]Center for Nanophase Materials Sciences (CNMS-ORNL), Oak Ridge, United States.

[3]Centro Nacional de Microscopía Electrónica (CNME), Madrid, Spain.

The roles of Mn and Al during the isothermal growth of partitioned pearlite under non-steady state conditions is analysed by comparing the phase compositions of austenite, ferrite, cementite ($\gamma+\alpha+M_3C$) within the three-phase field in the Fe-C-Mn and Fe-C-Mn-Al systems. When the steel composition lies within the three-phase region (austenite+ferrite+cementite), the eutectoid transformation proceeds with a continuous change in the austenite composition ahead of the advancing pearlite. This leads to a temporal increase in interlamellar spacing due to a slowdown in growth kinetics, causing the pearlitic lamellae to diverge. The goal is to study the kinetics and thermodynamics when divergent pearlite is obtained in both ternary and quaternary systems. Transmission electron microscopy, energy dispersive X-ray spectroscopy, and atom probe tomography (APT) measurements across the $\gamma/\gamma+\alpha$ and $\gamma/\gamma+M_3C$ interfaces were compared to theoretical values obtained by Thermocalc software to study the LE conditions across the interfaces at different isothermal decomposition times and to establish whether the pearlite is growing under the Negligible Partitioning Local Equilibrium (NPLE) or the Partitioning Local Equilibrium (PLE) modes for both Mn and Al alloying elements.

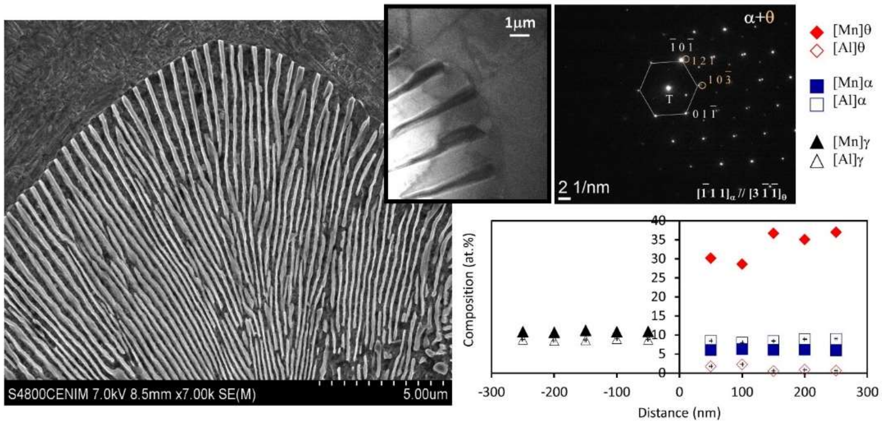

Pearlite formed in Fe-0.6C-10Mn-5Al (wt.%) at 670 ºC for 13 days. Crystallography and alloy distribution among austenite, ferrite and cementite.

F1c.1-3: Austenite formation.

Invited. **Microstructure evolution of line pipe steels during reheating.** Minyu Tseng, Joshua Swan, Sabyasachi Roy, Ruth Birch, Matthias Militzer, Warren Poole.

The University of British Columbia, Vancouver, Canada.

The desired microstructures and mechanical properties of line pipe steels can be achieved by carefully tailoring the thermo-mechanical process. In a hot mill, as-cast slabs undergo reheating, followed by rolling passes and run-out table cooling. This study focuses on austenite formation and grain growth during reheating which provides the initial microstructure for the subsequent processing steps and may affect the final product significantly. Austenite formation and grain growth tests were conducted for a Ti-Nb microalloyed line pipe steel using both as-cast and as-rolled materials. As-rolled or as-forged materials with more uniform microstructures have been typically employed for these studies, but the present work also focuses on as-cast materials to better reflect the actual manufacturing conditions. Microstructure evolutions were recorded in-situ by dilatometry for austenite formation and Laser Ultrasonics for Metallurgy (LUMet) for austenite grain growth. Further, ex-situ microstructure characterization was conducted in as-quenched samples by optical and electron microscopy. In particular, prior austenite grain reconstruction from Electron Backscatter Diffraction (EBSD) data provided insights into parent grain structures. Homogenous structures are observed in the as-rolled material with a clearly defined mean austenite grain size whereas complex heterogenous grain structures form with a mixture of small and very large grains in the as-cast material. These complex microstructures can be attributed to local variations in the distribution of Ti-rich carbo-nitrides that form during continuous casting and the associated spatial variation of pinning pressure for grain growth. This study enhances knowledge on microstructural evolution during reheating and its implication for optimizing steel processing routes.

Modelling the austenite formation in single pass laser heat treatments. Felipe Castro Cerda[1], Patricio Mendez[2].

[1]University of Santiago, Santiago, Chile.

[2]University of Alberta, Edmonton, Canada.

Laser heat treatment (LHT) is a fast, cost effective, and reliable strategy for surface engineering of alloys, whose main features and advantages have been thoroughly described in the literature. The microstructure after LHT is the result of rapid heating and cooling rates, with steep thermal gradients. The hardness achieved after LHT in steels is mainly due to the martensitic transformation of austenite formed during the thermal cycle. Therefore, the correct estimation of the austenite fraction formed during the heating and cooling stages becomes an important design parameter. A new model is hereby proposed, in which the initial microstructure consisted of ferrite and spheroidized cementite. Two essential features are implemented in the model: (i) the homogenization of austenite is concomitant with the dissolution of cementite and (ii) the cementite dissolution is estimated by the “invariant size” approximation. Three plain carbon steels of 0.18, 0.45 and 0.7 wt% carbon (nominal composition) in the quench and tempered condition were selected for this analysis. For each steel, single-pass laser heat treatments were carried using a 6 kW YLS-6000 IPG laser integrated with 4-axis CNC motion control system. The microstructure shows the well documented distinctive contrast between the hardened layer (mainly martensitic) and the base material. The microstructure reveals a clear transition zone, which is sharper as the carbon content increases. The new model shows a much better agreement than previous ones with the experimental results of case depth, denoting a sound physical description of the microstructure evolution during LHT cycles.

New insights into the influence of Al and Si on the austenitization of medium-Mn steel. Jiayu Li[1], Yunbo Xu[2], Daniel dos Santos Avila[3], Alexandros Banis[1], Jilt Sietsma[3], Roumen Petrov[1,3], Leo Kestens[1,3].

[1]Gent University, Gent, Belgium.

[2]Northeastern University, Shenyang, China.

[3]Delft University of Technology, Delft, the Netherlands.

Generally, Si and Al are the most common alloying elements in Fe-C-Mn based Medium-Manganese Steel (MMS), primarily functioning as carbide inhibitors. In this study, we found that compared with Si, the addition of Al can more effectively retard the austenite formation kinetics of MMS, thus inhibiting the austenite coarsening and promoting its C and Mn enrichment during intercritical annealing. This retardation has a profound effect on the microstructure evolution and mechanical properties of MMS. Based on thermo-kinetic analysis and experimental verification, we suggest that the essential reason for the reduced austenitization kinetics of Al-added MMS is the complex interaction between Al and Mn: although both Al and Si act as ferrite stabilizers, compared to Si (*i*) Al can greatly promote the austenite enrichment in C and Mn; and (*ii*) Al can rapidly reduce the chemical potential gradient of Mn during the partitioning local equilibrium (PLE) stage, forcing the partitioning rate of Mn to significantly slow down. Our work will change the existing view, no longer only focusing on the carbide inhibition and ferrite stabilisation effect of Si or Al addition. Instead, this study demonstrates that retardation of austenitisation kinetics via Al addition is a cost- and energy-effective approach to further refine the grain size of MMS. These findings can provide new insights into the optimization of composition design, microstructure tailoring, and mechanical properties of MMS.

F2a.1-2: Impurities and novel production methods (II).

Invited. **Science of dirty alloys - Improving recyclability of aluminum alloys.** Paul Chatron-Michaud[1,2], Sophie Cazottes[2], Olivier Dezellus[1], Michel Perez[2].

[1] Univ. Lyon, UCBL, LMI, CNRS, UMR 5615 Villeurbanne, France.

[2] Univ. Lyon, INSA Lyon, UCBL, MATEIS, CNRS, UMR 5510 Villeurbanne, France.

Aluminum recycling presents some difficulties, as mixing the alloying elements from different series in the recycling process leads to a reduction in the properties of so-called secondary aluminum, particularly ductility, which reduces the potential applications of this recycled aluminum. This decrease is usually attributed to the presence of Fe-rich brittle intermetallic compounds (IMC). The objective of this work is to improve the recycling sector's ability to produce alloys of interest by closing the loop on several wrought grades, avoiding downgrade to casting alloys. To do so, the methodology relies on a combination of experimental approaches and thermodynamic calculations to improve the predictive capacity of numerical simulation tools in compositional spaces they were not optimized for, to assess the impact of composition shift on the formation of detrimental IMC. Industrial alloys have been enriched to reproduce the consequences of recycling on the composition of secondary aluminum. The nature, size, shape and distribution of IMC have been successfully investigated by advanced techniques such as EDS, EBSD and XRD. Both massive samples and isolated IMC have been studied, thanks to a new take on the matrix selective dissolution technique (so called “Sibut” technique). This technique allowed a precise quantification of the different IMC in the enriched alloys through XRD and Rietveld refinement. The influence of several processing parameters on IMC such as cooling rate or homogenizing heat treatment have been studied. Experimental results have been also compared with numerical phase transformation models and thermodynamical calculations in order to challenge and optimize current databases.

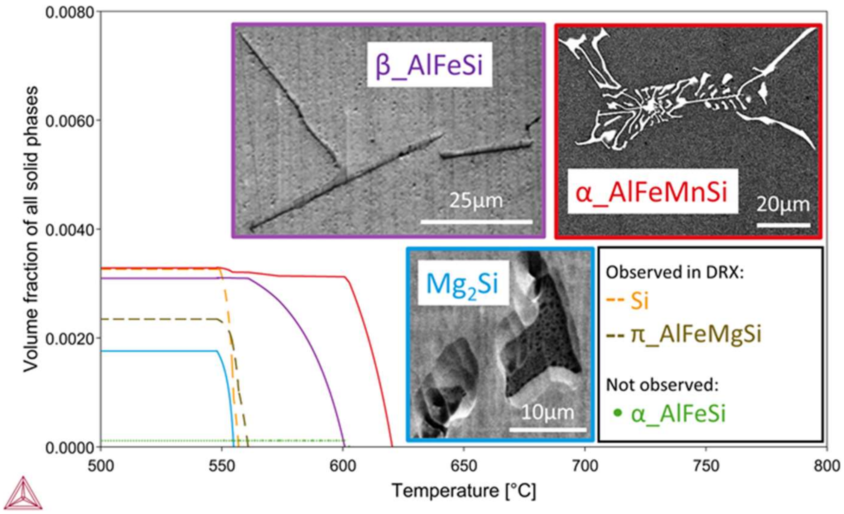

IMC in an enriched alloy after solidification and 1 K/s cooling: comparison between Thermo-Calc Scheil calculation and experimental observation

Mapping gangue effects on metallisation kinetics in hydrogen-based direct reduction. Yuxiang Wu, Lauren Sparrow, Ziyu Chen, Tian Zhang, Ma Jisheng, Ian Madsen.

Monash University, Melbourne, Australia.

The transition to green ironmaking presents a transformative opportunity for Australia's iron ore industry, aligning with global decarbonization goals. However, this shift poses significant challenges for existing ore grades, particularly Australian hematite ores, which contain various gangue oxides. This work investigates the effects of natural gangue species and additives on metallisation kinetics during hydrogen-based direct reduction. Utilizing in-situ synchrotron X-ray diffraction and 3D microscopy analysis, the study aims to elucidate microstructural transformation mechanisms, focusing on how gangue species influence the migration of reduced oxide interfaces and the formation of secondary phases (e.g., silicate), which restrict metallisation kinetics. The research points toward developing a kinetic map based on experimental data, offering foundational insights into the interplay between gangue content, temperature, and reduction kinetics. These findings will enhance impurity management across the steelmaking value chain, from beneficiation to electric smelting, supporting the transition to sustainable and efficient green steel production.

F2b.1-2: Pearlite (II), Senaatszaal.

Invited. **Multi-scale characterisation of subsurface microstructural evolution in a pearlitic rail steel induced by rolling contact tests.** Matteo Russo[1], Aurélien Saulot[1], Xavier Sauvage[2], Muriel Véron[3], Edgar Rauch[3], Patrice Chantrenne[1], Léo Thiercelin[4], Frédéric Lebon[5], Sophie Cazottes[1].

[1]INSA Lyon, Villeurbanne, France.

[2]Univ. Rouen Normandie, Rouen, France.

[3]Univ. Grenoble Alpes, Grenoble, France.

[4]Arts et Métiers Institute of Technology, Metz, France.

[5]Aix Marseille University, Marseille, France.

The ‘squat’-type defect is among the most concerning railway rail defects originating during service. Squats are characterised by a depression in the rail's running band that affects train dynamics and exacerbates rail degradation. This defect is associated with the propagation of subsurface cracks, potentially initiated by tribological surface transformations (TST) (Simon et al., 2013; Steenbergen, 2021). The latter are also known as White Etching Layers (WEL) and Brown Etching Layers (BEL) due to their appearance under an optical microscope. The mechanisms underlying WEL and BEL formation have been widely studied due to their impact on rail maintenance. Thermal and mechanical driving forces transform the original microstructure into a brittle nanostructure comprising phases such as residual austenite, depleted cementite, secondary carbides, martensite, and ferrite (Al-Juboori et al., 2019; Kumar et al., 2019). However, the effects of contact conditions, such as pressure, temperature, and shear stresses, on rail microstructure evolution are not yet fully understood. To clarify the influence of tribological parameters on the evolution of the microstructure, tests under controlled contact conditions were conducted using a tribometer that replicate the wheel/rail contact at a 1/10th scale. The test bench consists in a disc of diameter 70 mm (representing the wheel), rotating against a horizontal ring of diameter 2 m (the rail) (see Figure 1). A characterisation of the microstructural gradient using characterisation techniques down to the atomic scale was conducted, providing a detailed description of the sub-surface microstructure in link with the contact conditions.

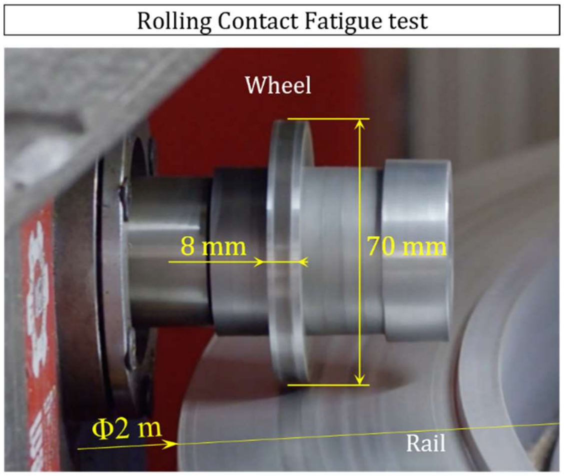

Test-rig used to replicate the wheel/rail contact conditions.

Quantitative evaluation of intrinsic mobility of interfaces with various characters during ferrite and pearlite transformations in Fe-C binary alloys. Yongjie Zhang[1], Haokai Dong[2], Kanon Sato[1], Takemasa Umeda[1], Goro Miyamoto[1], Tadashi Furuhara[1].

[1]Tohoku University, Sendai, Japan.

[2]Chinese Academy of Sciences, Ningbo, China.

Interface mobility is a key factor in predicting growth kinetics during phase transformations in steels, which is known to be strongly dependent on crystallographic characters, transformation temperature, and steel composition. In this study, to eliminate the extrinsic complexity caused by substitutional alloying elements, two Fe-C binary alloys with carbon contents of 0.07 mass% and 0.74 mass% were used to investigate the intrinsic interface mobility. The low-carbon alloy was isothermally transformed at 1023~1098 K, while the high-carbon alloy was decarburized at 1023 K to study the ferrite growth kinetics. Field emission-electron probe microanalyzer was used to measure the interfacial carbon content in austenite, and the intrinsic mobility of both incoherent interface for allotriomorphic and columnar ferrite, as well as semicoherent interface for Widmanstatten ferrite was evaluated based on the deviation in interfacial composition from local equilibrium and the interface velocity. The mobility of incoherent interface demonstrates an Arrhenius temperature dependence, whereas that of semicoherent interface appears to be more than one order of magnitude smaller. Additionally, the high-carbon alloy was also transformed at lower temperatures of 873~973 K to investigate the pearlite growth kinetics. After subtracting the energy consumed by lamella formation and carbon diffusion from the total chemical driving force, the mobility of incoherent interface for pearlite growth was evaluated using the net driving force for interface movement. The analysis reveals much larger mobility of pearlite than that of ferrite, accompanied by a non-Arrhenius temperature dependence, implying an essential difference in the growth behaviors of proeutectoid ferrite and pearlitic ferrite.

F2c.1-3: Intermetallics.

Invited. **Structurally complex intermetallic phases: understanding microstructure based on crystal structure.** Andreas Leineweber[1], Hanka Becker[1,2], Stefan Martin[1], Ulrich Meier[1], Lukas Richter[1], Guido Kreiner[1].

[1] Technical University Bergakademie Freiberg, Freiberg, Germany.

[2] Otto von Guericke University, Magdeburg, Germany.

The properties of intermetallic phases formed from transition metals *T*={Cr...Cu and higher homologues} and *B*={Zn and higher homologues as well as main-group metals} are, first of all, a topic of fundamental research. However, these phases can get technologically relevant in some heterogenous materials systems, where they develop in interdiffusion zones upon thermal processing. Examples are Sn-based soldering of Cu or Ni, or aluminizing or hot-dip galvanizing of iron and other transition metals. Investigation of the evolving microstructures developing upon interdiffusion reveals a wealth of phenomena, which have to be interpreted against the background of the sometimes structurally rather complex crystal structures of the intermetallic phases. It will be shown that rationalization of many microstructure phenomena is possible, if the complex, e.g., monoclinic or triclinic crystal structures (Ni_3Sn_4, $FeAl_2$, Fe_6Ga_5, Cu_7In_3) of the intermetallic phases are related with simpler, underlying structures. These structures are complex superstructures of “fcc”, “hcp”, and the “bcc” basic structures, for the latter including also ordered vacancies. If such a relation between structure of the intermetallic phase and of the underlying this relation is achieved, e.g., by formulating a lattice correspondence for this phase to the underlying basic structure, it turns out that microstructure features shown by this phase, such as habit planes, slip planes and orientation relationships are such which are typical for the underlying simple metal crystal structure. Basis for these findings are own experiments on diffusion couples and model alloys, investigated, in particular, using electron backscatter diffraction, but also data from the literature.

Formation of intermetallic CoSnX phases in the Sn-rich corner of the binary Co-Sn system. Stefan Martin, Andreas Leineweber.

TU Bergakademie Freiberg, Freiberg, Germany.

Due to the significant difference in the melting temperatures of Co and Sn, a cascade of peritectic reactions leads to the formation of numerous $CoSn_X$ intermetallic phases. The crystal structure and related polytypes of those phases can be reduced to an elementary arrangement of consecutive Sn and Co layers with distinct stacking sequences. This was evaluated using X-ray diffraction (XRD) on samples produced by arc melting and subjected to long-term heat treatments. Consequently, microstructures exhibiting a high density of stacking faults were observed, complicating the identification of the original phase. Certain transformation paths between different polymorphs have been evaluated. A comprehensive analysis of the observed microstructures, investigated through electron backscatter diffraction (EBSD) and TEM, was conducted to explore the interrelationships between the phases.

Precipitation behavior and microstructural evolution of σ phase and carbides in super austenitic stainless steels. Min Zhang, Yulin Gao, Zhunli Tan.

Beijing Jiaotong University, Beijing, China.

This study systematically investigates the precipitation behavior and microstructural evolution in super austenitic stainless steels, focusing on the σ phase and carbide phases ($M_{23}C_6$ and M_6C). Using Transmission Electron Microscopy (TEM), the morphology, crystallography, and orientation relationships (OR) of the continuously precipitated σ phase were characterized. The σ phase exhibited a habit plane of $(1\ 1\ \text{-}1)_{\gamma}/(0\ 2\ 0)_{\sigma}$ and preferentially extended along this plane due to lower distortion energy, forming an acicular morphology. The reduction in Cr and Mo content in the adjacent matrix decreased corrosion resistance, particularly in γ_2 regions of cellular σ phases, which had the lowest Pitting Resistance Equivalent (PRE). Additionally, the co-precipitation mechanisms of $M_{23}C_6$ and M_6C carbides were elucidated through crystallographic analysis. The OR between the γ matrix, $M_{23}C_6$, and M_6C phases were identified as $[\text{-}1\ 1\ 0]_{\gamma}//[\text{-}1\ 1\ 0]_{M23C6}//[\text{-}1\ 1\ 0]_{M6C}$ and $(1\ 1\ 1)_{\gamma}//(1\ 1\ 1)_{M23C6}//(1\ 1\ 1)_{M6C}$. $M_{23}C_6$ provided nucleation sites for M6C due to their structural compatibility, with no repeated habit plane observed. STEM-EDS analysis revealed the chemical formulas $(Cr_{17}Mo_3Fe_3)C_6$ for $M_{23}C_6$ and $(CrFe)_3Mo_3C$ for M_6C, while first-principles calculations confirmed the energy feasibility of the transformation from $M_{23}C_6$ to M_6C under high Mo content.This combined work provides critical insights into the precipitation behavior, microstructural evolution, and corrosion mechanisms of super austenitic stainless steels, laying a foundation for optimizing their performance in corrosive environments.

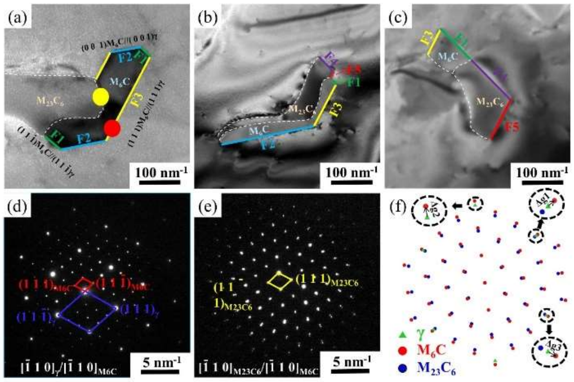

Posters

Quenching & Partitioning

Comparison of microstructure and mechanical properties after quench-temper and quench-partitioning heat treatment for a high silicon medium carbon cast steel. Saeed Hosseinreza[1], Habib Rastegari[2], Aliakbar Abedini[3].

[1]Research and development department of Isfahan, Casting Industries, Isfahan, Iran.

[2]Birjand University of Technology, Birjand, Iran.

[3]University of Birjand, Birjand, Iran.

In this research, the effect of Q&P and Q&T processes on microstructural evolutions and mechanical properties of a high silicon medium carbon cast steel was compared. For this purpose, the effect of various parameters including quenching temperature (230 and 250 °C), partitioning time (3, 8, and 15 min.), partitioning temperature (280 and 330 °C) as well as quenching media (oil and water) and tempering temperature (200 to 400 °C) was investigated. The results showed that the amount of retained austenite after quenching was approximately 13%, and after tempering at 350 °C, it reduced to about 8%; whereas in Q&P conditions, the highest and lowest amount retained austenite was 22.4% and 8.6% respectively. In some of Q&P conditions, the amount of austenite carbon concentration was more than the amount predicted by the CCE model (~1.2 wt%). In the Q&T process, the hardness and impact energy obtained from quenching in water and oil are almost similar values. For Q&T conditions, the highest impact energy was achieved by oil quenching and tempering at 200 °C. Increasing tempering temperature from 200 to 300 °C led to a decrease in impact energy, and at 350 °C it has slightly increased again. In the Q&P process, impact energy above 40J with a hardness of more than 40 HRC was achieved. Finally, a comparison of the results obtained for the Q&T and Q&P process showed that the Q&P process provides the best combination of hardness and impact energy for the investigated steel.

Austenite

Transformation of pancaked austenite in pipeline steel and its effect on the resistance to ductile fracture propagation. Alexey Gervasyev[1] Frank Barbaro[2], Leo Kestens[1,3], Roumen Petrov[1,3].

[1]Ghent University, Ghent, Belgium.

[2]Barbaro & Associates, Wollongong, Australia.

[3]Delft University of Technology, Delft, the Netherlands.

Pipeline steel is produced using thermomechanical controlled processing (TMCP), which employs accelerated cooling of deformed austenite leading to ferrite-bainite microstructures. This approach allows achieving high strength and toughness in compositions with low content of alloying elements. Niobium microalloying is used to suppress the austenite recrystallization during the last stage of hot rolling. The final microstructure is difficult to be described even qualitatively using optical or electron imaging. The Electron BackScatter Diffraction (EBSD) imaging technique can be used to create quantitative microstructural characteristics which can be correlated to mechanical properties of these steels. An overview of TMCP microstructures in pipeline steels and various ways of quantification are presented. The correlation of microstructural parameters with the resistance to ductile fracture propagation resistance is discussed.

Investigation of retained austenite stability in bearing steels. Mina Amiri[1], Per- Lennart Larsson[1], Lisa Toller-Nordström[1], Peter Hedström[1], Junbiao Lai[2], Annika Borgenstam[1].

[1] KTH Royal Institute of Technoloy, Stockholm, Sweden.

[2] SKF Research & Technology Development, Houten, the Netherlands.

The microstructure of bearing steels consists of martensite and retained austenite. Retained austenite can enhance the rolling contact fatigue lifespan, but can also lead to dimensional changes through deformation-induced transformation into martensite. Therefore, understanding the stability of retained austenite is critical in the development of bearing steels. In this study, the effect of mechanical loading on retained austenite stability was studied by conducting Brinell hardness testing and microstructural characterization. Finite element simulations were employed to estimate the influence of deformation on the retained austenite fraction and the results were compared with the experimentally determined fractions. Techniques including scanning electron microscopy, electron backscatter diffraction and X-ray diffraction were used to characterize the microstructure.

Phase transformation kinetics

A probabilistic approach to phase transformation kinetics. Gerben Krielaart.

Avans University of Applied Science, Breda, the Netherlands.

An alternative approach is proposed and discussed concerning the overall kinetics of phase transitions and phase transformations. The starting point is a general approach based on probability theory. This results in an equation describing phase transformation or transition rates in terms of transition or transfer probabilities, without recourse to a specific transition or transformation mechanism. The model can then be applied to various types of transformation and transition processes, taking account of the details particular to the process under consideration. In the case of heterogeneous phase transformations with preferred nucleation sites, as is the case in ferrous alloys and steels, this leads to a model that is based on physical quantities and phenomena like density, morphology, interface mobility and thermodynamic driving forces, which depend on the processing route. The transformation kinetics of heterogeneous

processes is also described as dependent on the microstructure evolution during the transformation process.

Tempering

Copper content and tempering synergy in tailoring the fatigue resistance of low-carbon steels.

Abhisek Mandal[1], Sumanta Bagui [2], Kapil Dev Sharma[1], Anish Karmakar[1].

[1]Indian Institute of Technology Roorkee, Roorkee, Uttarakhand-247667 India.

[2] CSIR-National Metallurgical Laboratory Jamshedpur - 831007, Jharkhand, India.

An attempt has been made to correlate the tempered martensitic structure embedded with different types of copper precipitates (crystal structure, shape, size, and distribution) with its low cycle fatigue (LCF response) of two copper-modified low-carbon (LCu-0.6 wt.% Cu and HCu-1.1 wt.% Cu) steels. After soaking in the complete austenite domain (920C-30m), two different tempering treatments, i.e., 630 °C and 170 °C, have been implied to the specimens prior to the LCF testing. The HCu specimens are showing finer structures at all tempering temperatures compared to the LCu ones. Moreover, the average KAM value is also higher in the HCu sample. The LCF tests were conducted in fully reversed strain-controlled mode to determine the cyclic stress response and strain life. At a lower tempering temperature of 170 °C, both HCu and LCu steels exhibit cyclic softening at a strain amplitude of 0.4%, whereas at higher strain amplitudes (>0.5%), cyclic hardening occurs with an increasing number of cycles for both compositions. However, the degree of hardening is greater in the case of HCu samples compared to LCu ones. At 630 °C, both HCu and LCu steels predominantly exhibit cyclic softening across all strain amplitudes (0.4%–1%) until fracture. Altogether, HCu steels demonstrate superior fatigue performance at both low and high tempering temperatures. A detailed microscopic analysis evidenced that high copper content in HCu samples enhances fatigue resistance via dislocation-precipitate interactions from incoherent FCC Cu precipitates and matrix interface.

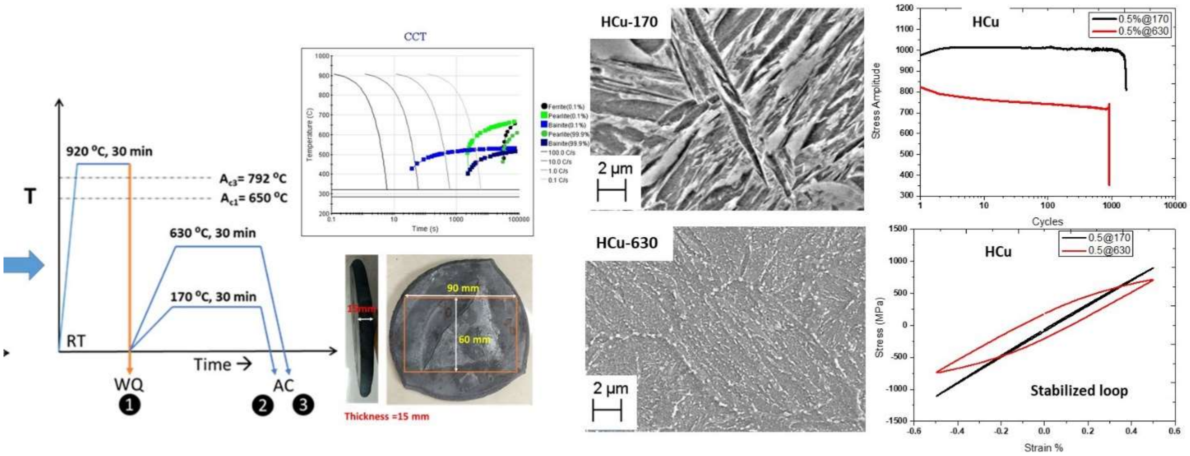

Effect of different tempering temperature on low-cycle fatigue properties of HCu steel at 0.5% strain amplitude.

Tempering of low alloy medium carbon steel under continuous fast heating and cooling conditions.

Cristofer Leandro Aravena Barria, Felipe Manuel Castro Cerda.

Universidad de Santiago de Chile, Santiago, Chile.

Traditional tempering methods, although reliable, are time and energy-intensive, often requiring hours to complete, depending on the steel type and process parameters. This study investigates ultra-rapid tempering using induction heating as a sustainable alternative to conventional tempering, highlighting its ability to achieve precise heating in a matter of seconds. These advantages could potentially reduce processing times and energy consumption, offering a more efficient solution for industrial applications. The present study involves the conventional salt bath quenching of cylindrical AISI standard 4140 steel tensile specimens. The austenitizing was carried out at 845°C for 20 minutes. Immediately after quenching, the tensile specimens were subjected to a tempering stage consisting of heating the sample at a constant heating rate of ~2E2 °Cs^{-1} to a peak temperature and immediately cooling in still air. Several peak temperatures in the range of 200 – 700 °C were applied using a 60 kHz induction furnace. The characterization was performed using optical and scanning electron microscopy, and X-ray diffraction (XRD) for phase quantification. Mechanical properties were evaluated through tensile tests and hardness measurements. The results of this work will provide valuable insights into the phase transformations occurring during continuous fast tempering cycles, enabling potential new processing conditions with an advantageous combination of strength and ductility.

Martensite

Assessment of the martensitic start temperature in carbon steels. Luciano Alexis Figueroa Maturana, Felipe Manuel Castro Cerda.

Universidad de Santiago de Chile, Santiago, Chile.

Martensitic steels are crucial in a wide range of industrial applications, including aerospace, automotive, structural, mining, and energy industries, due to their exceptional mechanical strength. The proper design of these steels requires the experimental determination of material parameters, such as the temperatures and times for transformation. However, these experimental methodologies are usually costly, time-consuming, and exhibit a significant variability. One of the key parameters in microstructure design is the martensitic transformation start temperature (Ms). The prediction of the Ms has been carried out using data from various experimental techniques, with dilatometry being the most commonly used. The empirical correlations derived from these studies are acceptable within a defined tolerance, but they lack predictive power. To improve the accuracy in estimating Ms temperature, it would be desirable to obtain data with better statistical representativity than expected from quench dilatometry experiments. Therefore, it's hereby proposed an approach is proposed that combines thermodynamic analysis of experimental data obtained through thermal analysis of heating and cooling curves at different rates on the Gleeble 563 thermomechanical simulator. This approach, complemented by microstructural characterization, will enable a deeper understanding of the martensitic transformation and facilitate the distinction between lath and plate martensite. Consequently, an accurate assessment of the Ms will not only enable the analysis of the predictability of thermodynamic models but also optimize the durability and performance of these steels in key sectors such as automotive and mining, contributing to greater industrial sustainability.

Strain solver

Efficient finite strain elasticity solver for phase-field simulations. Oleg Shchyglo, Muhammad Adil Ali, Hesham Salama.

ICAMS, Ruhr University Bochum, Bochum, Germany.

We present an effective mechanical equilibrium solution algorithm suitable for finite strain consideration within the phase-field method. The proposed algorithm utilizes a Fourier space solution in its core. The performance of the proposed algorithm is demonstrated using the St. Venant–Kirchhoff hyperelastic model, but the algorithm is also applicable to other hyperelastic models. The use of the fast Fourier transformation routines and fast convergence within several iterations for most common simulation scenarios makes the proposed algorithm suitable for phase-field simulations of rapidly evolving microstructures. Additionally, the proposed algorithm allows using different strain measures depending on the requirements of the underlying problem. The algorithm is implemented in the OpenPhase phase-field simulation library. A set of example simulations ranging from simple geometries to complex microstructures is presented. The effect of different externally applied mechanical boundary conditions and internal forces is also demonstrated. The proposed algorithm can be considered a straightforward update to already existing small strain solvers based on Fourier space solutions.

Elastic strain

Effect of nonlinear elasticity on microstructure evolution behavior using phase-field method. Jeonghwan Lee, Kunok Chang.

Kyung Hee University, Youngin-si, South Korea.

Elasticity significantly influences microstructural evolution, impacting morphology and, consequently, the mechanical performance of materials. Understanding elasticity is crucial for predicting system behaviors that affect structural integrity. Cahn and Larche developed an analytic model to study elastic effects on phase equilibria in binary alloys under coherent equilibrium. However, previous studies focused on linear elasticity based on Vegard's law, which assumes a linear relationship between lattice parameter and composition, overlooking the nonlinear behavior in real systems. To accurately predict material behavior, it is essential to account for both equilibrium composition and morphological changes caused by elasticity in non-equilibrium states. Thus, comprehensive simulations that consider both composition and morphology are crucial. To investigate the impact of nonlinear elasticity on microstructural evolution, we performed phase-field modeling, capturing changes in both composition and morphology across the system. While most phase-field models use linear elasticity based on Vegard's law, we incorporated nonlinear elasticity through a Taylor approximation to analyze its effects on microstructural evolution.

Diffusion

Quantitative analysis of diffusion equation when diffusivity is given as function of concentration. Yeonhak Chu[1], Ju-Seong Kim[2], Kunok Chang[1].

[1]Kyung Hee University, Yongin, South Korea.

[2]Korea Atomic Energy Research Institute, Daejeon, South Korea.

Fick's second law describes diffusion phenomena concerned with the concentration gradient. In a semi-infinite medium, the diffusion equation with constant diffusivity is solved by using the well-known error function analysis. However, when diffusivity is a function of concentration, a solution to the diffusion equation remains unclear. Previous studies demonstrated that an explicit solution can be derived by assuming that the diffusion coefficient varies as the positive nth power of concentration, $D=D_0(c/c_0)^n$. In this study, we extended the method to the case where n is the reciprocal of a natural number. To estimate the concentration profile and the Matano interface position as a function of diffusivity, we obtained concentration-time profiles and compared them under conditions of not only negatively but also positively deviated diffusivity. We also quantitatively evaluated the position of the Matano interface and iso-concentration lines with respect to time.

Isothermal Formation of Pearlite in Medium Mn Steel. Diego Jesús Zúñiga Montero, Dilan Sebastian Muñoz Vilches, Felipe Manuel Castro Cerda.

Universidad de Santiago de Chile, Santiago, Chile.

The evolution of pearlite transformation in medium-manganese steel, specifically in Fe0.5C5Mn and Fe0.5C5Mn1Co systems, remains insufficiently defined as the growth rate, final phase fraction and morphology, limiting treatment energy efficiency. Generally speaking, it is known the kinetics of pearlite transformation is influenced by factors like segregation, austenitic grain size, temperature, and alloy content. While low-alloy steels transform quickly under isothermal conditions, medium-manganese steels exhibit slower transformations due to diffusion of alloying elements, which extend treatment times, but not how they influence these systems. Experimental methods included software-based kinetic calculations, isothermal heat treatments, and microstructural experimental characterisation. Three critical temperatures were assessed: A_1-10 °C, A_1-50 °C, and 620 °C. Interrupted salt bath treatments on thin specimens ensured fast temperature homogenization. Dilatometry experiments were used as a complementary experimental technique to track in-situ phase evolution. The microstructural data analysis included the Underwood method for determining interlamellar spacing and Cahn and Hagel's approach for assessing the pearlitic growth rate. Results show that adding 1 wt.% cobalt to the Fe0.5C5Mn system enhances initial reaction kinetics and raises the final pearlite fraction compared to the ternary alloy. Treatment temperature has a similar effect. Distinct pearlite morphologies were observed; at 620 °C, interlamellar spacing is variable, like at lower temperatures at long times, but at short times the spacing remained largely constant. The hypotheses are based on the compositional change of the interface as it moves from a depleted to an Mn-enriched austenite given the growth rate results obtained.

Precipitation

Modelling the precipitation of carbonitrides during hot strip mill process. Yadvendra Yadvendra[1], Appa Rao Chintha[2], Henrik Larsson[1], Lars Höglund[1], Joakim Odqvist[1].

[1]KTH Royal Institute of Technology, Stockholm, Sweden.

[2]R&D, Tata Steel Limited, Jamshedpur, India.

Solid state precipitation is very important to understand while designing the alloys of desired properties. Size, shape, volume fraction and distribution of precipitates determine e.g. the mechanical and magnetic properties of the material concerned. There are various computational techniques used in the past to study the phenomenon with each having their own advantages and limitations. In this study, a numerical model based on NKW (Numerical Kampmann-Wagner) algorithm is being developed to study the complex carbonitride precipitation, VCN and NbCN, in micro-alloyed steels, coupled with plastic deformation mimicking the processes of Hot Strip Mill. The model is being integrated with the Thermo-Calc software for access to driving forces, equilibrium constituents and diffusional parameters of the active elements in precipitation. Part of this work has been done at Tata Steel India. Some preliminary simulation results are shown in the figure.

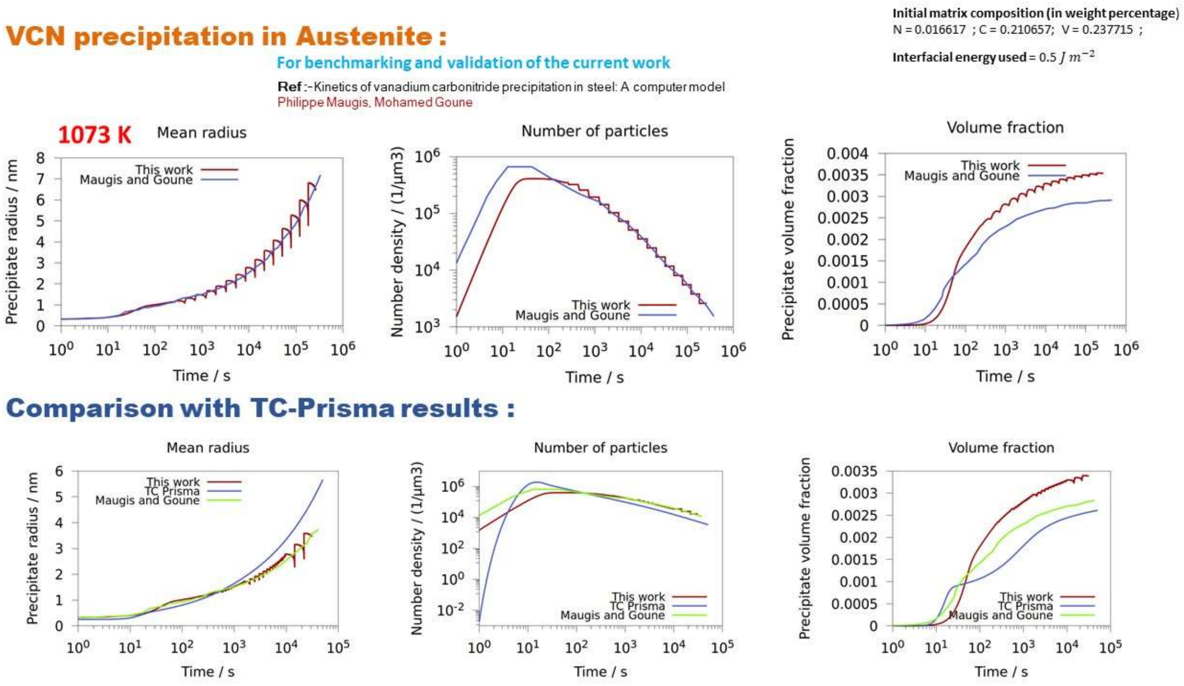

The effect of bath temperature on the microstructure and corrosion resistance of (Si, Ti) micro-alloyed Zn-6Al-3Mg alloy coating. Haotian Chen, Renbo Song, Zheyue Zhang.

University of Science and Technology Beijing, Beijing, China.

To further enhance the corrosion resistance of zinc-aluminum-magnesium coatings, trace amounts of Si and Ti alloying elements were added to the Zn-6Al-3Mg coating. This study investigated the impact of bath temperature on the microstructure and corrosion resistance of Zn-6Al-3Mg-0.1Si-0.05Ti coating. The results indicate that the addition of trace Si and Ti led to the formation of $(Al,Si)_3Ti$ and Mg_2Si within the coating. When the bath temperature was between 410-510 °C, the main microstructures of coatings were Al-rich dendrites, primary $MgZn_2$, and ternary eutectic. With an increase in bath temperature, the proportion of Al-rich dendrites gradually decreased, while the dendrite spacing increased. At a bath temperature of 600 °C, a significant amount of $Fe_2Al_5Si_x$ outburst structures formed within the coating, consuming Al atoms and preventing the formation of Al-rich dendrites. Molecular dynamics simulations suggest that this is related to the sudden increase in the diffusion coefficients of Al and Si atoms after 600 °C. Furthermore, when the bath temperature exceeded 510 °C, the proportion of lamellar ternary eutectic structures increased, while the proportion of reticular ternary eutectic structures decreased. Electrochemical results show that the coating exhibits the best corrosion resistance at a bath temperature of 450 °C, attributed to the high proportion of reticular ternary eutectic and fine Al-rich dendrites. The coating galvanized at 600 °C, lacking Al-rich dendrites, struggles to form a dense Al_2O_3 layer on its surface and is less capable of releasing Al^{3+} to form stable ZnAl-LDH during corrosion, resulting in the poorest corrosion resistance.

Computational design and thermal stability of novel alumina-forming martensitic steels at 550-650 °C. Cesar Fernandez-Jimenez[1], Isaac Toda-Caraballo[1], David San-Martin[1], Christopher Petersson[2], Peter Szakalos[2], Carlos Capdevila[1].

[1]National Center for Metallurgical Research (CENIM-CSIC), Madrid, Spain.

[2]Royal Institute of Technology (KTH), Stockholm, Sweden.

Alumina-forming martensitic steels were developed with the goal of combining the excellent oxidation and corrosion resistance of Alumina-forming austenitic stainless steels with the creep resistance and swelling resistance of ferritic-martensitic steels. Massive thermodynamic calculations have been performed under the Olson and Cohen approach for the estimation of the stacking fault energy to propose compositions aiming a microstructure formed by a martensitic matrix, stabilized with MX-type nano-precipitates. In addition, to achieve the capacity to form protective alumina scales, minimize the amount of retained austenite and avoid the formation of δ-ferrite, the element proportions of Cr, Ni and Al must be carefully balanced. Two Nb- and V-alloyed steels produced showed a primary martensitic microstructure with residual amounts of retained austenite and δ-ferrite. The microstructural characterization of the thermal stability of these alloys at 550 and 650 °C shows that the morphology of the martensitic package/block microstructure is preserved (**Figure 1**) in addition to a massive precipitation of B2-NiAl. The precipitation of this phase provides an initial hardening, though at long exposure times the coarsening of this phase along grain boundaries and in the matrix suggests that a suboptimal mechanical behaviour could be expected. Besides, their exposure to an oxygen-containing liquid lead environment at 550 and 650 °C for up to 1000 h reveals their capacity to generate an alumina scale, as characterised using electron probe microanalysis. The results achieved allows us to foresee the potential of these alloys for applications at intermediate temperatures in liquid lead environments for energy applications.

Isothermal phase transformation study of precipitates in ER312 duplex stainless steel. Ssu-Yun Lu[1], Shao-Pu Tsai[1], Te-Wei Lin[1, 2].

[1] National Taiwan University, Taipei, Taiwan.

[2] Walsin Lihwa Corporation, Tainan, Taiwan.

This study aims to investigate the isothermal phase transformation behavior of precipitates in ER312 duplex stainless steel. Initially, mechanical homogenization of the material is achieved through cold rolling instead of solution heat treatment. Subsequently, isothermal annealing is performed at various annealing temperatures and durations. The microstructural morphology, chemical composition, and phase distribution of ER312 duplex stainless steel samples subjected to different isothermal treatments are analyzed using optical microscope (OM), X-ray diffraction (XRD), and electron backscatter diffraction (EBSD). Based on these observations, a Time-Temperature-Transformation (TTT) diagram for ER312 duplex stainless steel is constructed. The findings are further validated through in-situ heating XRD experiments. Ultimately, the relationship between the phase proportions and annealing times at different annealing temperatures is established, providing valuable insights for the industrial applications of this duplex steel.

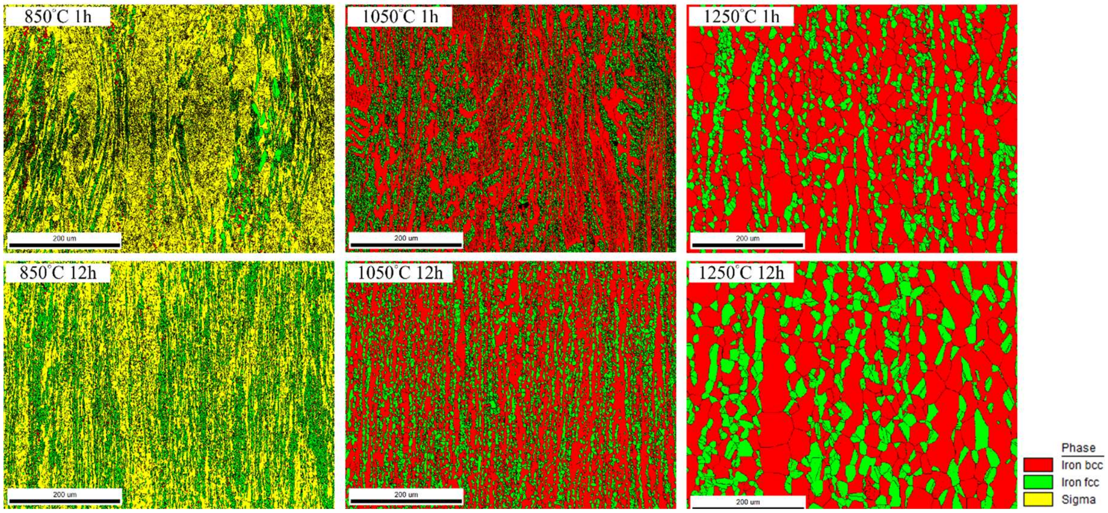

The EBSD phase maps of the ER312 sample held at 850 ℃, 1050 ℃, and 1250 ℃ for 1 h and 12 h, respectively.

A concise model for soft impingement during diffusion-controlled growth of spherical precipitates in the solid-state. Timo Brederode, Erik Offerman, Pina Mecozzi.

Delft University of Technology, Delft, the Netherlands.

The effect of soft impingement is modelled for the isothermal, diffusion-controlled growth of spherical precipitates in the solid-state. A two-stage soft impingement phase, isotropic growth in 3D and site saturation are assumed, which lead to a mean field approach for soft impingement. A mass balance is used in combination with a non-linear concentration profile approximation, instead of the ordinary linear concentration profile, to improve the description of growth under conditions of overlapping diffusion fields and low supersaturation. In addition, the capillary effects and dislocation assisted growth via pipe diffusion are discussed. The model has been applied to the growth of TiC-precipitates during tempering of a quenched Fe-C-Mn-Ti steel. The results are in good agreement with published experimental data of precipitate growth.

Investigation of the microstructure evolution in martensitic stainless steels during austenitization and quench. Alice Dautézac, María J. Santofimia.

Delft University of Technology, Delft, the Netherlands.

Many everyday items such as cutlery and razor blades are made from martensitic stainless steels. Due to their microstructure of tempered martensite and finely dispersed carbides, these materials exhibit not only a good corrosion resistance, but also a high hardness and a good workability. In this research, we investigate the microstructure evolution of the martensitic stainless steel AISI 420 during austenitization and quench. Its initial microstructure consists of a ductile ferritic matrix with uniformly dispersed spheroidal Cr-rich carbides. These carbides tend to partially or fully dissolve during austenitization, locally increasing the chromium content in the matrix. This leads to a local increase of the austenitization temperature, which might impede the transformation of the Cr-rich ferrite into austenite. The evolution of the Cr-rich carbides is first modelled with DICTRA, and then experimentally studied through dilatometry experiments. The microstructures are studied with optical microscopyand scanning electron microscopy. Energy dispersive X-ray spectroscopy, electron backscattered diffraction, and X-ray diffraction are used to investigate the local elemental distribution as well as the composition of the carbides and the present phases. This work sheds light on some of the mechanisms behind the microstructure evolution of martensitic stainless steels during processing, and hints at new possibilities in microstructure control.

Solidification

Solidification structure mathematical simulation research of pangang 37Mn5 oil well pipe steel.

Zhang Qiang.

Ansteel Group Anshan, Liaoning, China.

The production period of continuous casting at Pangang extracting vanadium and steelmaking plant does not align with the LF furnace processing period, leading to a decrease in steel temperature, increased power consumption, and limited continuous casting capacity. This study focuses on oil well pipe steel 37Mn5 produced by Pangang extracting vanadium and steelmaking plant. Under conditions where the amount of secondary cooling water remains constant, the commercial software ProCAST was used to simulate the effects of casting speed and superheat on the solidification structure. The reliability of the mathematical model simulation results was verified using production data, guiding the optimization of molten steel superheat and drawing parameters. Simulation results indicate that the casting speed can reach up to 2.0 m/min, with an axial crystal rate between 41% and 46% when the casting speed is within 1.5 to 2.0 m/min. This ensures oil well pipe quality while reducing production costs as casting speed increases.

Recrystallisation

Impact of boron and titanium on the mechanical properties and recrystallization behaviour of low carbon cold rolled and batch annealed HSLA steels.

Cécile Rampelberg[1,2], Christopher DiGiovanni[1], Tihe Tom Zhou[3], Chad Cathcart[3], Babak Shalchi Amirkhiz[1], Hatem Zurob[2], Colin Scott[1].

[1] CanmetMATERIALS, Hamilton, Canada.

[2] McMaster University, Hamilton, Canada.

[3] Stelco Inc, Hamilton, Canada.

High Strength Low Alloy (HSLA) steels are crucial in industries like automotive, construction, and transportation for their strong mechanical properties and cost-efficiency. In automotive applications, these steels improve vehicle safety, fuel efficiency, and reduce CO_2 emissions. Titanium addition (Ti) enhances strength through precipitation strengthening and controlled recrystallization, making Ti a cost-effective option for improving HSLA steels mechanical properties. Moreover, boron (B) added at ppm levels also significantly affects steel microstructures and properties [1]. This study investigates the impact of B on the recrystallization behavior and the performance of low-carbon Ti microalloyed steels during batch annealing. By analyzing the tensile stress-strain behavior and microstructural changes

(Fig1.), the study reveals that Ti+B microalloying improves strength in hot-rolled steel by increasing hardenability, which promotes finer ferrite grains and higher dislocation densities. However, the beneficial effect of B disappears after cold rolling and annealing. This effect is related to the solute drag effect of Ti being more influential than TiC particle pinning. Precipitation during the annealing of the cold-rolled material therefore results in coarser grains and reduced mechanical properties in the annealed product compared to the hot-rolled strip. These findings indicate that although B can improve hot-rolled properties, it poses challenges for cold-rolled and batch-annealed processes [2]. Optimizing microalloying elements and processing conditions, informed by insights into how B affects Ti microalloyed HSLA steels, is key to developing advanced materials with tailored properties for critical industrial applications.

[1] J. Takahashi, et al. Ultramicroscopy 159(2015)299–307.

[2] C. DiGiovanni, et al. Mat.Sc.&Eng. (2024) A, 147424.

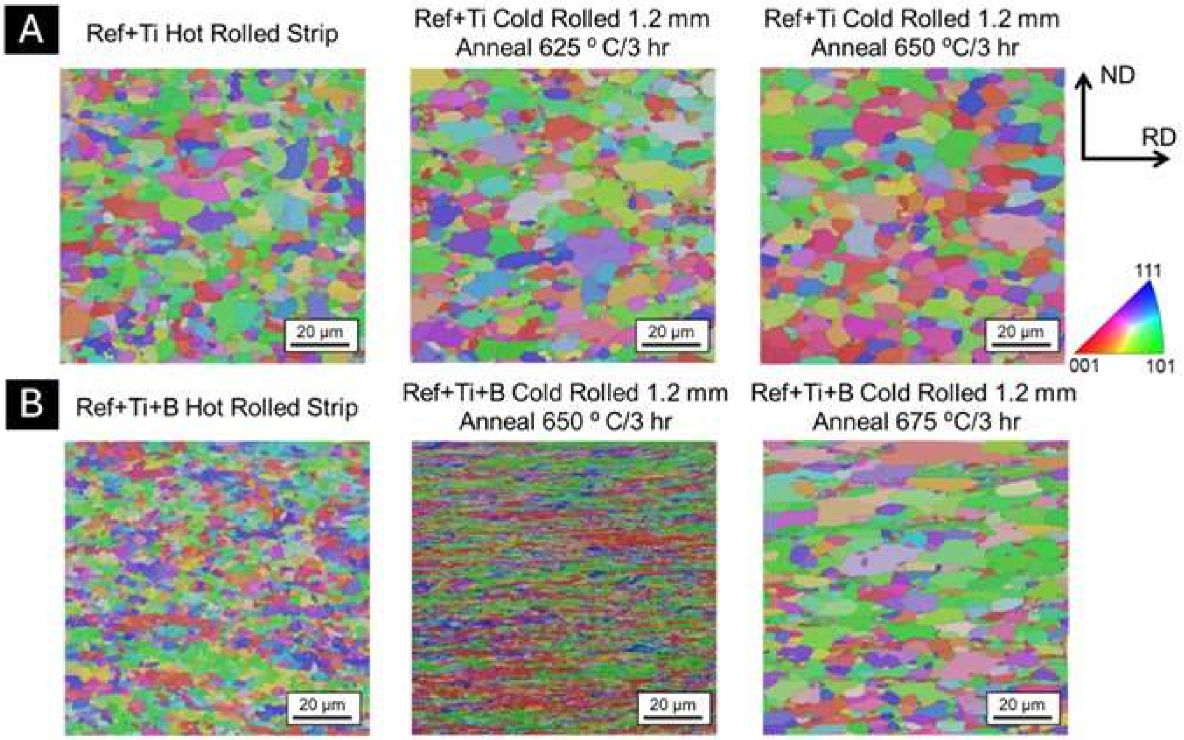

Figure 1: A) IPF maps for Ref+Ti steel. B) IPF maps for Ref+Ti+B steel.

Plasticity

Sequential γ-ε-α' transformation preserves high elongation in an ultrafine-grained high Mn steel.

Wei Xu[1], Lingyu Wang[1], Guangqi Dong[1], Jiahua Yuan[1], Jinliang Wang[2], Chenchong Wang[1], Minghao Huang[3].

[1]Northeastern University, Shenyang, China.

[2]Guangdong Ocen University, Zhanjiang, China.

[3]Hangzhou City University, Hangzhou, China.

While grain refinement is a prominent way to improve the yield strength of metastable austenitic steels, it usually leads to a reduction in the uniform elongation as γ-α' transformation tends to be suppressed. In the current study, it is found that the sequential γ-ε-α' transformation helps an ultrafine-grained high Mn austenitic steel maintain high uniform elongation while having more than doubled yield strength compared to the coarse-grained counterpart. The transformation kinetics of the ε and α' phases indicate that grain refinement increases the σ_s, delaying the transformation kinetics for both phases and decreases the maximum volume fraction of ε, but does not affect the final volume fraction of α', leading to sustained strain hardening and high uniform elongation. The differences in transformation kinetics can be reasonably explained by the intermediate ε phase and the variant selection phenomena in the γ-ε and ε-α' transformations. Grain refinement enhances variant selection of ε and increases strain energy, making the γ-ε transformation more difficult. Meanwhile, ε is rapidly consumed and transformed into α'. Together, these effects lead to a reduction in the maximum volume fraction of ε. The presence of the intermediate ε phase reduces the driving force, and the coordinated transformation of multiple α' variants reduces the strain energy, which together drive the sustained transformation of α'.The combination of a higher α' transformation rate and delayed transformation kinetics enables continued strain hardening, leading to high uniform elongation.

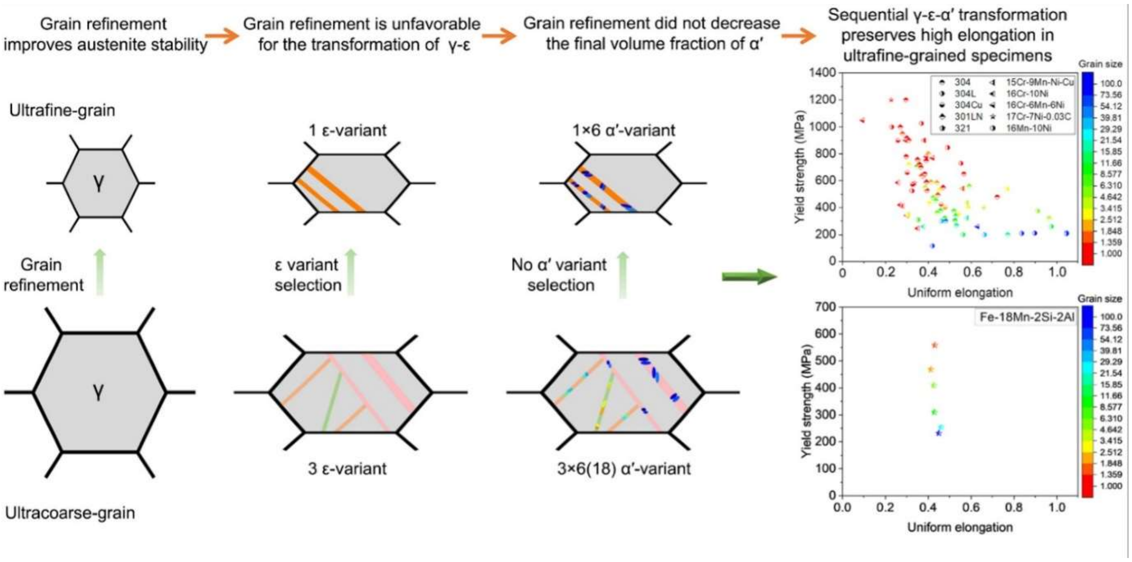

High entropy alloys

Structural and chemical analysis of multi-component alloys based on Ti, Nb, Zr, Ta, Ag prepared by arc-melting. Anna Benediktová, Palaniappan Subramanian, Michal Procházka, Zdeněk Jansa, Ján Minár.

University of West Bohemia, Plzeň, Czech Republic.

Multicomponent and high-entropy alloys are of great interest to researchers due to their unique properties, among which the potentially high chemical and structural stability is crucial. They are considered to be excellent candidates for use as biomaterials when appropriate component elements are used. Several Ti, Nb, Zr and Ta based alloys with the addition of Ag as an antibacterial agent were designed according to thermodynamic calculations and prepared by arc melting. Detailed structural and chemical analysis of the bulk material was carried out by diffraction techniques (XRD, SAED), scanning electron microscopy (SEM), and high-resolution transmission electron microscopy (HRTEM). The surface chemical states were investigated using X-ray photoelectron spectroscopy (XPS). The chemical stability of the alloys in phosphate-buffered saline (pH ~ 7.4) was evaluated using electrochemical methods such as potentiodynamic polarization and electrochemical impedance spectroscopy.

Microstructure and welding characteristics of single- and two-phase Al0.2CoCrFeNi produced by tailored thermomechanical treatments. Radha Ambe, Rajesh Korla, Subhradeep Chatterjee.

Indian Institute of Technology Hyderabad, Sangareddy, India.

Microstructure and mechanical properties of equiatomic CoCrFeNi have been shown to be tunable through controlled addition of Al, higher amounts which leads to the formation an ordered B2 phase in an FCC matrix. Here we investigate thermomechanical processing (TMP) and welding characteristics of an $Al_{0.2}$CoCrFeNi alloy with two different starting base metal (BM) microstructures. We show that the B2 forming range in this system can be extended to a lower-Al content by adopting a suitable annealing schedule after a cold working step. To isolate the effect of precipitates on the welding response from that of grain size, the cold rolled alloy is subjected to two different annealing schedules which result in the same grain size, but one BM contains B2 precipitates in an FCC while the other is single-phase FCC. Mechanical properties of the welded samples were compared with those of the base metal and correlated with the corresponding microstructures. The hardness of the weld fusion zone (FZ) is lower than the BM for both conditions and this is attributed to a relatively coarse dendritic microstructure of the FZ. Additionally, precipitate dissolution in the two-phase BM and increase in the grain size in the single-phase BM contribute to the decrease in hardness in the heat affected zone. Our results demonstrate the ability to precisely tailor the microstructure and properties of these alloys by adopting suitable TMP and highlight the role of precipitates on their welding response.

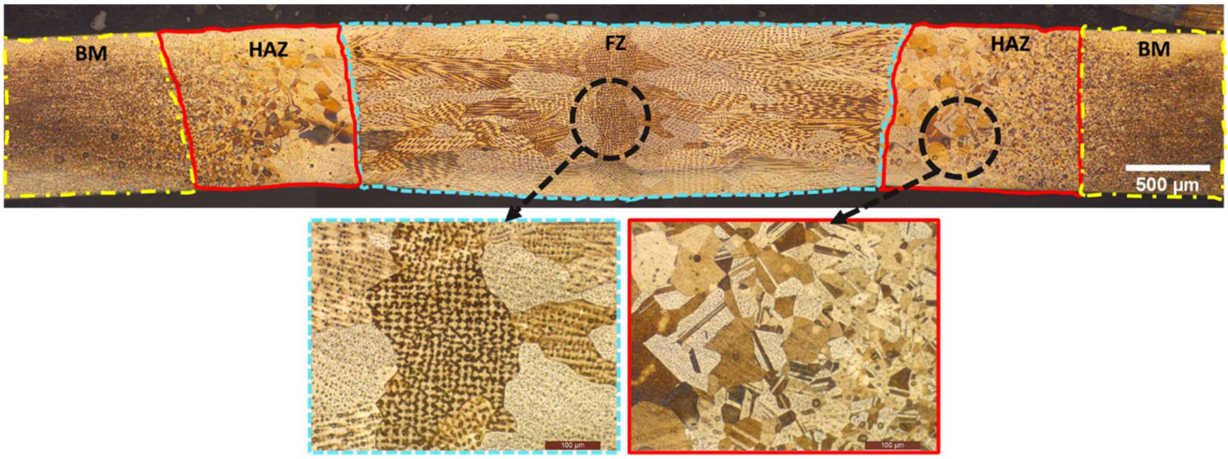

Macro- and microstructure of welded two-phase base metal revealing variation in structure across the weld

Additive manufacturing

In-situ heating TEM observation and high-temperature performance of sustainable Al-Fe alloys built by laser-powder bed fusion (L-PBF). Shao-Pu Tsai[1], Ji-Yun Wang[1], Verner Soh[2], Pei Wang[2], Tzu-Ching Tsao[1], Ming-Wen Chu[1], Ming-Hao Lee[1], Zhongji Sun[2], Yan Ma[3].

[1] National Taiwan University, Taipei, Taiwan.

[2] Agency for Science, Technology and Research (A*STAR) Singapore, Singapore.

[3] TU Delft, Delft, the Netherlands.

In this study, stepwise in-situ heating transmission electron microscopy (TEM) experiments were conducted on representative sustainable AlFe alloys produced by laser-powder bed fusion (L-PBF). The predominant microstructures observed in the build parts are cellular structures, which have been widely documented but less frequently discussed in the context of thermal stability. A critical threshold of 325 °C was identified, beyond which the cellular structures begin to decompose in conjunction with precipitate coarsening. The research also determined and presented the preferred precipitate nucleation sites and their subsequent coarsening kinetics. The use of Cs-corrected transmission electron microscopy revealed the presence of nanometre-sized crystalline embryos (~3.8 nm) within the cellular structure interiors in their as-built condition. Furthermore, their high-temperature mechanical behaviour is evaluated and discussed, indicating potential for future applications.

Microstructural development during wire arc additive manufacturing of bronze/stainless steel bimetallic structure. Mahdi Mahmoudiniya[1], Leo Kestens[1], Marcel Hermans[2].

[1] Ghent University, Ghent, Belgium.

[2] Delft University of Technology, Delft, the Netherlands.

In the present study, the wire arc additive manufacturing (WAAM) technique was used to produce a nickel aluminium bronze/ 410 stainless steel bimetallic part. The printed stainless steel part revealed a martensitic microstructure with a minor amount of retained austenite, while the bronze part showed a microstructure composed of different ƙ-precipitates within a Cu-rich matrix. A complicated microstructural gradient was also observed across the interface. Simultaneous electron backscattered electron diffraction (EBSD) and energy dispersive spectroscopy (EDS) revealed the presence of some Liquid metal embrittlement (LME) cracks in the heat-affected zone (HAZ) of 410 stainless steel. Reconstruction of prior austenite microstructure showed that LME cracks have propagated along the prior austenite grain boundaries.

Materials for energy

Multiphysics Simulation of Flow-Assisted Erosion of Main Steam Pipeline of iSMR. Homin Yu, Kunok Chang, Jeongho An.

Kyung Hee University, Yongin, South Korea.

The steam generator in a nuclear reactor heats the feedwater to produce steam. In the Korean-developed small modular reactor iSMR, a helically coiled tube design allows steam to discharge directly to the turbine through the discharger, bypassing components such as moisture separators. However, this configuration may lead to erosion, as high-speed steam droplets impact component surfaces. Although most studies on erosion in nuclear power plant environments focus on turbines, existing findings are challenging to apply to steam pipes due to environmental and design differences. Furthermore, studies specifically addressing droplet-induced erosion in main steam pipelines are limited. Thus, research on potential erosion in small modular reactor pipelines is essential to enhance reactor efficiency, safety, and component lifespan. This study analyzes the components of the iSMR main steam pipeline, such as the L-shaped pipe, where liquid droplet erosion is expected. Using the particle tracing module in COMSOL Multiphysics, we conducted a Flow-Assisted Erosion (FAE) analysis to predict erosion levels based on changes in fluid velocity and temperature.

Microstructure Effects on Oxidation in Carbon Steels. Patricia Libertad Gatica Godoy, Felipe Manuel Castro Cerda.

Universidad de Santiago de Chile, Santiago, Chile.

High temperature oxidation has the potential to modify the microstructure and thereby the surface properties of steel. Although the oxidation of iron and steel has been thoroughly reviewed (Chen et al. and Chang et al.), few studies address the influence of initial microstructure on the oxidation of carbon steel; Baud's work being an example. This research aims to contribute to elucidating how the initial microstructure and carbon content affect the kinetics and the morphology of the oxide layer on steel, giving a different perspective on the oxidation process and its impact on material performance. For this purpose, isothermal oxidation treatments were carried out at 890°C and 750°C for steels of 0.2%, 0.45%, and 0.7% nominal carbon content. The experimental set-up consisted of a controlled atmosphere furnace, which was held under vacuum conditions until the isothermal oxidation temperature was reached. This methodology ensures that the oxidation of the three steel chemistries begins at either the stability range of austenite (890 °C) or austenite and ferrite (750 °C). Optical microscopy and scanning electron microscopy (SEM) techniques were used to identify and quantify the phases present during oxidation. The observed kinetics of oxidation and the distribution of oxides are consistent with the literature for the case of 890 °C (fully austenitic range). The oxide layer formed at 890°C is adherent, whereas at 750°C the oxide layer is easily detached from the surface. In some cases, decarburization was observed to be associated with blister formation in the oxide layers.

Modeling the microstructure-dependent hydrogen redistribution during hydrogen storage applications. Konstantina Traka, Jilt Sietsma, María J. Santofimia.

Delft University of Technology, Delft, the Netherlands.

Understanding how hydrogen redistributes in the metallic microstructure is of high importance nowadays. This is because it allows an estimation of the metal’s ability to trap and de-trap hydrogen, and hence enables a microstructure-based material choice and longevity estimation for hydrogen storage (e.g. cargo tanks, fuel tanks, pipelines), where both leakage and metal embrittlement must be eliminated. In this work, we apply a physics-based model in different steel microstructures, the framework of which has already been qualitatively validated for carbon redistribution. In this model, the concurrent evolution of hydrogen phase partitioning and trapping at / de-trapping from defects is considered. These defects are grain boundaries, dislocations, and block boundaries, in cases where martensite is also present. The model describes the local, time-dependent distribution of hydrogen, considering a multi-component local thermodynamic equilibrium between all different lattice types, i.e the austenite solid solution, the ferrite / martensite solid solution, the defects of austenite, and the defects of ferrite / martensite. Due to the multi-structure local thermodynamic equilibrium computed during the hydrogen kinetics, the simulations capture also the de-trapping from these high solubility sites, e.g. austenite and defects, due to the equilibrium trap concentration that is affected by the hydrogen transport from solid solution. This is crucial because it enables the derivation of quantitative results regarding the actual diffusion length of hydrogen in the material, which is the main indicator of hydrogen leakage and / or embrittlement.

Sustainable metallurgy

High-throughput mapping of ferrite growth kinetics in residual-containing steel. Alexy Decroocq[1,2], Sébastien Allain[2], Imed-Eddine Benrabah[2], Benoit Denand[2], Alexis Deschamps[1], Guillaume Geandier[2], Hugo Landeghem[1].

[1]SIMaP Grenoble, France.

[2]Institut Jean Lamour, Nancy, France.

Steel is a critical metallic material in large number of applications, in particular in energy and transport applications, current and future. The global annual production of steel, at around 2 Gt is also a major contributor to anthropic greenhouse gas emissions. This large footprint can be reduced by increasing the amount of scrap recycling using electric arc furnaces. This steelmaking route displays a very contained environmental footprint but is reserved today to low-added value products (construction steel). The main hurdle to producing high-added-value advanced high-strength steel that way is the presence of residual elements in scraps, which cannot be practically removed from the liquid steel. The presence of these elements, even in amounts no greater than a few hundred ppm, alters the transformation of austenite into ferrite and hinders the microstructural control necessary for the production of AHSS. The purpose of the present study is to advance the knowledge base on the effect of residuals such as Sn and Sb on the transformation kinetics using high-throughput *in situ* characterization. This characterization, relying on compositionally-graded samples and synchrotron X-ray diffraction, enables a reliable assessment of the effect of those residuals on the transformation kinetics, and in particular of their interaction with the austenite/ferrite transformation interface. This assessment is complemented by select *ex situ* atom probe experiments to confirm this interaction. The results are used to calibrate numerical models that will ultimately help processing high-residual steels.

On the use of ammonia as reducing agent for green steelmaking. Matteo Villa[1, 2], Basit Ali[2], Marcel Somers[2].

[1]Polytechnic University of Bari, Bari, Italy.

[2]Technical University of Denmark Kgs. Lyngby, Denmark.

Steel production is currently the largest source of CO_2 emissions to the atmosphere from industrial activity. Green steel would be obtained with minimal (ideally none) CO_2 emission by directly reducing iron ore with carbon-free gases which are also obtained without releasing CO_2, i.e. green H_2 and green NH_3. As compared direct iron reduction by H_2, NH_3-based processing has received close to no attention. In this work, we applied thermogravimetry coupled to mass spectroscopy during the in-situ investigation of the reduction process of various iron oxides, including a natural iron ore from Uganda of particularly high purity. The efficiency of reduction in NH_3 and NH_3/H_2 mixtures were compared to reduction in H_2, which is considered as benchmark. Various sets of experimental conditions, e.g. various types of time-temperature cycles, gas flow rates, iron oxide types, etc were investigated. The role of porosity was investigated with nano-scale tomography. The data provides information on the relative effectiveness of the various reductive atmospheres as well as the associated kinetics. Such information is essential for further research in the field of NH_3-based green steelmaking.

A sustainable approach to develop high silicon steels using hydrogen reduced sponge iron powder. Sindhu Banothu, Gautam Jai Prakash.

University of Hyderabad, Hyderabad, India.

The increasing demand for energy-efficient electrical steel necessitates the exploration of innovative processing techniques. Hydrogen-reduced sponge iron, a sustainable and eco-friendly iron source, offers a promising alternative to traditional steelmaking processes. This research aims to develop a novel approach to produce Fe-Si alloys with superior magnetic properties, focusing on reducing energy consumption and environmental impact. Fe-Si alloys were produced by alloying hydrogen-reduced sponge iron with 4% silicon. The alloys were then processed through casting and warm rolling at 600°C with an 80% reduction. Subsequently, samples were annealed at 900°C, 1100°C, and 1200°C to induce recrystallization and texture development. Microstructural characterization techniques, including X-ray diffraction (XRD), optical microscopy, and electron backscatter diffraction (EBSD), were employed to investigate the deformation behaviour, microstructure and texture evolution during warm thermomechanical processing. The findings of this study provide valuable insights into the microstructure and texture development of Fe-4%Si alloys produced using hydrogen-reduced sponge iron and warm rolling. The results demonstrate the potential of this approach to produce high-performance electrical steel with improved magnetic properties.

PTM25

7 - 11 July 2025, Delft

GHENT UNIVERSITY

TU Delft

KTH VETENSKAP OCH KONST

WE WOULD LIKE TO THANK OUR SPONSORS:

GGS Groeien met Groen Staal

Thermo-Calc Software

micress®

TATA

CAMECA® SCIENCE & METROLOGY SOLUTIONS / AMETEK®

JOURNAL OF ALLOYS AND COMPOUNDS

www.PTM2025.eu

PTM25